DETERMINING INTERFACIAL ADHESION PERFORMANCE AND RELIABILITY FOR MICROELECTRONICS APPLICATIONS USING A WEDGE TEST METHOD

Hitendra Kumar Singh

Thesis submitted to the faculty of the

Virginia Polytechnic Institute and State University

in partial fulfillment of the requirements for the degree of

Master of Science

in

Engineering Mechanics

David A. Dillard, Chairman

John G. Dillard

Scott W. Case

August, 2004

Blacksburg, Virginia

Keywords: interfacial fracture energy, subcritical crack growth, temperature, diffusion, wedge test, glass-epoxy interface, silicon-epoxy interface, adhesion, delamination, fracture mechanics.

DETERMINING INTERFACIAL ADHESION PERFORMANCE AND RELIABILITY FOR MICOELECTRONICS APPLICATIONS USING A WEDGE TEST METHOD

Hitendra K. Singh

(ABSTRACT)

Fracture mechanics is an effective approach for characterizing material resistance to interfacial failure and for making interface reliability predictions. Because interfacial bond integrity is a major concern for performance and reliability, the need to evaluate the fracture and delamination resistance of an interface under different environmental conditions is very important. This study investigates the effects of temperature, solution chemistry and environmental preconditioning, in several solutions on the durability of silicon/epoxy and glass/epoxy systems. A series of experiments was conducted using wedge test specimens to investigate the adhesion performance of the systems subjected to a range of environmental conditions. Both silicon and glass systems were relatively insensitive to temperature over a range of 22-60°C, but strongly accelerated by temperatures above 60°C, depending on the environmental chemistry and nature of the adhesive system used.

Silicon/commercial epoxy specimens were subjected to preconditioning in deionized (DI) water and more aggressive solution mixtures prior to wedge insertion to study the effect of prior environmental exposure time on the system. The wedge test data from preconditioned specimens were compared with standard wedge test results and the system was insensitive to preconditioning in DI water but was affected significantly by preconditioning in aggressive environments. Plots describing $\frac{da}{dt}$ - G (crack velocity versus applied strain energy release rate) characteristics for a particular set of environmental conditions are presented and a comparison is made for different environmental conditions to quantify the subcritical debonding behavior of systems studied. A kinetic model to characterize subcritical debonding of adhesives for microelectronic applications is also proposed based on molecular interactions between epoxy and a silane coupling agent at the interface and linear elastic fracture mechanics, which could help predict long-term deterioration of interfacial adhesion.

ACKNOWLEDGMENTS

I wish to express my sincere appreciation to my advisor, Dr. David A. Dillard for his valuable time, advice, guidance and support through my study and research at Virginia Tech and for his steadfast patience, understanding, and encouragement over the last two years.

I also wish to acknowledge my other committee members Dr. John G. Dillard and, Dr. Scott W. Case for serving on my advisory committee, as well as for useful suggestions and guidance on my research work.

I would like to particularly thank Dr. Thomas C. Ward for teaching me about adhesives and adhesives research from a both a practical and fundamental standpoint.

I would like to thank former research scientist Dr. Kai-tak Wan, Dr. Zuo Sun, and Dr. Shu Guo in the Adhesion Mechanics Lab for useful discussions and great help in this work.

A special mention of thanks goes to Mr. Marshal H. McCord in the ESM Dept. at Virginia Tech for his great assistance in this work.

I would like to thank every one involved in the Hewlett-Packard project including Sandra Case, Emmett P. O'Brien, Davis Xu, Shu Guo, Harpreet Singh Chadha, Mike Christopher and Jeremy Garrett. I would like to gratefully acknowledge the financial support from Hewlett-Packard Company. I wish to thank Paul Reboa, Joshua Smith, Ellen Chappell, Brad Benson, Alok Sharan, Tom Deskins, Jami Barone, and Rhonda Pierce, of Hewlett-Packard for their assistance and advice in this work.

I am grateful to the Center for Adhesive and Sealant Science for fostering an interdisciplinary environment for the adhesion research, and would like to thank the Engineering Science and Mechanics Department at Virginia Tech for providing the research facilities.

Thanks are also due to Ms. Shelia Collins, Ms. Loretta Tickle and Ms. Joyce Smith in the ESM Dept. and Ms. Tammy Hiner at the Center for Adhesive and Sealant Science at Virginia Tech for their help over the years.

I owe my sincere appreciation to my friends, and relatives, who have supported and encouraged me over the years.

Finally, I extend my profound appreciation to my beloved mom, my aunt Dr. Kusum Singh and my uncle Dr. Mahendra P. Singh for their inspiration, love, care, and support and blessings over the years.

TABLE OF CONTENTS

LIST OF FIGURES

LIST OF TABLES

1 INTRODUCTION

1.1 Background

Many aspects of our lives—transportation, communication, computers, home entertainment, medical equipment, and instrumentation—have been profoundly affected by the microelectronics revolution. This dynamic industry is propelled by constant technological changes, which have brought improved and innovative products to the end user. Polymers play a critical role in the advancement of the microelectronics industry. The ever-increasing demand for high-performance portable electronics has resulted in pushing the electronics industry to extend technology limits in terms of higher packaging density, lower cost, lighter weight, and greater performance. Polymers are widely used in electronic packaging as adhesives, encapsulants, insulators, dielectrics, and conducting elements for interconnects [1, 2]. In recent years, there has been a significant increase in the use of polymers as adhesives for these applications as well. Adhesives are able to offer numerous advantages ranging from weight reductions to increased durability, which is very important to the microelectronics industry.

The use of adhesives in joining materials with different characteristics is of major importance for sealing, bonding, and adhering in microelectronic applications. However, there are many problems associated with adhesive bonding and typical areas under research and development are the reliability and durability of adhesive joints and their environmental resistance. Durability can be improved by making the interphase more stable and by increasing the moisture resistance of adhesives. A study of the factors responsible for the failure of adhesive joint in extreme environments will lead to a better understanding of the delamination mechanism, providing long-term solutions to problems associated with the adhesion and hence more reliable electronics assemblies. This research explores the reliability and durability aspects of adhesive joints subjected to different environmental conditions for microelectronic applications.

1.2 Research Objective

Adhesives form an integral part of a wide variety of fabricated products and offer many advantages including improved stress distribution, enhanced fatigue resistance and reduced component weight. As a result, the use of adhesive bonding in joining materials

with different characteristics is of major importance in a variety of microelectronic applications. Although most microelectronics devises are never subjected to liquid environments, the areas like microfluids, biomedical (e.g. implants) provide a harsh service environment for the adhesives. Many polymeric systems exhibit a significant drop in adhesive joint performance upon exposure to warm, moist environments. Several factors that affect the durability of an adhesive joint include the substrate, surface chemistry of the substrate, solution chemistry, testing temperature, adhesive, and exposure time and temperature. The effect of test temperature, environmental preconditioning and, liquid chemistry is evident from the results shown later in this thesis. Moisture absorbed by the system may affect interfacial adhesion by attacking strained bonds at the interface as well as lead to reversible and irreversible changes in the polymer. With the presence of moisture and temperature, the initiation and slow propagation of debonding between encapsulants and substrates are important problems that may influence the durability of the devices. Combinations of moisture and temperature are often major threats to adhesive bond durability.

This study aims at improving our understanding of the mechanisms of adhesion degradation of surface treated silicon and glass wafers bonded with a commercial and a model epoxy. The objective is to investigate the effect of environmental conditions on the behavior of silicon/epoxy joints and to formulate reliability models for practical electronics assemblies. X-ray photoelectron spectroscopy (XPS) studies on samples that were fractured and studied in different environments reveal changes in the surface chemistry and mode of failure of the adhesive joint. A fracture mechanics-based approach was utilized to study the durability of adhesive joint and obtain a better understanding of the failure mechanisms of the given adhesive system. A new tentative empirical model to characterize subcritical debonding of silicon/epoxy joints is developed based on subcritical debond behavior and linear elastic fracture mechanics, which could model long-term degradation and lifespan of interfacial adhesion.

1.3 Organization of this Thesis

This study is divided into six chapters and each chapter is briefly described as follows.

Chapter 1 gives a brief description of background information related to this research and presents the objective and significance of this study along with the organization of this thesis.

Chapter 2 provides a literature review covering a brief discussion on various theories of adhesion, and a review of fracture mechanics fundamentals and the wedge test method. A brief introduction to surface analysis, as well as bulk polymer characteristics, is also provided.

In Chapter 3, various mechanisms and physical models of diffusion in adhesive systems are discussed. This chapter surveys the general trends in environmental failure of adhesives and reviews some of the diffusion models to characterize diffusion in polymers.

Chapter 4 is entitled "Understanding Subcritical Delamination Mechanisms in Epoxy Bonds to Silicon and Glass Adherends". This chapter investigates the effect of environment on the subcritical behavior of a silicon/epoxy and glass/epoxy system. This chapter is written in paper format for formal publication in several journals.

Chapter 5 discusses predictive modeling along with the results obtained from fitting the existing empirical relationships to the wedge test data. At the closure of this thesis, Chapter 6 summarizes the important conclusions and future work in this area.

1.4 References

1. J. H. Lau, "Large High-I/O Solder-Bumped Flip Chip Technology," *Flip-chip Technologies*, McGraw-Hill, New York, **4**, 158-171, 1996.
2. R. S. Bauer, "Application of Epoxy Resin in Electronics", *Polymers for Electronics and Photonics* (Edited by C. P. Wong), Academic Press, **7**, 287-331, 1993.

2 LITERATURE REVIEW

2.1 Theories of Adhesion

Adhesion science is a multidisciplinary field and an area of research that presents many challenges. The actual mechanisms of adhesion have been investigated for years; several theories have been proposed in an attempt to provide an explanation for observed adhesion phenomena. However, no single theory explains adhesion in a general, comprehensive way [1]. Intimate molecular contact between adhesive and substrate is a necessary, but not sufficient, condition for effective bonding. There must also be sufficiently strong forces acting across the interface to hold an adhesive joint under an applied load. The nature of these forces is not fully understood, however there are widely recognized theories of adhesion as reviewed by Wake [2] and Kinloch [3]. There are five fundamental theories of adhesion: adsorption theory, mechanical interlocking theory, diffusion theory, electrostatic theory, and chemical bonding theory, which are explained here briefly.

2.1.1 Adsorption

Adsorption is the most widely accepted of the adhesion theories [3]. The adsorption theory proposes that, provided sufficiently intimate intermolecular contact is achieved at the interface, the materials will adhere because of the attractive forces acting between the atoms in the two surfaces and are much stronger with proximity depending on separation distance as per the Lennard-Jones model. The most common of the forces leading to adsorption are secondary or van der Waal's forces (dipole-dipole interactions and induced dipole-dipole interactions), which are responsible for the attraction of electrically neutral bodies to one another. In addition, acid-base interactions and hydrogen bonds, which are generally considered as a type of acid-base interaction, may also contribute to intrinsic adhesion forces and have been studied in depth by Fowkes [4-6]. Many researchers [7-8] have experimentally demonstrated that the mechanism of adhesion in many joints involves interfacial secondary forces and calculated attractive forces between two surfaces are considerably higher than the experimentally measured strength of adhesive joint. The discrepancy has been attributed to voids, defects or other geometric irregularities, which may cause stress concentrations during loading [9].

To obtain good adsorption, intimate contact must be reached such that van der Waal's interactions or acid-base interactions or both can take place; hence good wetting is essential. According to Young's equation, the surface tensions (liquid/vapor: γ_{lv}, solid/liquid: γ_{sl} and solid/vapor: γ_{sv}) at the three phase contact point, as shown in Figure 2.1, are related to the equilibrium contact angle, θ, through:

$$\gamma_{sv} = \gamma_{sl} + \gamma_{lv} Cos(\theta)$$

One other factor that influences adhesive joint strength is the ability of the adhesive to spread spontaneously on the substrate when the bond is initially formed [10]. For spontaneous wetting to occur:

$$\gamma_{sv} \geq \gamma_{sl} + \gamma_{lv}$$

Under the umbrella of the adsorption theory, two adsorption distinctions have been made: chemisorption and physisorption [11]. The latter refers to the condition where a material is physically adsorbed, or held together by secondary forces, whereas chemisorption involves ionic, covalent or metallic interfacial bonds formed across the interface [12]. Chemisorption is discussed further under chemical bonding theory in this review.

2.1.2 Mechanical Interlocking

The mechanical interlocking theory of adhesion states that good adhesion occurs only when an adhesive penetrates into the pores, holes, crevices, and other irregularities of the adhered surface of a substrate, and locks mechanically to the substrate. The adhesive must not only wet the substrate, but also have the right rheological properties to penetrate pores and openings in a reasonable time. To be effective, the adherend surface must have sufficient numbers of microscopic undercutting or root-like cavities. Mechanical interlocking can produce strong adhesive bonds that are resistant to hydrolytic and thermal degradation [12]. Evidence of this theory is most notably shown by the adhesion of polymers to textiles [13] or metals [14]. Venables [15] reported that mechanical interlocking is critical for good bond strength and long-term durability for metal-polymer bonds, especially in anodized aluminum-polymer systems.

Packham et al. [11] demonstrated that the adhesion of a polymer to anodized aluminum was dependent on mechanical interlocking of the adhesive in the pores of the aluminum oxide. Several researchers [16-18] demonstrated an increase in the joint

strength resulting from factors such as an increase in surface area, improved kinetics of wetting, or an increase in the extent of plastic deformation.

2.1.3 Diffusion

The diffusion theory was originally proposed by the Russian scientist Voyutskii [19]. He proposed that the intrinsic adhesion of high polymers to themselves, and to each other, is due to mutual diffusion of polymer molecules across the interface. This theory is applied to adhesion in polymer-polymer systems and states that adhesion of two polymer surfaces is due to the intermingling of polymer chains at a molecular level. This requires that the macromolecules or chain segments of polymers possess sufficient mobility and are mutually soluble and compatible [11, 20]. To describe the self-diffusion phenomenon of polymers, several theories have been proposed: entanglement coupling [21], cooperativity [22], and reptation [23]. According to the reptation model, Wu [24] has proposed that for the interdiffusion between two compatible polymers, the thickness of the interdiffused region, x(t), is proportional to the square root of time, $t^{1/2}$, and inversely proportional to the number of monomers per chain, N. Some evidence has demonstrated that the interdiffusion phenomenon exists in mobile and compatible polymers and may promote intrinsic adhesion. The diffusion theory, however, has found limited application where the polymer and adherend are not soluble or the chain movement of the polymer is constrained by highly crosslinked polymers, crystalline structures, or for polymers below their glass transition temperature. Also, because limited to polymer to polymer bonds, this mechanism is not applicable to other systems, such as the silicon/polymer system being studied in this thesis.

2.1.4 Electrostatic

The electrostatic theory originated in the proposal that if two metals are placed in contact, electrons will be transferred from one to the other, forming an electrical double layer (EDL), which gives a force of attraction. The basis of the electrostatic theory of adhesion relies on the difference in electronegativities of materials coming in contact with each other. An attractive force is attributed to the transfer of electrons across the interface, creating positive and negative charges that attract one another. For example, when an organic polymer is brought into contact with a metal adherend, electrons are transferred from the metal into the polymer, creating an attractive electrical double layer.

The electrostatic forces at the interface (i.e. in the EDL) account for resistance to separation of the adhesive and the substrate. The electrostatic theory states that the strength of the adhesive bond is a result of electrostatic forces formed when an electropositive material donates charge to an electronegative material, thus creating an electrostatic double layer at the interface. Some controversies have arisen surrounding the electrostatic theory owing to the fact that the EDL could not be identified without separating the adhesive bond. Possart [25] revealed that the energy required to peel a low density polyethylene (LDPE) film from aluminum foil is about 600 times that of the stored electrostatic energy. On the other hand, this theory does account for the electric discharges observed when a piece of pressure sensitive tape is quickly debonded from a rigid substrate by rapid peeling.

This theory finds much application in colloid science [26], but has found little practical use in engineering because of the large number of parameters it requires for predicting adhesion.

2.1.5 Chemical Bonding

The chemical bonding mechanism suggests that primary chemical bonds may form across the interface. According to this theory, a chemical reaction between two materials coming into contact is responsible for adhesion [3, 27]. The adhering phases undergo chemical reaction with each other to form covalent bonds at the surface. In order to form sufficient chemical bonds, intimate contact between two materials must be achieved. This can be achieved by employing by proper surface treatments or by using various coupling agents which requires mutually reactive chemical groups tightly bound at the substrate and coating surfaces. The coupling agents and adhesion promoters are frequently used to help in fixing the adhesive at the surface by chemical reaction [28-30]. An example is hybrid inorganic-organic material being synthesized with the sol-gel technology where Si-OH groups of react with the surface hydroxyl groups of the substrates. Chemical bonds are strong and make a significant contribution to the intrinsic adhesion in some cases. For example, primary chemical forces have energies ranging between 60-1100 kJ/mol, which are considerably higher than the bond energies of secondary forces (0.08-5 kJ/mol) [12].

2.2 Fracture testing

2.2.1 Development of Fracture Mechanics

The problem of adhesion can not be completely comprehended by consideration of the interfacial properties alone. Other parameters such as geometry, applied and residual stresses, and interfacial flaw populations are also important [31]. Fracture mechanics is the field of solid mechanics that permits these aspects to be considered and deals with the behavior of cracked bodies subjected to stresses and strains that can arise from applied loads or self-equilibrating stress fields (e.g. residual stresses). The study of the stresses caused by flaws and the material's resistance to failure form the basis for the field of fracture mechanics. The power of fracture mechanics lies in the fact that local crack tip phenomena can, to a first order, be characterized by relatively easily measured global parameters, e.g. crack length and nominal global stress (calculated in the absence of the crack), together with finite geometry correction factors.

There are two approaches to linear elastic fracture analysis: the stress intensity factor approach and the energy release rate criterion. The stress intensity factor approach, based on the work of Irwin [32], develops the concept that the fracture toughness should be measured in terms of resistance to crack propagation. According to this approach, fracture occurs when the applied stress intensity factor, K, exceeds a critical value, K_c, which is a material property. The energy criterion, based on the pioneering research of Griffith [33], states that the crack growth is energetically favorable when the decrease in the potential energy (during an incremental crack growth) is equal (or exceeds) the energy absorbed by the fracture process. This energy criterion is a measure of the energy required to create a unit surface area, and the critical energy parameter is usually referred to as the critical strain energy release rate, G_C .

According to the energy balance viewpoint [33], during an increment of crack extension ∂a , there can be no change in the total energy, *E*, of the cracked body. Te total energy *E* was viewed as being composed of the potential energy of deformation, Π , and the free surface energy, *S*. Therefore, during crack extension:

$$dE = d\Pi + dS = 0 . \qquad (1)$$

The rate of change of potential energy with respect to crack extension, ∂a , in a planar component of thickness, *b* is defined as the energy release rate, *G*:

$$G = \frac{-d\Pi}{b\partial a} \tag{2}$$

If the surface energy density is denoted by γ then $dS = 2\gamma b\partial a$ for the two increments of fracture surfaces formed during crack extension. Equation 1 and 2 can be combined to yield

$$G = 2\gamma \tag{3}$$

as the criterion for crack extension in a brittle solid. Equation 3 represents the balance that is achieved at the point of crack initiation between the energy provided by the loaded component and the energy required for the creation of new surface or the fracture resistance. The fracture resistance is a characteristic of the material, whereas the energy release rate depends upon the loading and geometry of the crack component.

The most common method of determining the energy release rate is to consider the change in component compliance as a crack grows in it. The potential energy of the component is the difference between the strain energy, *U*, and the work done by the force:

$$\Pi = U - P\Delta \tag{4}$$

Where P is the force and Δ is the associated displacement through which P does work. For linear elastic material, and small displacements, the strain energy $U = \frac{1}{2}P\Delta$ and Equation 2 and 4 yield

$$G = \frac{P}{2b}(\frac{\partial\Delta}{\partial a}) \tag{5}$$

The compliance, *C*, of a linearly elastic component is given by $C = \frac{\Delta}{P}$, and the energy release rate in Equation 5 becomes

$$G = \frac{P^2}{2b}(\frac{\partial C}{\partial a}) \tag{6}$$

which is powerful because it can be used to determine energy release rates directly from load-displacement records of fracture toughness tests without the need for any further stress analysis.

The stress intensity factor approach, developed by Irwin [32], focuses attention on the mechanical environment near the tip of a crack. In general, cracks may be stressed in three different modes as shown in Figure 2.2: mode I, the cleavage or tensile opening

mode; mode II, the in-plane shear mode; and mode III, the antiplane shear or tearing mode. Williams [34] resolved the problem of modes I and II but mode I was also given by Irwin. From linear elastic theory, the general solution, also called the Irwin-Williams solution, is expressed as the expansion of a series whose first terms are written (as an example) as:

$$\sigma_{ij} = \frac{K}{(2\pi r)^{1/2}} f_{ij}(\theta) + T\delta_{1i}\delta_{1j} + C_{ij2}(\theta) r^{\frac{1}{2}} + \ldots + C_{ijn}(\theta) r^{\frac{n-1}{2}} + \ldots \tag{5}$$

where σ_{ij} are the components of the stress tensor at a point, r and θ are the cylindrical polar coordinates of a point with respect to the crack tip, and K is the stress intensity factor which is linearly proportional to the magnitude of the stress intensity near the crack and is a function of the applied load and geometry of the structure in which crack is located. The second term of the expansion for mode I loading, called the "T-stress" or "component T", is a constant. The higher order terms are negligible as one approaches the crack tip. For mode I loading, the stresses in the vicinity of a crack tip may be developed from Equation 5 to yield the expression below:

$$\begin{bmatrix} \sigma_{11} \\ \sigma_{22} \\ \tau_{12} \end{bmatrix} = \frac{K_I \cos\frac{\theta}{2}}{\sqrt{2\pi r}} \begin{bmatrix} 1 - \sin\frac{\theta}{2}\sin\frac{3\theta}{2} \\ 1 + \sin\frac{\theta}{2}\sin\frac{3\theta}{2} \\ \sin\frac{\theta}{2}\sin\frac{3\theta}{2} \end{bmatrix} + \begin{bmatrix} T \\ 0 \\ 0 \end{bmatrix} + 0[r^{1/2}] \tag{6}$$

$$\sigma_{33} = 0 \text{ (plane stress)} \tag{7}$$

$$\sigma_{33} = \upsilon(\sigma_{11} + \sigma_{22}) \text{ (plane strain)} \tag{8}$$

$$\tau_{23} = \tau_{13} = 0 \tag{9}$$

where υ is the Poisson's ratio. From Equation 6 it is evident that as $r \to 0$ then the stress $\sigma_{ij} \to \infty$ and hence stress alone does not make a reasonable local failure criterion. Since the level of K_I uniquely defines the stress field around the crack, Irwin postulated that the condition:

$$K_I \geq K_{IC} \tag{10}$$

represented a fracture criterion, where K_{IC} is a critical value for crack growth in the material and is a material property and often termed as fracture toughness. The SI units of

K are in MPa$\sqrt{m}$ to represent a realistic physical order of magnitude. This elemental dimensional consideration sometimes allows for easy determination of K. Thus, for a crack of length 2a in an infinite plate loaded by a remote uniform tensile stress, σ (as shown in Figure 2.3), the two characteristic quantities are a and σ, and K_I from [35] is:

$$K_I = \sigma \sqrt{\pi a} \tag{11}$$

The above has considered the aspect of cracks located in "bulk" material, but the second important case is that of cracks at, or very close to a bimaterial interface. However, a problem arises when the joint is subjected to solely tensile loads applied normal to the crack, which is located along or parallel to the interface. These loads will induce both tensile and shear stress around the crack tip and both K_1 and K_2 terms are needed to describe the stress field [36]. However, K_1 and K_2 terms no longer have the clearly defined physical significance, as in the bulk materials case. Mathematical modeling [37-43] has shown that, for linear-elastic materials, the local stresses ahead of the crack tip at a bimaterial interface are proportional to:

$$\frac{f(K_1, K_2)}{(2\pi r)^{1/2}} \begin{Bmatrix} \sin \\ \cos \end{Bmatrix} (\zeta \ln r) \tag{12}$$

where ζ is a 'bimaterial constant' and is a function of the moduli and Poisson's ratios of the two materials forming the interface and is given by:

$$\zeta = \frac{1}{2\pi} \ln[(\frac{\beta_a}{\mu_a} + \frac{1}{\mu_s}) / (\frac{\beta_s}{\mu_s} + \frac{1}{\mu_a})] \tag{13}$$

where μ_a and μ_s are the shear moduli of the adhesive and substrate, respectively, κ_a and κ_s are the functions of the Poisson's ratios of the adhesive, υ_a, and substrate, υ_s, such that:

$$\kappa_j = 3 - 4\upsilon_j \text{ for plane strain and}$$

$$\kappa_j = (3 - \upsilon_j)/(1 + \upsilon_j) \text{ for plane stress} \tag{14}$$

$$j = a \text{ or } s \text{ as required.}$$

Unlike the bulk material case, a major consequence of Equation 12 is that very close to the crack tip, the stresses are oscillatory and have the highly improbable property of changing signs with increasing frequency as $r \to 0$. A further complication is that the

analysis results in a logarithmic term of a dimensional parameter, r, and thus the crack tip stresses, and values of K, become a function of the measuring units of r.

From Equation 12 the values of K_1 and K_2 for an interfacial central crack of length $2a$ in an infinite sheet under only tensile applied stress, σ_o, are given by [40]:

$$K_1 = \sigma_o \frac{\{(2\pi)^{1/2}[\cos(\zeta \ln 2a) + 2\zeta \sin(\zeta \ln 2a)]\}}{\cosh(\pi\zeta)} (a)^{1/2} \tag{15}$$

and

$$K_2 = \sigma_o \frac{\{-(2\pi)^{1/2}[\sin(\zeta \ln 2a) - 2\zeta \cos(\zeta \ln 2a)]\}}{\cosh(\pi\zeta)} (a)^{1/2} \tag{16}$$

The logarithmic term of a dimensional parameter, a, present in Equation 15 and 16 leads to the value of K dependent upon the units of a and makes it difficult to evaluate the mode I and mode II contributions independently of each other. Also, even if the mode I and mode II contributions are evaluated independently, the problem of combining them so as to propose a fracture criterion that takes both into account immediately arises. Several researchers [44-46] have suggested that for cracks at, or near, an interface a combined interfacial stress intensity factor, K_{iC}, for crack growth may be defined such that:

$$K_{iC} = (K^2{}_1 + K^2{}_2)^{1/2} \tag{17}$$

The main advantage of this approach, apart from combining the mode I and II contributions, is that by taking the root of the sum of the squares the length term is eliminated. Hence, the values of K_{iC} may be ascertained without the ambiguity of the stress intensity factor being a function of the units of the length.

Many problems arise and have yet to be resolved when applying the stress intensity factor approach to cracks in adhesive joints and therefore, many researchers adopted the energy balance approach over the stress intensity factor approach when studying crack growth in joints and deduced a value of G_C from Equation 4 via a theoretical or experimental determination. However, for engineering design and life-prediction, the stress intensity factor approach could possibly be of greater benefit if some of the above aspects were clarified and validated.

2.2.2 Wedge Test

Wedge test double cantilever beam specimens, as shown in Figure 2.4, are often used to evaluate the durability of adhesive bonds. The wedge test is a commonly utilized method to test the performance of fractured and stressed adhesive joints when exposed to different environments. This fracture test is an ASTM standard (ASTM D 3762) and utilizes a mode I specimen configuration. By driving a wedge into one end, an initial crack is introduced, exposing the crack tip directly to the test environment while under opening stress. By following the propagation of the debond with time, the debond kinetics can be established. The driving force for debond propagation comes primarily from the stiffness of the deformed beams separated by the wedge and this driving force decreases rapidly as the crack propagates. The introduction of the crack results in creation of two new surfaces (each of area A), and release of elastic energy stored in the beams. Calculations of *G*, used in this study, were obtained using Cognard's [47] relationship:

$$G = \frac{3}{16}\frac{B\Delta^2 Eh^3}{ba^4} \tag{11}$$

where the different terms are defined in Figure 2.4.

An important assumption in this test is that adherends should not deform plastically. This is usually not a problem when using thick and stiff adherends. The available strain energy release rate decreases with debond propagation, which results in the crack stopping at some equilibrium or threshold value, the value itself dependent upon the system conditions. One of the disadvantages of the wedge test is that it is often necessary to remove the specimens from the test environment to make crack length measurements. Also, the cracks may not be easy to view, as in the case of opaque specimens, or may propagate unevenly across the specimen width. The wedge test may be used to test the adhesive or cohesive strength depending upon whether the crack propagates at the adhesive interface or within the polymer itself (cohesive failure). This test can also be used to compare different surface treatments, especially when the mode of failure is interfacial.

A wedge test provides an effective way of testing the effect of different environmental conditions on the bond performance. In this test, the environment attacks closer to the bondline and directly at the site of the initiated crack and often leads to interfacial fracture surfaces.

2.3 Surface Analysis and Bulk Polymer Durability

2.3.1 Surface Characteristics

2.3.1.1 The Role of Interphase

The interphase is defined as the region of finite thickness with a gradient between the bulk adherend and bulk adhesive in which the adhesive penetrates and alters the adherend's properties or in which the presence of the adherend influences the chemical and/or physical properties of the adhesive. Sharpe [48] is credited with the first use of "interphase" to describe the boundary layers between adhesive and substrate. He emphasizes the importance of characterizing such boundary layers when analyzing the adhesive/substrate structure. Recent theories in adhesion science state that a three dimensional interphase, which exists between the substrate and bulk adhesive in an adhesive-bonded joint, governs the mechanical resistance and durability of the joint. Cuthrell [49] showed by penetrometry and microscopic observations that, for an epoxy resin molded either in metal or polytetrafluoroethylene (PTFE), a gradient in properties was found from the polymer surface adjacent to the mold to a depth of several hundred microns into the polymer bulk. Unfortunately, the boundaries of the interphase are difficult to define, and the interphase can extend from a few nanometers (nm) to a few thousand nm, depending on the system [50]. Sancaktar [51] has stated that adequate analysis and understanding of the interphase "is critical for design of efficient bonded structures and composite materials." Mechanisms of environmental degradation leading to failure in the interphase include:

1) Displacement of adhesive from the adherend (e.g. by water) due to the rupture of secondary bonds at the adhesive/adherend interface,

2) Mechanical weakening and failure of the oxide layer, and

3) Failure in a boundary layer of adhesive close to the substrate surface (i.e. in the interphase), which has properties differing from the bulk adhesive.

The mechanical properties of an adhesive material near the interface have been observed to differ from those in the bulk adhesive [51]. This boundary layer may well possess a different chemical and physical structure than the bulk adhesive, e.g. different molecular weight or crosslink density [52]. Since, the polymer chains in an interphase are stressed due to adsorption of polymer molecules on a substrate, either by primary or secondary bonding, these stressed polymer chains are more prone to chemical

degradation than the unstressed bulk polymer chains. Since metals and metal oxides are common catalysts in organic reactions, the metallic substrate might catalyze a chemical reaction of a polymeric material at an adhesive/substrate interface. Dillingham and Boerio [53] report such catalysis of an epoxy cure reaction by hydroxyl groups present on the aluminum oxide substrate surface. Thus, the existence of an interface can significantly affect the properties of the adhesive in the interphase region.

2.3.1.2 Surface Pretreatments

Surface pretreatment for the substrate materials is often necessary prior to adhesive bonding to replace a preexisting weak oxide layer with a more stable one. To achieve optimum adhesion durability, modifying the native substrate surface is often necessary. The basic objectives of any particular surface pretreatment may be manifold but the main aims are usually one or more of the following:

1) To remove loosely bonded surface contamination,
2) To create a microscopically rough and stable oxide layer, and
3) To provide intimate contact between the two interacting materials on a molecular scale [3].

Aside from a thorough cleaning, the chemical modification of a metal surface is one of the most powerful ways of enhancing interaction with an adhesive. A clean surface will rapidly absorb low-energy absorbates, such as hydrocarbons, which create a weak boundary layer on the metal oxide, lowering the surface energy substantially [54], preventing successful wetting of the substrate, and limiting adhesion. Since the adhesive/metal oxide interface is often susceptible to environmental attack and because improving the durability of the interphase is the prime concern, a large body of literature describes various methods and processes for cleaning semiconductor substrates [55-57]. These surface treatments are often categorized based on the surface roughness obtained during the treatment.

Basic aqueous solutions with the addition of oxidizers or acidic formulations [47] are used to remove organic surface contaminants [58]. To remove the native oxide on silicon, fluorine-containing reagents are used for etching in aqueous solution or in the gas phase [59-61]. However, wet chemical cleaning methods suffer from environmental concerns with materials handling and disposal, and the fact that such cleaning procedures often leave trace amounts of residue on the surface which present additional problems for

downstream processes. On the other hand, plasma pretreatments are environmentally benign and energy efficient processes commonly used in semiconductor processing and offer an attractive means to alter surface characteristics because they combine the features of safety, cleanliness and cost effectiveness while enhancing adhesion performance. Plasma processes can remove surface contaminants, introduce polar groups onto the surface to increase the surface energy, and increase the wettability of a substrate [62, 63], thereby improving adhesion. For example, oxygen containing plasmas introduce hydroxy, carbonyl, carboxy, and peroxy polar groups to the surface. Surface modification via plasma treatment is a non-solution surface treatment method for improving adhesion [64]. Plasma treatments that utilize nonpolymerizing gases are an effective means of removing carbon-containing contaminants from the surface, in addition to physically and chemically altering the surface of the adherend incorporating desired chemical functionalities to promote interaction and adhesion with the selected adhesive. An advantage of utilizing plasma processes to pretreat substrates is that typically only the top few microns of the surface are affected, leaving the bulk properties intact [65]. The various reactive species in the plasma (electrons, ions, free radicals and metastable species) interact with the polymer surface and can introduce different functional groups and chain crosslinking. Plasma modification can be tailored to improve the surface properties of the material by the nature of the gas or gases present in the plasma. However, the modification of the surface is not permanent and surface chemistry can change progressively.

Argon plasma treatment is generally preferred prior to the deposition of APS (3-aminopropyltriethoxysilane) to further enhance adhesion performance and durability on silicon surfaces. Silane coupling agents significantly improve adhesion between inorganic oxides and polymer resins [66]. Molecules defined as “coupling agents” are chemicals that promote adhesion between mineral phases and organic phases. The coupling agent, usually an organofunctional alkyltrialkoxysilane, is a hybrid that contains both organic and inorganic functionalities, thus allowing it to act as a chemical bridge between two dissimilar materials. Organofunctional alkyltrialkoxysilanes are most often used as coupling agents with a typical formula R-$(CH_2)_n$-silicon$(OR')_3$ where R' is an alkyl group, R is a functional group and n = 0-3 [67]. The alkoxy group –silicon$(OR')_3$ is capable of undergoing hydrolysis , in turn interacting with an inorganic substrate (e.g. metal oxides

or hydroxides) via hydrogen bonding with the organofunctional group, R (e.g. $-NH_2$), may be tailored to react with a specific adhesive. Silane coupling agents are commonly deposited utilizing a sol-gel reaction and may form monolayer or multilayers depending on sol-gel solutions and substrate. The application of these materials increases adhesive bond strength and resistance to moisture by improving wettability and/or strengthening the interphase of the inorganic acid and organic boundary layers [66]. Although there is extensive documentation on the use of organosilanes as adhesion promoters, the effectiveness of a coupling agent in a bonded system is highly specific and dependent on the substrate, polymer, and silane deposition parameters.

2.3.1.3 Surface Analysis Techniques

The objective of surface analysis is to determine the chemical composition of the outer few atomic layers of a solid surface where contaminants, process residues, diffusion products, and impurities are typically present. The composition of the outer most atomic layers of a material plays a critical role in properties such as: chemical activity, adhesion, wettability, electrostatic behavior, corrosion resistance, bio-compatibility, etc. Surface analysis is accomplished by using a probe beam to stimulate the emission of electrons, ions from a surface and analyzing the emitted charged particles which provide elemental, chemical state, or molecular structure information. The average analysis depth of most surface analysis techniques is approximately 0.5-5 nm, with the exact analysis depth dependent on the specific technique. Because surface analysis experiments are typically performed in an ultra high vacuum (UHV) environment, surface analysis techniques are generally applied to solid surfaces. Both organic and inorganic materials may be analyzed, depending on the technique. Various methods used to study the surface are Field Emission Scanning Electron Microscopy (FE-SEM), Optical Microscopy, Auger Electron Spectroscopy (AES), Atomic Force Microscopy (AFM), and X-Ray Photoelectron Spectroscopy (XPS). Since XPS was used in the present study to analyze the surface of the fractured specimens, a brief discussion is given here.

2.3.1.3.1 XPS Technique

X-ray photoelectron spectroscopy (XPS) has evolved into a powerful surface analysis technique over the last twenty years and is arguably the most popular surface analysis technique because of the excellent qualitative and quantitative elemental analysis it

provides. This technique uses a monochromatic X-ray source, usually Mg K_α (1253.6 eV) or Al K_α (1486.6 eV) to study the composition and chemical state of the surface region of a sample. X-ray photoelectron spectroscopy utilizes photo-ionization and energy-dispersive analysis of the emitted photoelectrons from inner-shell orbitals [68] to identify the chemical constituents of materials, and allows identification and quantification of atomic elements as well as information on the chemical state of the substituents at solid surfaces [69]. Generally, the electrons of atoms with highly electronegative substituents groups exhibit higher binding energies than the same atoms bound to groups with lower electronegativity [70].

The detection of photoelectrons requires that the sample be placed in a high vacuum chamber. The energy of the photoelectrons is analyzed by an electrostatic analyzer and the photoelectrons are detected by an electron multiplier tube or a multichannel detector. Because energy is conserved, the kinetic energy of the emitted electron plus the energy required to remove it from its orbital must equal the X-ray energy. The kinetic energy, E_K, of these photoelectrons is determined by the energy of the X-ray radiation, $h\nu$, and the electron binding energy, E_b, as given by:

$$E_K = h\nu - E_b \tag{12}$$

The experimentally measured energies of the photoelectrons are given by:

$$E_K = h\nu - E_b - \varphi \tag{13}$$

where φ is the work function of the spectrometer [68]. The energy level diagram for XPS is shown in Figure 2.5. The electron binding energies are dependent on the chemical environment of the atom, making XPS useful to identify the oxidation state of an atom. The photoelectrons and auger electrons emitted from the sample are energy separated by an electron energy analyzer and photoelectrons are then analyzed by an electrostatic analyzer. Detailed analysis of the absolute and relative binding energies and relative peak intensities corresponding to the direct photoionization of core levels can provide data on structure and bonding in systems. Because the escape depth of the ejected electron is limited, typically to 5 to 10 nm, XPS is an excellent technique for analyzing the near-surface region of the sample of interest.

2.3.2 Polymer Durability

Since the early 1960s, the subject of polymer durability has been of great interest and importance. Long-term stability in the presence of heat, light, atmospheric oxygen, and other agents, in many cases, is the limiting factor in the use of polymers in high-performance applications. Understanding polymer degradation mechanisms is often an important part of being able to predict the long-term reliability of individual components and systems. As polymeric materials with improved durability have been developed, the potential applications for polymeric materials have become even more demanding. Prior to use, the long-term durability of these materials must be clearly demonstrated, requiring either real-time testing of materials beyond one lifetime of service [70] or development and validation of accelerated aging [71] and/or lifetime prediction methods [72, 73]. The growing emphasis on quality and reliability of products has resulted in the ability to predict the aging behavior and useful lifetimes of polymers in application environments.

Different aging mechanisms can lead to a decrease of material or product properties which leads to non-fulfillment of requirements. Aging mechanisms can be divided into two major groups, according to the different influences and the affecting mechanisms:

1) Physical aging mechanisms, and
2) Chemical aging mechanisms.

Physical and chemical aging mechanisms are influenced by environmental factors. Their effects on the molecular structure of the material can describe the difference between physical and chemical mechanisms.

Physical aging is a phenomenon caused by material evolution towards thermodynamic equilibrium [74]. When a polymeric material is reduced below its glass transition temperature (T_g), it does not immediately achieve thermodynamic equilibrium; rather, the material evolves towards this state. Unless the temperature is very close to T_g, this evolution will typically take months or years to complete. During this period, physical properties such as compliance and modulus change continuously. Also, the viscoelastic properties of the polymer change, the creep and relaxation rates decrease, as does the damping. Physical aging mechanisms lead to reactions that affect molecular arrangement, the structure of the polymer material and their inter-molecular forces or secondary valence forces. The extent of physical aging, a function of aging time and temperature, is reflected in physical property changes, such as an increase in density and T_g, and in

mechanical property changes [75, 76], such as an increase in modulus and tensile yield strength and a decrease in fracture toughness. Generally, physical aging mechanisms are reversible and by increasing the temperature of the sample above its glass transition temperature its past history can be expunged. The ability to account for the effects of physical aging is critical to the design of engineering structures involving advanced polymers and polymer composites.

Chemical aging mechanisms change the polymer structure irreversibly in contrast to reversible physical aging mechanisms. Under moderate conditions, the degradation of the polymer is attributed to chemical aging but the analysis of the chemical evolution of a polymeric material is complex because it includes many mechanisms that vary in importance. The free space that exists between molecular chains in polymers allows the polymer to absorb fluids to which they are exposed, especially those with similar solubility parameters. Such absorption physically weakens the polymer and may also chemically attack the polymer. The kinetics of these processes is governed by diffusion and chemical kinetics, both of which are governed by Arrhenius relationships with regard to the influence of temperature. Testing via accelerated aging is a recommended technique for a very different reason: the difficulty of extrapolating the data collected in non-accelerated conditions. Accelerated aging can be defined as a procedure that seeks to determine the response of a device or material under normal-usage conditions over a relatively long time, by subjecting the product for a much shorter time to stresses that are more severe or more frequently applied than normal environmental or operational stresses. Since, the functional properties of a polymer depend on the properties of its constituent materials the performance of these materials is related to the rate of degradation of their inherent structure and configuration over time. This degradation is primarily chemical—a combination of effects arising from oxidative chain scission, oxidation hydrolysis, changes in crystallinity, and other factors that may be environmentally dependent. Any factor that can reasonably affect the functional properties of the product over time should be included in the accelerated testing program. Many accelerated-aging techniques used for the qualification testing of polymers are based on the assumption of zero-, first-, and pseudo-first-order chemical reactions following the Arrhenius reaction rate function. The testing is conducted at higher than usual levels—whether of temperature, humidity, radiation, temperature cycling, chemical

environment, or other factors. The results at these accelerated stress conditions are then correlated to those at normal operating or storage conditions using a physically appropriate statistical model. While useful information can be gained from accelerated aging studies, one must treat these data very carefully, as complex degradation mechanisms and synergistic effects can cause accelerated/ predicted results to vary considerably from real time aging behavior. The difficulty in any accelerated aging testing lies in the identification of the detrimental chemistry. An accelerated aging experiment is unacceptable whenever the nature of the dynamic process that controls the weathering is different during the testing procedure.

Polymers are routinely called upon to perform reliably in applications in which they may be exposed to a wide range of environmental stresses. The ability to characterize and monitor their degradation is crucial in determining the service life of components and systems that use these materials. Understanding polymer degradation mechanisms is often an important part of being able to predict the long-term reliability of individual components and systems. A variety of approaches has been used to evaluate and/or predict polymer durability. Oxidative weight loss [72, 73], micro-cracking behavior and extrapolation of mechanical properties after accelerated isothermal aging [71] have been investigated as accelerated aging and lifetime prediction methods for elevated temperature applications. The stress simulation approach [77], where a polymeric system is treated as a "black box" to which were applied all the physicochemical stresses that exist in the environment e.g. light, heat, mechanical strains, O_2, liquid and gaseous water, O_3, and pollutants, has been used to study and understand the phenomenon causing the degradation of the system. Some negative aspects of stress simulation approach include control of the important aging parameters. The detrimental effects of these parameters can not be rationalized because many different chemical evolutions might have the same physical consequences and since physical and chemical stresses can be applied simultaneously, the actual origin of the observed degradation is often difficult to identify.

The ability to accurately predict changes in polymer properties is of critical importance. Modeling the kinetics of polymer deterioration is difficult and complex, and the difficulty is compounded by the fact that a single-rate expression of degradation or change developed over the short term may not be valid over the long-term service life of the product or material being studied. The data collected in the laboratory can not be

safely extrapolated based on a simple correlation between the variations of the macroscopic physical properties in the artificial and natural conditions. To convert the data from the laboratory to the environment, the chemical evolution of the polymer must be analyzed. In order to design a test plan that accurately models the time-correlated degradation of polymers, it is necessary to possess an in-depth knowledge of the material composition and structure, end-product use, assembly and sterilization process effects, failure-mode mechanisms, and storage conditions. The testing regimen should be designed to provide data that are appropriate to whatever criteria the polymer must ultimately satisfy.

2.4 References

1 B. O. Bateup, "Surface Chemistry and Adhesion," *International Journal of Adhesion and Adhesives*, **1,** 233-239, 1981.

2 W. C. Wake, "Theories of Adhesion and Uses of Adhesives: A Review," *Polymer*, **19**, 291-308, 1978.

3 A. J. Kinloch, "Review: The Science of Adhesion Part 1. Surface and Interfacial Aspects" *Journal of Materials Science*, **15**, 2141-2166, 1980.

4 D. L. Allara, F. M. Fowkes, J. Noolandi, G. W. Rubloff, M. V. Tirrell, "Bonding and Adhesion of Polymer Interfaces," *Materials Science & Engineering*, **83**, 213-226, 1986.

5 F. M. Fowkes, D. W. Dwight, D. A. Cole, T. C. Huang, "Acid-base Properties of Glass Surfaces," *Journal of Non-Crystalline Solids*, **120**, 47-60, 1990.

6 F. M. Fowkes, "Role of Acid-Base Interfacial Bonding in Adhesion," *Journal of Adhesion Science and Technology*, **1**, 7-27, 1987.

7 J. R. Huntsberger, "The Mechanics of Adhesion", *Treatise on Adhesion and Adhesive,* (Edited by R. L. Patrick), Marcel Decker Inc., New York, **1**, 119-123, 1967**.**

8 W. C. Wake, "Theories of Adhesion and Adhesive Action", *Adhesion and the Formulation of Adhesives,* Applied Science Publisher, New York, **5**, 93-94-3, 1966.

9 A. J. Kinloch, "The Science of Adhesion: Surface and Interfacial aspects", *Journal of Materials Science*, **15**, 2141-2166, 1980.

10 L. H. Sharpe and H. Schonhorn, "Advances in Chemistry Series," *American Chemical Society*, Washington, **43**, 189-192, 1964.

11 D. E. Packham, "The Mechanical Theory of Adhesion - Changing Perceptions", *Journal of Adhesion*, **39**, 137-144, 1992.

12 A. J. Kinloch, "Mechanisms of Adhesion," *Adhesion and Adhesives: Science and Technology*, Chapman and Hall, New York, **3**, 57-66, 1987.

13 S. G. Abbott, "Control of the Bonding Process in a Medium Technology Industry," *International Journal of Adhesion and Adhesives*, **5**, 7-11, 1985.

14 D. E. Packham, K. Bright, B.W. Malpass, **"**Mechanical Factors in the Adhesion of Polyethylene to Aluminum," *Journal of Applied Polymer Science,* **18**, 3237-3247, 1974.

15 J. D. Venables, "Adhesion and Durability of Metal-Polymer Bonds," *Journal of Materials Science,* **19**, 2431-2453, 1984.

16 K. Bright, B. W. Malpass, D. E. Packham, "Adhesion of Polyethylene to Metals", *Nature*, **223**, 136-1361, 1969.

17 J. R. Evans and D. E. Packham, "Adhesion of Polyethylene to Metals: The Role of Surface Topography," *Journal of Adhesion*, **10**, 177-191, 1979.

18 C. W. Jennings, "Surface Roughness and Bond Strength of Adhesives," *Journal of Adhesion*, **4**, 25-38, 1972.

19 S. S. Voyutskii, "Adhesion of High Polymers," *Autohesion and Adhesion of High Polymers*, Interscience, New York, **5,** 140-149, 1963.

20 B. Ellis, "Epoxy Resin Adhesives," *Chemistry and Technology of Epoxy Resins*, Blackie Academic & Professional, London, **7**, 208-209, 1993.

21 J. Klein, "The Self-diffusion of Polymers," *Contemporary Physics*, **20**, 611-629, 1979.

22 S. F. Edwards and J. W. V. Grant, "The Effect of Entanglements on the Viscosity of a Polymer Melt, "*Journal of Physics A-Mathematical & General*, **6**, 1186-1195, 1973.
23 F. Brochard and P. G. De Gennes, "Polymer-Polymer Interdiffusion", *Europhysics Letters*, **1**, 221-224, 1986.
24 S, Wu, H.-K. Chuang, C. D. Han, "Diffuse Interface between Polymers: Structure and Kinetics," *Journal of Polymer Science*, Polymer Physics Edition, **24**, 143-159, 1986.
25 W. Possart, "Experimental and Theoretical Description of the Electrostatic Component of Adhesion at Polymer Metal Contacts," *International Journal of Adhesion and Adhesives*, **8**, 77-83, 1988.
26 R. D. Vold and M. J. Vold, "Theory and Stability of Hydrophobic Dispersions," *Colloid and Interface Chemistry*, Addison-Wesley Publishing Company Incorporated, Massachusetts, **8**, 261- 287, 1983.
27 L. H. Lee, "Chemical Bonding and Intermolecular Forces," *Fundamentals of Adhesion*, Plenum Press, New York, **3**, 6-16, 1991.
28 E. P. Plueddemann, "Adhesion through Silane Coupling Agents," *Fundamentals of Adhesion*, Plenum Press, New York, **2**, 79-151, 1991.
29 P. S. Ho, P. O. Hahn, J. W. Bartha, G. W. Rubloff, F. K. LeGoues, B. D. Silverman, "Chemical Bonding and Reaction at Metal/Polymer Interfaces," *Journal of Vacuum Science & Technology*, **3**, 739-745, 1985.
30 R. Haight, R. C. White, B. D. Silverman, P. S. Ho, "Complex Formation and Growth at the Cr- and Cu-Polyimide Interface," *Journal of Vacuum Science & Technology*, **6**, 2188-2199, 1988.
31 M. D. Thouless, "The role of Fracture Mechanics in Adhesion," *Materials Research Society, Proceedings from MRS Symposia*, **119**, 51-62, 1988.
32 G. R. Irwin, "Analysis of Stresses and Strains Near the End of a Crack Traversing a Plate," *Journal of Applied Mechanics*, **24**, 361-364*,* 1957.
33 A. A. Griffith, "The Phenomenon of Rupture and Flow in solids," *Philosophical Transactions*, **221,** 163-198, 1920.
34 W. L. Williams, "On the Stress Distribution at the Base of a Stationary Crack," *Journal of Applied Mechanics*, **24**, 361-364, 1957.
35 A. H. Hult and F. A. McClintock, "Elastic-plastic Stress and Strain Distribution around Sharp Notches under Repeated Shear," *International de Mecanique Applique*, **2**, 51-58, 1957.
36 A. J. Kinloch, "Fracture Mechanics of Adhesive Joints," *Adhesion and Adhesives: Science and Technology*, Chapman and Hall, New York, **7**, 274-276, 1987.
37 M. L. Williams, "The Stresses Around a Fault or Crack in Dissimilar Media," *Bulletin of the Seismological Society of America*, **49**, 199-204, 1959.
38 F. Erdogan, "Stress Distribution in a Homogeneous Elastic Plane with Cracks," *Journal of Applied Mechanics*, **30**, 232-236, 1963.
39 J. R. Rice and G. C. Sih, "The Bending of Plates of Dissimilar Materials with Cracks," *Journal of Applied Mechanics*, **31**, 477-482, 1965.
40 J. R. Rice and G. C. Sih, "Plane Problems of Cracks in Dissimilar Media," *Journal of Applied Mechanics*, **32**, 418-423, 1965.
41 B. M. Malyshev and R. L. Salganik, "The Strength of Adhesive Points Using the Theory of Fracture," *International Journal of Fracture Mechanics*, **1**, 114-128, 1965.

42 A. H. England, "A Crack between Dissimilar Media," *Journal of Applied Mechanics*, **32**, 400-402, 1965.
43 M. L. Williams, "Review of Continuum Mechanics Factors in Adhesive Fracture," *Adhesive Joints: Formation, Characterstics, and Testing* (Edited by K. L. Mittal), Plenum Press, New York, **6**, 703-738, 1984.
44 R. T. Fenner, A. J. Kinloch, E. Thrusabanjong, and J. Williams, *Unpublished work*, 1986.
45 S. G. Sawyer and R. B. Anderson, "Collocated Interfacial Stress Intensity Factors for Finite Bimaterial Plates," *Engineering Fracture Mechanics*, **4**, 605-616, 1972.
46 A. Piva and E. Viola, "Biaxial Load Effects on a Crack between Dissimilar Media," *Engineering Fracture Mechanics*, **13**, 143-174, 1980.
47 J. Cognard, "The Mechanics of the Wedge Test", *Journal of Adhesion*, **20**, 1-13, 1986.
48 L. H. Sharpe, "The Interphase in Adhesion", *Journal of Adhesion*, **4**, 51-64, 1972.
49 R. E. Cuthrell, "Macrostructure and Environment-Influenced Surface Layer in Epoxy Polymers," *Journal of Applied Polymer Science*, **11**, 949- 952, 1967.
50 C. U. Ko, E. Balcells, T. C. Ward, J. P. Wightman, "Effect of Surface Topography on the Relaxation Behavior of Thin Polysulfone Coatings on Pretreated Aluminum Substrates," *Journal of Adhesion*, **28**, 247-260, 1989.
51 E. Sancaktar, "Recent Approaches in Constitutive Behavior and Testing of Structural Adhesives," *Applied Mechanics Review*, **49**, 128-138, 1996.
52 F. J. Boerio, D. J. Ondrus, R. G. Dillingham, *Adhesion Science Review: Proceedings of the 5th Annual Program/Review Workshop of the Virginia Tech Center for Adhesion Science* (Edited by H. F. Brinson, J. P. Wightman, T. C. Ward), Virginia Tech Center for Adhesion, Blacksburg, Virginia, 1987.
53 R. G. Dillingham, F. J. Boerio, "The Effect of a Multicomponent Silane Primer on the Interphase Structure of Aluminum/Epoxy Adhesive Joints," *Journal of Adhesion*, **24**, 315-320, 1987.
54 D.M. Mattox, "Deposition Processes," *Vacuum Technology and Coating*, **7**, 11-33, 2000.
55 J. D. Venables, "Adhesion and Durability of Metal-Polymer Bonds," *Journal of Materials Science*, **19**, 2431-2453, 1984.
56 A. Mahoon, "Titanium Adherends," *Durability of Structural Adhesives* (edited by A. J. Kinloch), Applied Science, New York, **6**, 259-275, 1983.
57 G. D. Davis, "Surface Treatments of Aluminum and Titanium-From Basic Research to Production Failure Analysis", *Surface and Interface Analysis,* **17**, 439-447, 1991.
58 R. Divan, N. Moldovan, and H. Camon, "Roughning and Smoothing Dynamics During KOH Silicon Etching," *Sensors and Actuators A: Physical*, **74**, 18-23, 1999.
59 J. A. Shields and B. Rangarajan, US Patent 6207582, 2001.
60 C. N. Wu and C. L. Yang, US Patent 6303482, 2001.
61 J. W. Butterbaugh and D. C. Gray, Eur. Patent 688045, 1995.
62 H. Biederman, S. M. Ojha and L. Holland, "The Properties of Fluorocarbon Films Prepared by R. F. Sputtering and Plasma Polymerization in Inert and Active Gas," *Thin Solid Films*, **41**, 329-339, 1977.
63 W. J. Van Ooij, F.J. Boerio, A. Sabata, D.B. Zeik, C.E. Taylor, S.J. Clarson, "Metal Surface Preparation by Plasma-Polymerized Films," *Journal of Testing and Evaluation*, **23***,* 33-40, 1995.

64 C. A. Harper, "Development and Fabrication of IC Chips", *Electronic Assembly Fabrication,* McGraw-Hill, New York, **2**, 96-98, 2002.
65 F. Denes, "Synthesis and Surface Modification by Macromolecular Plasma Chemistry," *Trends in Polymer Science*, **5**, 23-31, 1997.
66 E. P. Plueddemann, "Adhesion through Silane Coupling Agents," *Fundamentals of Adhesion*, Plenum Press, New York, **2**, 79-151, 1991.
67 W. D. Bascom, "Primers and Coupling Agents," *Engineered Materials Handbook: Adhesives and Sealants,* ASM International, **3**, 254-258, 1990.
68 A. B. Christie, "X-ray Photoelectron Spectroscopy," *Methods of Surface Analysis* (Edited by J. M. Walls), Cambridge University Press, New York, **5**, 127-168, 1989.
69 H. M. Tong and L. Nguyen, "XPS/SIMS/AES for Surface and Interface Characterization of Thin Polymer Films", *New Characterization Techniques for Polymer Films,* John Wiley and Sons Incorporated, New York, **11,** 291-300, 1990.
70 R. J. Morgan, E. Shin, C. Dunn, E. Fouch, B. Jurek, A. Jurek, "Durability of Composites for Potential High Speed Civil Transport Applications," *Proceedings of the 39th International SAMPE Symposium*, **39,** 1564-1575, 1994.
71 J. A. Hinkley and J. J. Yue, **"**Oxidative Aging of Thermoplastic Polyimide Films," *Journal of Applied Polymer Science*, **57**, 1539-1543, 1995.
72 R. Kiefer, J. J. Yue, J. A. Hinkley, "Kintetic Mapping of Oxidative Weight Loss in Polyimide Composites," *Journal of Advance Materials*, **26**, 55-59, 1995.
73 L. J. Burcham, R. F. Eduljee, and J. W. Gillespie, Jr., "Investigation of the Microcracking Behavior of Bismaleimide Composites during Thermal Aging," *Polymer Composites*, **16**, 507-517, 1995.
74 A. J. Kovacs, R. A. Stratton, and J. D. Ferry, "Dynamic Mechanical Properties of Polyvinyl Acetate in Shear in the Glass Transition Temperature Range," *Journal of Physical Chemistry*, **67,** 152-161, 1963.
75 J. L. Sullivan, "Creep and Physical Aging of Composites," *Composite Science and Technology*, **39**, 207-232, 1990.
76 R. L. Hastie, and D. H Morris, "The Effect of Physical Aging on the Creep Response of a Thermoplastic Composite," *ASTM STP 1174*, (Edited by C. E. Harris and T. S. Gates), Philadelphia, PA, 163-185, 1993.
77 Jacques Lemaire, "Predicting Polymer Durability," *Chemtech*, **26**, 42-47, 1996.

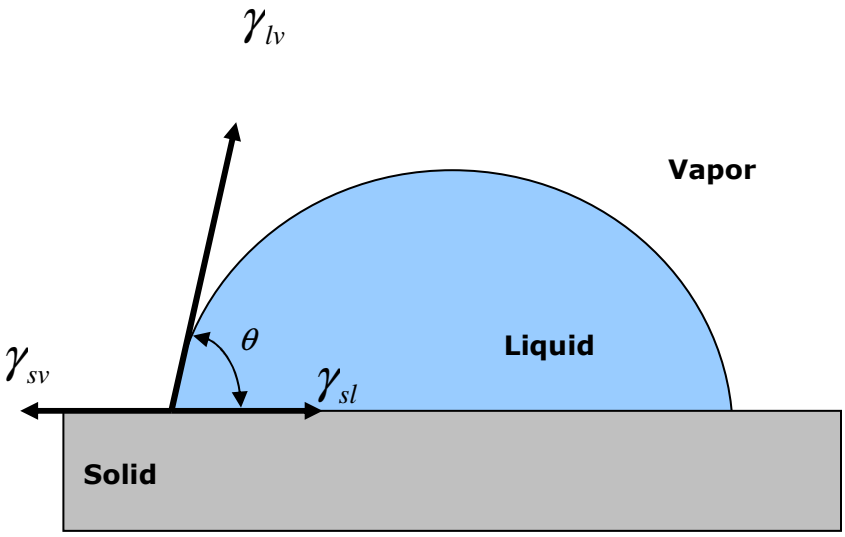

Figure 2.1 Schematic illustration of the surface energies present at the contact point of a liquid droplet on a solid substrate.

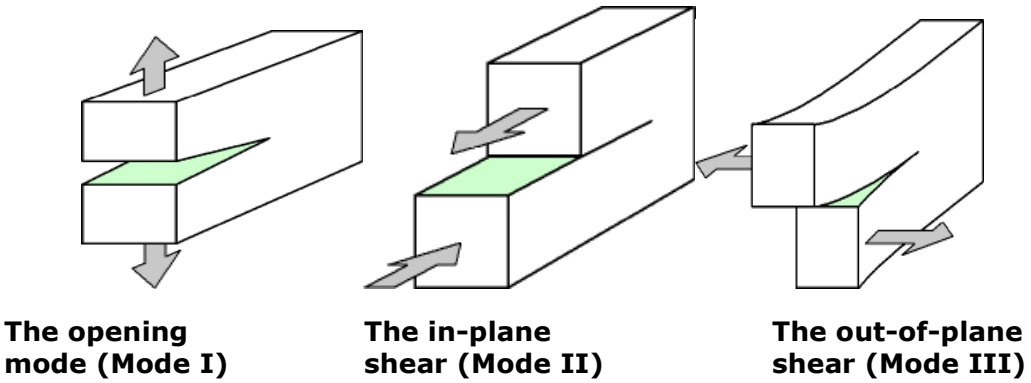

Figure 2.2 Three basic modes of crack tip deformation.

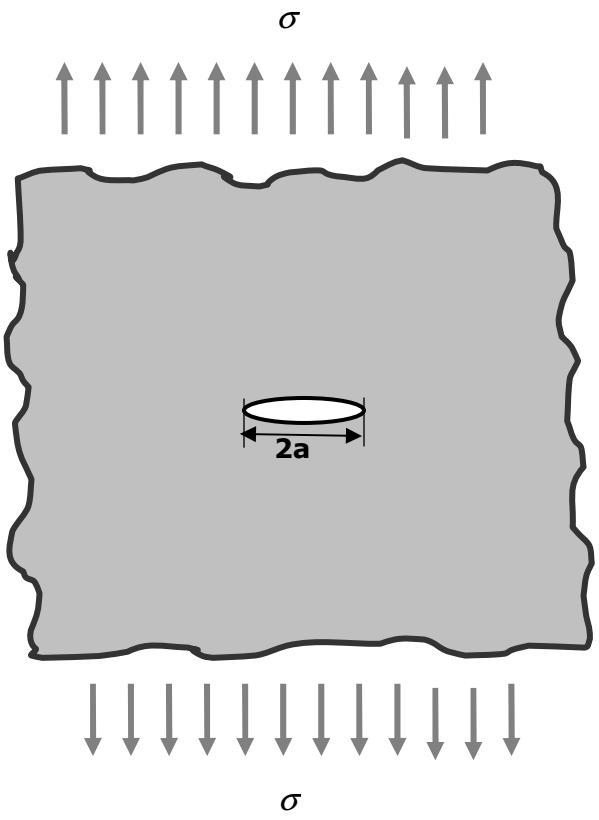

Figure 2.3 Crack in an infinite plate under uniform tension.

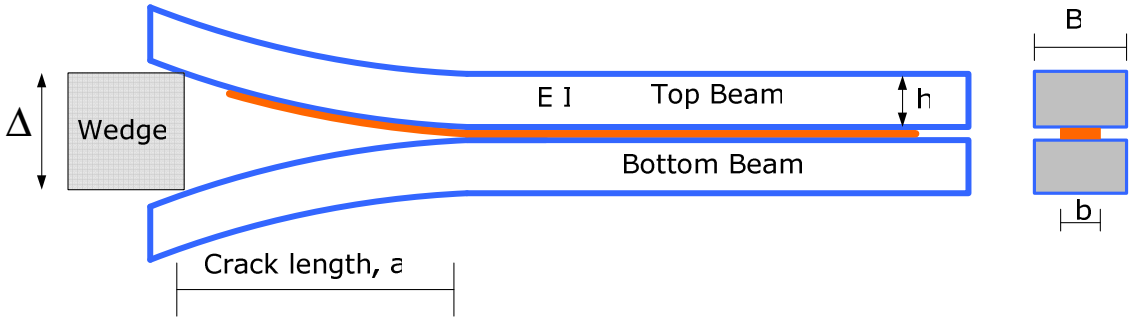

Figure 2.4 Schematic illustration of the wedge test showing different parameters used in the calculation of strain energy release rate, *G*.

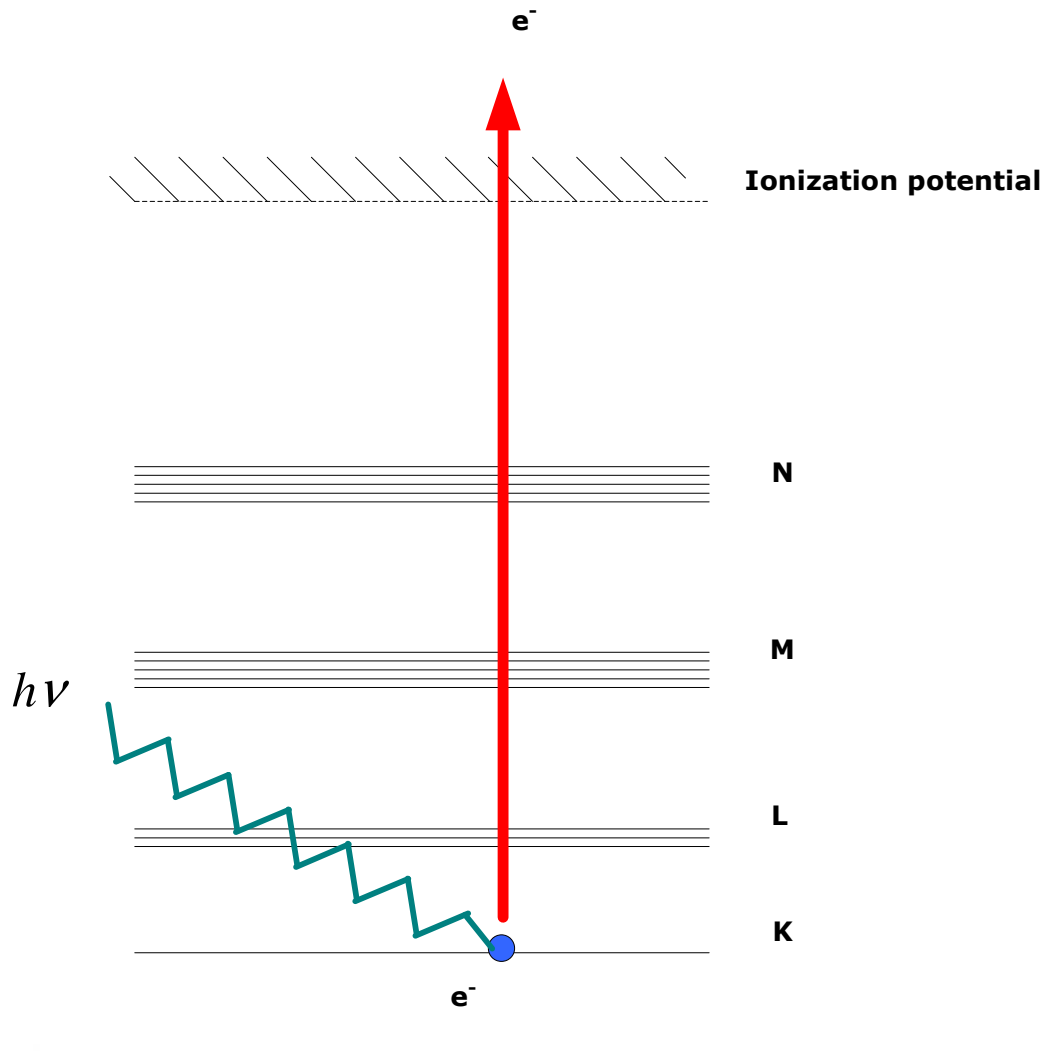

Figure 2.5 Energy-level diagram for XPS.

3 MECHANISMS AND PHYSICAL MODELS OF DIFFUSION IN ADHESIVE SYSTEMS

Diffusion in adhesive systems is an important phenomenon. Diffusion in adhesive systems is passive, if the driving force is purely a brownian molecular motion, but diffusion can also be activated by the effects of external physical forces such as electrical, osmotic, or convective forces. When adhesive joints are exposed to specific environments, a considerable loss in joint strength is typically observed, owing to the diffusion of environmental species into the polymer or changes within the interphase. This chapter reviews the mechanisms of diffusion as regards to theoretical descriptions of Fickian and non-Fickian behavior. Various physical models based on different physical concepts are briefly discussed. Emphasis has been given on the model of Vrentas and Duda [1-8] and model based on Arrhenius theory [9] and model in an attempt to illustrate their applicability over a wide range of temperatures and concentrations to the system under testing. The effect of water or any other aggressive solutions on the adhesive and the interface is also presented.

3.1 Introduction

Water gives some of the greatest problems in the environmental stability of adhesive joints. The presence of small amounts of water in a polymer has previously been shown to affect a variety of properties [10, 11]. Water may plasticize and accelerate creep or relaxation in the adhesive [12], swell the adhesive, and degrade mechanical properties. Water can also lead to unwanted chemical reactions in the adhesive [13], as well as the formation of cracks and crazes [14, 15]. The performance of an adhesive joint depends on the activity of water at the crack tip. Hence, water is considered a critical factor in determining the durability of an adhesively bonded joint. Kinloch [10] showed that the exposure of an aluminum alloy/epoxy polyamide joints adhesive joint to a hot-wet environment results in considerable loss of joint strength. Water is a highly polar molecule that can permeate through most organic adhesives, and migration of water to an interface with a high-energy surface adherend is practically inevitable. Water can enter either by diffusion through the bulk adhesive layer or by wicking along the adhesive-adherend interface, displacing the adhesive from the substrate. Also, in some bonded

systems (e.g. wood or composites), moisture can diffuse through the adherends themselves. The effective lifetime of an adhesive joint is related to the kinetics of diffusion of water molecules, along with the nature and extent of water-induced plasticization in the system.

Diffusion is the process responsible for the movement of matter from one region to another [16], and is often due to random molecular motion. According to Cussler [17], diffusion can be predicted and modeled by various theories. The fundamental principle of diffusion is based on Fick's laws, which describe the macroscopic transport of matter by a concentration gradient. Fick's first law [18] models for steady state diffusion whereas Fick's second law is used to describe transient phenomena where the concentration profile varies during diffusion. There are two basic types of diffusion behavior [19]:

(1) Fickian diffusion

(2) Non-Fickian diffusion

Alfrey et al. [20] proposed a classification according to the diluent diffusion rate (R_{diff}) and the polymer relaxation rate (R_{relax}) for Fickian and non-Fickian diffusion. The amount of diluent absorbed per unit of area at time t, M_t, is represented by:

$$M_t = kt^n \tag{1}$$

where k is a constant and n is a parameter related to the diffusion mechanism.

3.1.1 Fickian Diffusion

Description of diffusion at the macroscopic level is based on Fick's hypothesis [18], which assumes proportionality between the flux and the concentration gradient of the physical quantity diffused. The diffusion takes place by random jumps (or random walk) of the penetrant molecule in the polymer with little interaction with the polymer matrix. Fickian diffusion is more common in rubbery materials that have flexibility and mobility, larger free volumes, and have relatively fast relaxation times, allowing easier penetration of the diluent [21]. Fickian diffusion is characterized by systems in which diluent diffusion rate, R_{diff}, is significantly slower than the polymer relaxation rate, R_{relax} ($R_{diff} << R_{relax}$). Fickian diffusion is often observed in polymer networks when the temperature is well above the glass transition temperature, T_g, of the polymer. The amount of the diluent absorbed per unit area is proportional to the square root of time in homogeneous and

isotropic systems i.e. the spreading rate of the diffusing quantity and the velocity at which the front progresses are proportional to the square root of time:

$$M_t = kt^{1/2} \quad (2)$$

The exponent 1/2 has a very fundamental background and reflects at the macroscopic scale the random motion of the quantity diffused at the microscopic level, for which the mean square of displacement is proportional to time (t) [22]. Fickian diffusion has been accepted as universal for more than a hundred years and applied to a vast number of phenomena including heat conduction, moisture transport in porous materials and ionic and membrane transport [23-25].

3.1.2 Non-Fickian Diffusion

The diffusion process does not always follow the standard Fickian model and is, in general, referred to as anomalous or non-Fickian diffusion phenomena, which is caused by viscoelastic effects in the polymer–solvent system. Deviation from ideal Fickian diffusion or non-Fickian diffusion is mainly observed in glassy polymers when diluent activity is high [26] and the diluent diffusion rate is faster than the polymer relaxation rate ($R_{diff} >> R_{relax}$). There are two general cases of non-Fickian diffusion: two-stage absorption and Case II diffusion.

Two-stage absorption is typical for polymers that exhibit structural relaxation induced by the adsorption of the penetrant. In this case, the relative mass uptake curve is composed of two stages, an initial fast Fickian absorption, followed by a slow non-Fickian absorption that, on the typical time scale of an experiment, never reaches an asymptote. In some cases, such as in epoxies and other polymers, water will absorb in two stages, but for different reasons than mentioned previously: the first stage where water molecules attach to the polymer chain via hydrogen bonding, referred to as "bound" molecules, disrupt the interchain hydrogen bonding, inducing swelling, and plasticize the polymer, followed by a second stage association where the water molecules that are free to move through the holes, or free volume, are often referred to as "unbound" molecules. Because this unbound moisture is filling free volume, it does not cause dimensional changes of the polymer.

Case II is another form of non-Fickian diffusion characterized by a step-like concentration profile with a sharp diffusion front. The diluent penetration front advances

at a constant rate, thus the amount of the diluent absorbed per unit area is directly proportional to time:

$$M_t = kt \tag{3}$$

In this model, the diffusion occurs faster in the swollen material and the relative mass uptake appears linear with time whereas for Fickian diffusion, the relative mass uptake appears linear with the square-root of time.

However, a dramatic change in the relative mass uptake is indicative of damage to the adhesive. A large mass loss upon sorption may often be attributable to leaching of specific components or low molecular weight species from the adhesive. A large mass gain in composites or adhesive coatings can be indicative of fluid accumulation at the interface of the matrix and filler or between the adhesive and substrate.

3.2 Kinetics and Physical Models of Diffusion in Polymers

3.2.1 Kinetics of Water Absorption and Distribution

According to Crank [16], the amount of substance diffusing in the z-direction across a plane of unit area in unit time is known as flux, and is related to the concentration gradient $\frac{\partial C}{\partial z}$ by Fick's first law,

$$J = F_z = -AD\frac{\partial C}{\partial z} \tag{4}$$

where J is the flux, j is the flux per unit area, A is the area across which the diffusion occurs, D is the diffusion coefficient or diffusivity, C is the concentration, and $\frac{\partial C}{\partial z}$, the gradient of the concentration along the z axis. This is usually applied to steady-state diffusion, where concentrations at points within the system are not varying with time, which is not the case when uptake is occurring. The build up or decay of a diffusing species in a small volume-element is given by Fick's second law, which states that the rate of change of concentration in a volume element of a membrane is proportional to the rate of change of concentration gradient at that point in the field. The derivation considers that the change of concentration with time in the element is controlled by the fluxes crossing six faces, as represented by Figure 3.1. In Cartesian coordinates, Fick's second law in three dimensions is:

$$\frac{\partial C}{\partial t} = D[\frac{\partial^2 C}{\partial x^2} + \frac{\partial^2 C}{\partial y^2} + \frac{\partial^2 C}{\partial z^2}] \quad (5)$$

If diffusion is restricted to the z-direction, such as a case of a thin film absorbing a fluid, where diffusion into the edges of the film can be ignored, the second law can be simplified to:

$$\frac{\partial C}{\partial t} = D\frac{\partial^2 C}{\partial z^2} \quad (6)$$

where C is the concentration (kg m^{-3}) of penetrant or absorbed fluid, t is the time (seconds), z is position (m), and D is the diffusion coefficient or diffusivity (m^2 sec^{-1}) of the penetrant in polymer. The most common method for characterizing adsorption processes and calculating the diffusion coefficient is by a mass-uptake experiment. For a free polymer film of thickness 2*L* with a uniform initial concentration (C_0) and the surface is kept at a uniform concentration (C_S), the solution to Fick's Law in terms of concentration is [16]:

$$C^* = \frac{C(x,t) - C_0}{C_S - C_0} = 1 - \frac{4}{\pi}\sum_{n=0}^{\infty}\frac{(-1)^n}{2n+1}\exp\left[-\frac{D(2n+1)^2\pi^2 t}{4L^2}\right]\cos\left(\frac{(2n+1)\pi x}{2L}\right) \quad (7)$$

where *C(x, t)* is the concentration of penetrant in the polymer at any time *t* and distance *x*. Figure 3.2 shows the normalized concentration profile for diffusion of 0.1 M NaOH in the commercial adhesive (supplied by Hewlett Packard Company) at 60°C for the sandwich specimen (no shim, *L* = 2.5 mm) plotted against the normalized thickness of an epoxy layer of thickness 2L, calculated using Equation 7 based on the diffusivity, *D*, of distilled water [27]. The solution to Fick's Law can be put in terms of the average mass of the substance diffusing in the polymer by integrating Equation 7 across the thickness 2*L* of the free polymer film [28]. The expression for the concentration as a function time and distance for diffusion in a bilayer film, as shown in Equation 7, can also be found in the work of McKnight and Gillespie [29]. Based on Fick's law, Shen and Springer [28] derived an appropriate expression, for the calculation of the fractional water uptake as follows:

$$\frac{M_t}{M_\infty} = 1 - \frac{8}{\pi^2}\sum_{n=0}^{\infty}\frac{1}{(2n+1)^2}\exp\left[-\frac{D(2n+1)^2\pi^2 t}{4L^2}\right] \quad (8)$$

where M_t is the mass of absorbed fluid at any time t, and M_∞ is the equilibrium or final mass of absorbed fluid. The relative mass uptake is the scaled average water concentration; a fraction ranging from zero at $t = 0$, to one at $t = \infty$.

Fick's law may not satisfactorily describe water diffusion in polymeric materials as other factors may be involved, e.g. temperature, stress state in the polymer, and concentration of penetrant.

3.2.2 Physical Models for Diffusion in Polymers

Diffusion in polymers has been studied by various techniques such as gravimetric [30], membrane permeation [31], fluorescence [32], and dynamic light scattering [33]. The availability of these techniques and various others like NMR help in understanding polymer morphology and structure [34] as well as transport phenomena [35], and data on diffusion have become more available. The theoretical models, based on different physical concepts such as obstruction effects, free volume effects, and hydrodynamic interactions, have been reviewed [36] and their applicability to polymers is discussed here briefly.

- Diffusion models based on obstruction effect

This theory regards polymer chains as motionless relative to the diffusing molecules. This approximation is based on the assumption that the self-diffusion coefficient of the polymer is negligible as compared to the diffusant. Various models based on this theory are the Maxwell-Fricke [37-40], Mackie and Meares [41, 42], Ogston et al [43], and hard sphere theory [44] models.

- Diffusion models based on hydrodynamic theory

This theory takes into account the hydrodynamic interactions present in the system. These interactions include frictional interactions between the solute and the polymer, the solute and the diluent, and between diluent and the polymer. This consideration allows the description of diffusion in more concentrated regimes, when the polymer chains start to overlap. Various models based on this theory are Cuckier [45], Altenberger et al [46], Phillies [47-49], and Gao and Fagerness [50] models.

- Diffusion models based on free volume theory

The free volume concept in polymer science is well known and has found uses in discussing physical properties such as viscosity, diffusion in liquids, viscoelasticity, electrical conductivity, the glass transition, and plastic yielding. Free volume is the fraction of the volume not occupied by the polymer. The free volume diffusion theory implies that the void fraction is the dominant factor, as diffusivity is proportional to both the kinetic velocity and the probability of finding enough free volume for the hopping of a penetrant molecule from site to site. The rearrangement of free volume creates holes through which diffusing molecules can pass. Various models like Fujita's [51], Yasuda et al [52], Peppas and Reinhart [53, 54] and the model of Vrentas and Duda are based on free volume theory. The model of Vrentas and Duda is applicable over a wide range of temperatures and concentrations, and is described briefly here:

3.2.2.1 The Model of Vrentas and Duda

A major contribution to free volume theory was made by Vrentas and Duda [1-8]. The free volume theory of Vrentas and Duda takes into account several physical parameters such as temperature, activation energy, diluent size, and molecular weight of the diffusant. The approach of Vrentas and Duda is based on the following assumptions:

a. The mixing of the polymer and diluent partial specific volumes does not lead to volume change.
b. The polymer thermal expansion coefficient is approximated to the average values over the temperature interval of interest.
c. The total hole free volume of the system is computed by using the free volume parameters $\frac{K_{11}}{\gamma_1}$ and $\frac{K_{21}}{\gamma_2}$, which are determined from pure component data for diluent and polymer.

For the case of a binary system, the model of Vrentas and Duda is expressed by the following equation:

$$D = D_{01} \exp\left[-\frac{E}{RT}\right] \exp\left[-\frac{\omega_1 V_1 + \omega_2 \xi V_2}{\frac{K_{11}\omega_1(K_{21} - T_{g1} + T)}{\gamma_1} + \frac{K_{12}\omega_2(K_{22} - T_{g2} + T)}{\gamma_2}}\right] \qquad (9)$$

where D_{01} is the diluent self-diffusion coefficient in the absence of polymer, E is the activation energy for a diluent jump, ω_i is the weight fraction of the i^{th} component, V_i is

the specific volume needed for one jumping unit of component i, ξ is the ratio of the volume of the diluent jumping unit to that of the polymer jumping unit, γ_i represents the overlap factor for the free volume for pure component i, K_{11} and K_{21} are the free volume parameters, and K_{21} and K_{22} are the polymer free volume parameters which are defined as:

$$K_{11} = V^*_1 T_{g1}[\alpha_1 - (1 - f^G_{H1})\alpha_{c1}] \tag{10}$$

$$K_{21} = [\frac{f^G_{H1}}{\alpha_1 - (1 - f^G_{H1})\alpha_{c1}}] \tag{11}$$

where α_1 is the coefficient of the thermal expansion of the diluent, α_{c1} is the thermal expansion coefficient for the sum of the specific occupied volume and the specific interstitial free volume, V^*_1 is the free volume occupied by the diluent at 0 K, and f^G_{H1} is the average fractional hole free volume.

3.2.2.2 Model Based on Arrhenius Theory

The Arrhenius form is well known and commonly used to describe various rate processes such as chemical reactions and diffusion. The Arrhenius equation relates the temperature dependence of a chemical reaction [9] and is given as:

$$K = A \exp(-\frac{E_a}{RT}) \tag{12}$$

where K is the kinetic rate of chemical reaction, E_a is the activation energy, and A is the pre-exponential factor. This relation can also be written as:

$$\log K = \log A - \frac{E_a}{RT} \tag{13}$$

and can be used to estimate E_a from a plot of K versus 1/T. The activation energy of a diffusant can also be calculated by diffusion experiments at different temperatures using the Arrhenius equation [46, 55, 56].

$$D = A \exp(-\frac{E_a}{RT}) \tag{14}$$

The Arrhenius model is valid only in dilute systems because the diffusion rate is limited by the energy required for the diffusing species to escape its present surroundings and move into an adjacent environment. However, in moderate to high concentration solutions, the diffusion process is limited by the polymer molecular motion [56].

3.3 Effect of Water on the Adhesive and Interface

Many adhesive joints tend to be weakened by exposure to a wet environment. Moisture diffusion in polymers is associated with the availability of molecular-sized holes within the polymer and the polymer-water affinity. In some cases, where both adherend and adhesive are hydrophilic, water may migrate to and accumulate at the interface, causing spontaneous separation of the adhesive from the adherend. According to Comyn [57], two fundamental problems which arise with water are its widespread occurrence and the fact that adhesives are hydrophilic. The polar groups often used to confer good adhesion are inherently hydrophilic. The basic factors that affect the rate of water transport and the corresponding loss of adhesion in coatings are listed by Leidheiser and Funke [58] as:

1. Time of exposure,
2. Effect of the substrate,
3. Effects of type of coating,
4. Effect of temperature, and
5. Effect of contaminants in water.

From the work of Leidheiser and Funke [59] and the literature regarding environmental degradation of adhesives, there are clearly some general trends. However, these trends are far from conclusive given the diversity of adhesive systems (adhesive, substrate, and interface) and exposure conditions (temperature and fluid), and the possible interactions among the parameters.

3.3.1 Effect of Water on the Adhesive

The reduced durability of an adhesive system in the presence of moisture has long been known through studies showing substantially decreased joint strength and reliability. The detrimental effect of moisture may relate to water absorption and a plasticizing effect in the polymer network. In general, water can be viewed as an efficient, homogeneous plasticizer that depresses the glass transition of the polymer and disrupts the interfacial region between the substrate and the organic phase. Water is an unusual fluid, and is more complex in structure and behavior than typical organic plasticizers. Some effects of water on polymers are reversible, like plasticization (results in lowering the T_g and modulus of the adhesive) and swelling, and so are accompanied by a recovery upon

removal of water. Other mechanisms are irreversible and cause permanent changes in the performance of polymers.

Several attempts have been made by Kelley and Beuche [59] and Fox [60] to relate the depression of T_g to free volume theories of the glass transition. Ivanova [61] demonstrated that the introduction of water in the polymer causes swelling, which may introduce swelling stresses in the system. Antoon and Koenig [62] demonstrated that hydrolytic attack of water takes place in the epoxy films and hydrolytic effects are enhanced under tensile stress in alkaline water. Moisture causes structural damage by introducing microcavities or crazes in polymeric materials [63, 64] and the formation of these structural damages can further accelerate the diffusion process [65], causing an adhesive joint to fail. Berger and Henderson [66] demonstrated that the ability of hydroxyl groups on the polymer to hydrogen bond with water plays a major role in the ability of the polymer to absorb water and the rate of absorption.

3.3.2 Effect of Water on the Interface

Water acts aggressively on bonded joints. The detrimental effects of water may include attacking the substrate/adhesive interface, which degrades joint durability. The locus of failure moves from being cohesive within the adhesive to being interfacial. Gledhill, Kinloch and Shaw [67] have shown that there is a critical level of water concentration, C_c, in the adhesive layer in the joint, below which environmental attack is prevented. For an epoxy system, the estimated value of critical water concentration is about 1.35-1.45%, and the critical humidity is around 50-65% [68-71]. The rate of attaining this concentration appears to be governed by the rate of water diffusion through the adhesive and this is accelerated by temperature and, possibly, by stress [72]. The loss of adhesion and swelling in the epoxy at this critical concentration may be attributed to one of the following mechanisms.

1. The rupture of interfacial bonds: This may involve the rupture of secondary bonds due to displacement of adhesive from the metal oxide by water ingression or a more complex reaction sequence, e.g. the hydrolysis of interfacial covalent bonds. The chemical reactions between absorbed water molecules and the OH groups of the polymer may cause breaking of inter-chain hydrogen bonds resulting in the displacement of adsorbed OH groups from the surface of the substrate.

2. Subtle changes occurring in the oxide structure e.g. hydration, which causes a mechanical weakening of the oxide layer. The rate of loss of strength is faster if tensile or shear stresses are present [67].

Gledhill and Kinloch [71] suggested that for adhesive joints, where only secondary forces are the mechanism of adhesion, the intrinsic stability of the adhesive/substrate interface in the presence of an absorbed liquid may be evaluated from a consideration of the thermodynamic work of adhesion. Usually, the work of adhesion for a dry adhesive/substrate has a positive value, indicating thermodynamic stability of the interface. However, the introduction of water may induce a negative value of the work of adhesion, which indicates that the interface is unstable and the adhesive may be easily displaced from the substrate by water. Water can also chemically degrade the interface by interacting with the adhesive and the substrate or probably chemical bonds across the interface. Studies have suggested that a boundary layer of adhesive exists adjacent to the substrate surface and this boundary possesses a different physical and chemical structure such as lower crosslink density [73] or a lower concentration of filler particles [74]. Brockmann *et al* [75] proposed that the hydrolysis of boundary layer of the adhesive might be an important mechanism of environmental attack, though other researchers [76-78] suggest that water attack on the metal oxide layer is a more likely failure mechanism of adhesive joints. In some circumstances, substrate corrosion may occur in adhesive joints and act as a factor that weakens the performance of the adhesive joint.

3.4 Conclusion

Diffusion in polymer systems is a complicated process which depends on the properties of the diffusant, the polymer network, and the diluents. Various models have been put forward to understand the diffusion process under different circumstances, but estimating and predicting the diffusion remains a difficult task. Different adhesive joints may fail in different ways but the resistance of the adhesive joints to moisture attack is related to the adhesive properties as well as to the substrate metallization. However, when considering both cohesive and interfacial degradation, it is found that interfacial failure is often the dominant failure which can be attributed to the concept of surface free energy and interfacial free energy. A review of the available literature on interfacial diffusion reveals that, in general, the rate of interfacial diffusion, or the presence of fluid at the interface becomes more critical to the lifetime of the adhesive joint. It is possible for

water to be present in the bulk and at the interface yet the integrity of the adhesive bond can be preserved if the interface is strong. The role of interfacial diffusion becomes less important and the rate limiting step for failure becomes the chemical reaction at the interface for strong interfaces. The detrimental effects of diffusion in DI water and other aggressive mixtures used in this study, and possible weakening of interface for different adhesive systems might be the possible reason behind observed subcritical behavior (as presented in the following chapters) in different environmental conditions.

3.5 References

1. J. S. Vrentas and J. L. Duda, “Diffusion in Polymer-Solvent Systems. I. Reexamination of the Free Volume Theory", *Journal of Polymer Science: Polymer Physics*, **15**, 403-416, 1977.
2. J. S. Vrentas and J. L. Duda, “"Diffusion in Polymer-Solvent Systems. II. A Predictive Theory for the Dependence of Diffusion Coefficients on Temperature, Concentration, and Molecular Weight", *Journal of Polymer Science: Polymer Physics*, **15,** 417-439, 1977.
3. J. S. Vrentas, J. L. Duda, H. C. Ling, “Self Diffusion in Polymer-Solvent-Solvent Systems”, *Journal of Polymer Science: Polymer Physics*, **22**, 459-469, 1985.
4. J. S. Vrentas, J. L. Duda, H. C. Ling,” "Free-Volume Theories for Self-Diffusion in Polymer-Solvent Systems. I. Conceptual Differences in Theories", *Journal of Polymer Science: Polymer Physics*, **23**, 275-288, 1985.
5. J. S. Vrentas, J. L. Duda, H. C. Ling, A. C. Hou,” "Free-Volume Theories for Self-Diffusion in Polymer-Solvent Systems. II. Predictive Capabilities", *Journal of Polymer Science: Polymer Physics*, **23**, 289-304, 1985.
6. J. S. Vrentas, C. M. Vrentas**, “**Solvent Self-Diffusion in Crosslinked Polymers”, *Journal of Applied Polymer Science*, **42,** 1931-1937, 1991.
7. J. S. Vrentas, C. M. Vrentas, **“**A New Equation Relating Self-Diffusion and Mutual Diffusion Coefficients in Polymer-Solvent Systems”, *Macromolecules*, **26,** 6129-6131, 1993.
8. J. S. Vrentas, C. M. Vrentas, J. L. Duda. "Comparison of Free-Volume Theories", *Journal of Polymer Research*, **25**, 99-101, 1993.
9. C.T. Reinhart and N.A. Peppas: "Solute Diffusion in Swollen Membranes. II. Influence of Crosslinking on Diffusive Properties", *Journal of Membrane Science*, **18**, 227-239, 1984.
10. A. J. Kinloch, “Interfacial Fracture Mechanical Aspects of Adhesion Bonded Joints-Review”, *Journal of Adhesion*, **10**, 193-219, 1979.
11. T. Nguyen, W. E. Byrd, D. P. Bentz, “Quantifying Water at the Organic Film/Hydroxylated Substrate Interface”, *Journal of Adhesion*, **48**, 169-194, 1995.
12. V. J. McBreirty, C. M. Keely, F. M. H. Coyle, H. Xu and J.K. Vij, “Hydration and Plasticization Effects in Cellulose Acetate: Molecular Motion and Relaxation”, *Faraday discussions*, **103**, 255-268, 1996.
13. M. K. Antoon, J. L. Koenig, "Irreversible Effects of Moisture on the Epoxy Matrix in Glass-Reinforced Composites", *Journal of Polymer Science: Polymer Physics Ed*, **19**, 197-212, 1981.
14. Y. Diamant, G. Marom, L. J. Broutman, “The Effect of Network Structure on Moisture Absorption of Epoxy Resins”, *Journal of Applied Polymer Science*, **26**, 3015-3025, 1981.
15. C. D. Shirrell and J. L. Halpin, “Moisture Absorption and Desorption in Epoxy Composite Laminates”, *ASTM Special Technical Publication*, **617**, 514-528, 1977.
16. J. J. Crank, “The Diffusion Equations”, *The Mathematics of Diffusion*, Clarendon Press, Oxford, **1**, 1-5, 1956.
17. E. L. Cussler*,* “Diffusion in Concentrated Solutions,” *Diffusion: Mass Transfer in Fluid Systems*, 2nd ed., Cambridge University Press, Cambridge, **3**, 50-78, 1997.
18. A. Fick, “Ueber Diffusion”, *Annals of Physical Chemistry*, **94**, 59-86, 1855.
19. H. L. Frisch. “Sorption and Transport in Glassy Polymers—a Review”, *Polymer Engineering and Science*, **20,** 2-13, 1980.

20. T. Alfrey Jr., E. F. Gurnee, W. G. Lloyd," Diffusion in Glassy Polymers", *Journal of Polymer Science,* **12**, 249-261, 1966.
21. R. A. Grinsted, L. Clark, J. L. Koenig, **"**Study of Cyclic Sorption-Desorption into Poly (methyl methacrylate) Rods Using NMR Imaging", *Macromolecules*, **25**, 1235-1241, 1992.
22. A. Einstein, *Annals of Physics*, **17,** 549-560, 1905.
23. H. S. Carslaw and J. C. Jaeger, "Change of State," *Conduction of Heat in Solids*, Clarendon Press Oxford, **2**, 282-296, 1959.
24. J. Philip, "Theory Of Infiltration," *Advances in Hydroscience and Engineering*, **5,** 215-96, 1969.
25. J. Darnell , H. Lodish & D. Baltimore, "Principles of Cellular Organization and Function," *Molecular Cell Biology*, Scientific American Books Incorporated, New York, **1**,132-134, 1986.
26. L. A. Wiesenberger, J. L. Koenig, **"**NMR Imaging of Diffusion Processes in Polymers: Measurement of the Spatial Dependence of Solvent Mobility in Partially Swollen PMMA Rods", *Macromolecules*, **23**, 2445-2453, 1990.
27. Emmett P. O'Brien, "Durability of Adhesive Joints Subjected To Environmental Stress," *Ph.D. Dissertation*, Virginia Tech, Chapter 2, 2003.
28. C. H. Shen and G. S. Springer, "Moisture Absorption and Desorption of Composite Materials", *Journal of Composite Materials*, **10**, 2-20, 1976.
29. S. H. McKnight, J. W. Gillespie, Jr., "In-Situ Examination of Water Diffusion to the Polypropylene-Silane Interface Using FTIR-ATR**",** *Journal of Applied Polymer Science*, **64**, 1971-1985, 1997.
30. D. S. G. Hu and K. J. N. Chou, "Kinetics of Water Swelling and Development of Porous Structure in Ionic Poly (acrylonitrile-acrylamide-acrylic acid) Hydrogels", *Polymer*, **37**, 1019-1025, 1996.
31. B. A. H. Smith, M. V. Sefton, "Permeability of a Heparin Polyvinyl-Alcohol Hydrogel to Thrombin and Antithrombin-III", *Journal of Biomedical Materials Research*, **22**, 673-685, 1988.
32. M. B. Wisnudel, J. M. Torkelson, "Small-Molecule Probe Diffusion in Polymer Solutions: Studies by Taylor Dispersion and Phosphorescence Quenching", *Macromolecules*, **29**, 6193-6207, 1996.
33. A. C. Van Asten, W. T. Kok, R. Tilssen, H. Poppe, "Characterization of Thermal Diffusion of Polystyrene in Binary Mixtures of THF/Dioxane and THF/Cyclohexane", *Journal of Polymer Science: Polymer Physics Ed.* **34,** 283-295, 1996.
34. R.W. Korsmeyer and N.A. Peppas: "Effect of the Morphology of Hydrophilic Polymeric Matrices on the Diffusion and Release of Water Soluble Drugs", *Journal of Membrane Science*, **9**, 211-227, 1981.
35. D. Hariharan and N.A. Peppas, "Modelling of Water Transport and Solute Release in Physiologically Sensitive Gels", *Journal of Controlled Release*, **23**, 123-136, 1993.
36. L. Masaro and X. X. Zhu, "Physical Models of Diffusion for Polymer Solutions, Gels and Solids", *Progress in Polymer Science,* **24**, 731-775, 1999.
37. R. Allen Waggoner, Frank D. Blum, J. M. D. MacElroy, **"**Dependence of the Solvent Diffusion Coefficient on Concentration in Polymer Solutions", *Macromolecules*, **26**, 6841-6848, 1993.

38. P. C. Griffiths, P. Stilbs, B. Z. Chowdhry, M. J. Snowden, "NMR Studies of Solvent Diffusion in Poly (N- Isopropylacrylamide) Colloidal Microgels", *Colloid and Polymer Science*, **273**, 405-411, 1995.
39. E. Cheever, F. D. Blum, K. R. Foster, R. A. Mackay, "Self-Diffusion of Water in Ionic and Non-Ionic Microemulsions", *Journal of Colloid and Interface Science*, **104**, 121-129, 1985.
40. S. Pickup and F. D. Blum, "Self-Diffusion of Toluene in Polystyrene Solutions", *Macromolecules*, **22**, 3961-3968, 1989.
41. J. S. Mackie and P. Meares, "The Diffusion of Electrolytes in a Cation-Exchange Resin membrane", *Proceedings of the Royal Society of London*: *Series A*, **232,** 498-509, 1955.
42. J. H. Wang, **"**Theory of the Self-diffusion of Water in Protein Solutions: A New Method for Studying the Hydration and Shape of Protein Molecules", *Journal of the American Chemical Society***, 76**, 4755-4763, 1954.
43. A. G. Ogston, B. N. Preston, J. D. Wells, "On the Transport of Compact Particles through Solutions of Chain-Polymers", *Proceedings of the Royal Society of London*: *Series A*, **333**, 297-316, 1973.
44. L. Johansson, C. Elvingson, J. E. Lofroth, "Diffusion and Interaction in Gels and Solutions", *Macromolecules*, **24,** 6024-6029, 1991.
45. R. I. Cuckier, "Diffusion of Brownian Spheres in Semidilute Polymer Solutions", *Macromolecules*, **17**, 252-255, 1984.
46. A. R. Altenberger, M. Tirrell, J. S. Dahler, "Hydrodynamic Screening and Particle Dynamics in Porous Media Semidilute Polymer Solutions and Polymer Gels," *Journal of Chemical Physics*, **84,** 5122-5130, 1986.
47. G. D. J. Phillies, "Universal Scaling Equation for Self-Diffusion by Macromolecules in Solution," *Macromolecules,* **19,** 2367-2376, 1986.
48. G. D. J. Phillies, "Dynamics of Polymers in Concentrated Solution: The Universal Scaling Equation Derived," *Macromolecules*, **20**, 558-564, 1987.
49. G. D. J. Phillies, "The Hydrodynamic Scaling Model for Polymer Self-Diffusion," *Journal of Physical Chemistry*, **93**, 5029-5039, 1989.
50. P. Gao, P. E. Fagerness, "Diffusion in HPMC Gels. I. Determination of Drug and Water Diffusivity by Pulsed-Field-Gradient Spin-Echo NMR," *Pharmaceutical Research***, 12,** 955-964, 1995.
51. H. Fujita, "Diffusion In Polymer Diluent Systems", *Advances in Polymer Science*, **3,** 1-47, 1961.
52. H. Yasuda, C. E. Lamaze, L. D. Ikenberry, "Permeability of Solutes through Hydrated Poloymer Membranes: Diffusion of Sodium Chloride," *Macromolecular Chemistry*, **118**, 19-35, 1968.
53. N. A. Peppas and S. R. Lustig, "Solute Diffusion in Hydrophillic Network Structures", *Hydrogels in Medicine and Pharmacy*, Boca Raton: CRC Press, **1,** 57-83**,** 1987.
54. N.A. Peppas, and C.T. Reinhart: "Solute Diffusion in Swollen Membranes. I. A New Theory," *Journal of Membrane Science*, **15**, 275-287, 1983.
55. B. Nystrom, M. E. Moseley, W. Brown, J. Roots, "Molecular Motion of Small Molecules in Cellulose Gels Studied by NMR**",** *Journal of Applied Polymer Science,* **26**, 3385-3393, 1981.

56. A. R. Waggoner, F. D. Blum, J. M. D. McElroy, "Dependence of the Solvent Diffusion Coefficient on Concentration in Polymer Solutions", *Macromolecules,* **26**, 6841-6848, 1993.
57. J. Comyn, "Kinetics and Mechanism of Environmental Attack", *Durability of Structural Adhesives,* (Edited by A. J. Kinloch), Applied Science Publishers, London and New York, **3**, 85-131, 1985.
58. H. Leidheiser, W. Funke, "Water Disbondment and Wet Adhesion of Organic Coatings on Metals - A Review and Interpretation", *Journal of the Oil Colour Chemists Association,* **70**, 121-132, 1987.
59. F. N. Kelley and F. J. Beuche, "Viscosity and Glass Temperature Relations for Polymer-Diluent Systems", *Journal of Polymer Science,* **50**, 549-556, 1961.
60. T. G. Fox, *Bulletin of the American Physical Society,* **1**, 123, 1956.
61. K. I. Inanova, R. A, Patrick, S. Affrosman, "Investigation of Hydrothermal Ageing of a Filled Rubber Toughened Epoxy Resin Using Dynamic Mechanical Thermal Analysis and Dielectric Spectroscopy, *Polymer*", **41**, 6787-6796, 2000.
62. M. K. Antoon, J. L. Koenig, "Irreversible Effects of Moisture on the Epoxy Matrix in Glass-Reinforced Composites", *Journal of Polymer Science: Polymer Physics Edition*, **19**, 197-212, 1981.
63. A. Apicella, L. Nicolais, G. Astarita, E. Oriole, "Effect of Thermal History on Water Sorption, Elastic properties and Glass Transition of Epoxy Resins", *Polymer*, **20**, 1143-1148, 1979.
64. Y. Diamant, G. Marom, L. J. Broutman, "The Effect of Network Structure on Moisture Absorption of Epoxy Resins", *Journal of Applied Polymer Science*, **26**, 3015-3025, 1981.
65. D. M. Brewis, J. Comyn, J. L. Tegg, "The uptake of Water Vapor by an Epoxide Adhesive Formed from the Diglycidyl Ether of Bisphenol-A and Di-(1-aminopropyl-3-ethoxy) Ether", *Polymer*, **21**, 134-138, 1980.
66. C.M. Berger, C. L. Henderson, "The Effect of Humidity on Water Sorption in Photoresist Polymer Thin Films", *Polymer*, **44**, 2101-2108, 2003.
67. R. A. Gledhill, A. J. Kinloch, S. J. Shaw, "A Model for Predicting Durability", *Journal of Adhesion,* **11**, 3-15, 1980**.**
68. A. J. Kinloch, "Interfacial Mechanical Fracture Aspects of Adhesive Bonded Joints-A Review", *Journal of Adhesion*, **10**, 193-219, 1979.
69. D. M. Brewis, J. Comyn, A. K. Raval, A. J. Kinloch, The Effect of Humidity on the Durability of Aluminum-Epoxide Joints", *International Journal of Adhesion and Adhesives,* **10**, 247-253, 1990.
70. R. A. Gledhill and A. J. Kinloch, "Environmental Failure of Structural Adhesive Joints", *Journal of Adhesion*, **6**, 315-330, 1974.
71. D. R. Lefebvre, K. M. Takahashi, A. J. Muller and V. R. Raju, "Degradation of Epoxy Coatings in Humid Environments: The Critical Relative Humidity for Adhesion Loss", *Journal of Adhesion Science and Technology*, **5**, 201-227, 1991.
72. D. R. Lefebvre, D. A. Dillard, H. F. Brinson, "A Model for the Diffusion of Moisture in Adhesive Joints.2. Experimental", *Journal of Adhesion*, **27**, 19-40, 1989.
73. J. Comyn, C. C. Horley, D. P. Oxley, R. G. Pritchard, and J. L. Tegg, "The Application of Inelastic Electron Tunneling Spectroscopy to Epoxide Adhesives", *Journal of Adhesion,* **12**, 171-188, 1981.
74. K. W. Allen, H. S. Alsalim, and W. C. Wake, *Faraday Spec. Disc.,* **2**, 38, 1972.

75. W. Brockmann, "Durability of Metal Polymer Binds," *Adhesion Aspects of Polymeric Coatings* (edited by. K. L. Mittal), Plenum Press, New York, **3**, 265-180, 1983.
76. J. D. Venables, "Adhesion and Durability of Metal-Polymer Bonds," *Journal of Materials Science*, **19**, 2431-2453, 1984.
77. G. D. Davis, P. L. Whisnant and J. D. Venables, "Sub-adhesive Hydration of Aluminum Adherends and its Detection by Electrochemical Impedance Spectroscopy," *Journal of Adhesion Science and Technology*, **9**, 433-442, 1995.
78. A. J. Kinloch, M. S. G. Little and J. F. Watts, "The Role of the Interphase in the Environmental Failure of Adhesive Joints," *Acta Materialia,* **48**, 4543-4553, 2000.

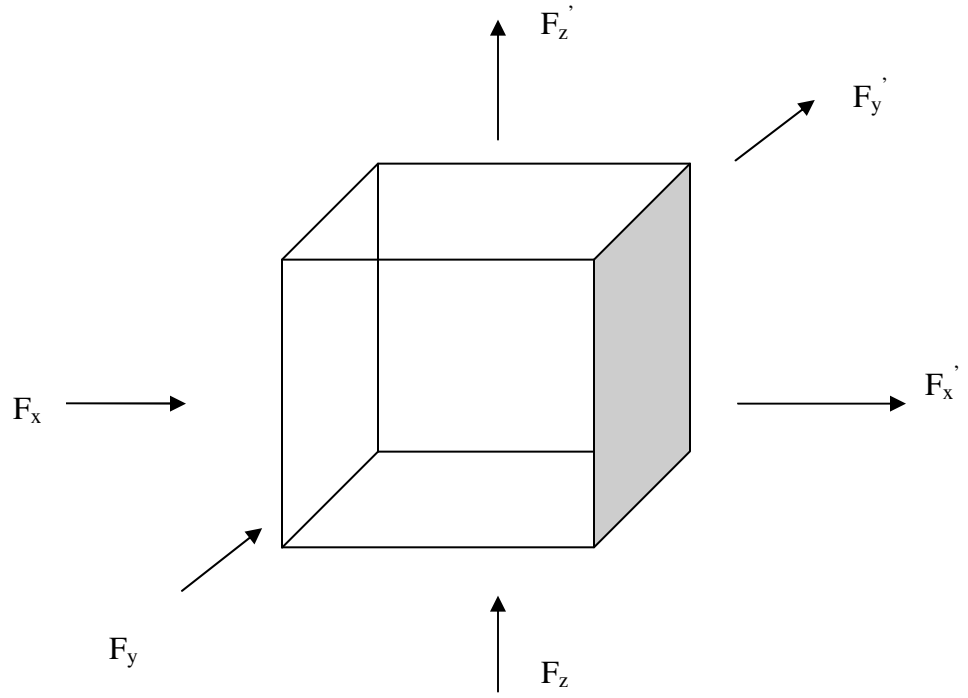

Figure 3.1 Fluxes entering and leaving a cartesian volume element.

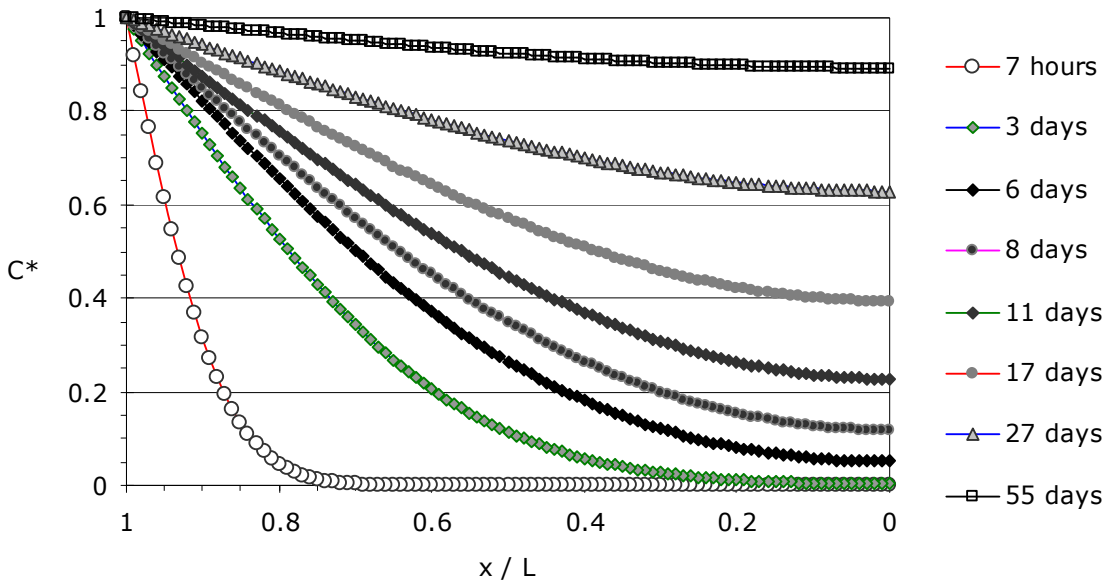

Figure 3.2 Normalized concentration (C^*) as a function of normalized distance from the edge (x/L) calculated using Equation 7 based on the diffusivity, ($D=1.14 \pm 0.11 \times 10^{-8}$ cm^2/sec), of distilled water. $x/L = 1$ is the edge and $x/L = 0$ is the center of the sensor, and L = 2.5 mm. Source: Reference 74.

4 UNDERSTANDING SUBCRITICAL DELAMINATION MECHANISMS IN EPOXY BONDS TO SILICON AND GLASS ADHERENDS

4.1 Abstract

This study investigates the effects of temperature, solution chemistry and environmental preconditioning, in several liquid chemistries, on the durability of silicon/epoxy and glass/epoxy systems. A series of experiments was conducted using wedge test specimens to investigate the adhesion performance of the systems subjected to a range of environmental conditions. Both silicon and glass system's performance was relatively insensitive to temperature over a range of 22-60°C, but strongly accelerated by temperatures above 60°C, depending on the environmental chemistry and nature of the adhesive system used.

Silicon/commercial epoxy specimens were subjected to preconditioning in deionized (DI) water and more aggressive liquid mixtures prior to wedge insertion to study the effect of prior environmental exposure time on the system. The wedge test data from preconditioned specimens were compared with standard wedge test results and the system was found to be insensitive to preconditioning in DI water but shown to have been affected significantly by preconditioning in aggressive environments. Plots describing $\frac{da}{dt}$ - G (crack velocity versus applied strain energy release rate) characteristics for a particular set of environmental conditions are presented and a comparison is made for different environmental conditions to quantify the subcritical debonding behavior of systems studied.

Key Words: Subcritical crack growth, wedge test, preconditioning, debonding rate, threshold, fracture mechanics, silicon/epoxy bonds, durability, and environmental effects.

4.2 Introduction

Fracture mechanics is an effective approach for characterizing material resistance to interfacial failure and for making reliability and durability predictions. Semiconductor packaging industries use fracture energy as the parameter for avoiding crack growth in

designing and predicting durability for microelectronic packages [1]. Fracture mechanics can be used to predict failures of assemblies due to subcritical crack growth, which lead to crack propagation at very low values of strain energy release rate and can be a dominant mechanism particularly when products operate under humid environments. The original theory for subcritical crack growth in glass based on thermally activated kinetics was developed by Hillig and Charles [2, 3]. Water-assisted subcritical crack growth in glass has been measured by Wiederhorn [4-6], Helfinstine [7], Maugis [8], Simmons and Freiman [9], Mecholsky et al. [10], Wiedmann and Holloway [11], and Freiman [12-14]. Similar behavior has also been measured in other brittle inorganic materials by Hartley and Wilshaw [15], Nadeau [16], Tonneau et al. [17], and Evans and Linzer [18]. Akin to stress corrosion cracking in bulk materials like glasses [2, 4, 19, 20] and polymers [21, 22], time dependent subcritical debonding often occurs at much lower mechanical loads than required to cause catastrophic failure.

Interfacial bond integrity is a major concern for performance and reliability of modern electronic devices and therefore, the need to evaluate the fracture resistance and long term durability of various interfaces in the presence of moisture is very important. Kinloch et al. [23], Mostovoy and Ripling [24], and Ripling et al. [25] reported water-assisted subcritical crack growth measurements along polymer/ metal interfaces. Water-assisted subcritical crack growth has also been measured along polymer/glass interfaces by Ritter [26], Conley et al. [27], Lane [28, 29], Hohlfelder [30], Kook [31], Bhatnagar [32], and Dauskardt et al. [33]. Although subcritical debond mechanisms at interfaces are not clearly understood, there seems to be a possible interaction between strained atomic bonds and environmental species [2, 4, 34, 35]. Subcritical debonding may be driven by residual stresses, thermo-mechanical cycling, and the presence of moisture. Residual stresses arise due to thermal expansion mismatch and polymer curing strains. The thermal cycles during device operation may produce significant thermo-mechanical cycling. Moisture may be present in the materials themselves during manufacturing or processing operations. Moisture ingression into the adhesive or along the interface lowers the energy required for debond extension and may be dependent upon the level and nature of stress concentrations in the adhesive layer [36]. Holubka and Chun [37], Kinloch [38], Ooij [39], Landrock [40], Plueddemann [41], Gledhill et al. [42], Bascom [43], and Goodman and Rhys [44] have identified hydrolysis as the primary cause for weakening of

polymer/metal interfaces. There is very little understanding of the actual debond mechanisms at crack tips because of the complex nature of delamination. However, the kinetics of debond growth depends on the activity of the environmental species at the crack tip, which in turn depends on the operating temperature. The basic principles illustrated by Hutchinson & Suo [45] can be used to model the interfacial fracture mechanics where a crack propagates along the interface between two materials.

A schematic illustration of the resulting crack growth rate versus crack driving energy ($\frac{da}{dt}$- G), taken from Gurumurthy et al. [46], is shown in Figure 4.1. The relationship between $\frac{da}{dt}$ and G typically results in a sigmoidal shape which incorporates the familiar velocity regions: region I, stress dependent chemically assisted crack propagation; region II, transport controlled debonding; and region III is associated with critical fracture events and for classic fracture of bulk glasses is independent of the environment, where changes in slope indicate changes in the rate limiting step for crack advance [20, 21, 47]. Since the energy release rate provided to the crack tip in our tests is far below the critical value, region III was not included in the measurements. When comparing different environmental conditions and adhesive systems at a constant velocity, the applied crack driving energy decreases as the aggressiveness of the environment or chemical activity increases. The $\frac{da}{dt}$-G curve can adopt several different shapes that are characteristic of the mechanism of interfacial degradation.

Curley et al [48] made theoretical predictions of the fatigue lifetime of adhesive joints based on mechanical fatigue data by modeling the ($\frac{da}{dN}$) versus G curve and then calculating the number of cycles until failure based on an initial flaw size and the applied stress in the joint. The approaches developed in fatigue ($\frac{da}{dN}$) can be extended to $\frac{da}{dt}$ versus G experiments. The plots of $\frac{da}{dt}$- G revealed important information about the system, including:

1. Effect of preconditioning in deionized (DI) water and other aggressive solutions,
2. Effect of test temperature on the system,

3. $G_{threshold}$ as a function of preconditioning time, preconditioning temperature and test temperature, and
4. Debonding velocity in the plateau region.

The primary objective of this study was to characterize and model subcritical debonding of silicon/epoxy and glass/epoxy interfaces utilizing a wedge test geometry in conditions mimicking service conditions of the microelectronic devices for which they are intended. The wedge test is a commonly utilized method to test the durability of fractured and stressed adhesive joints when exposed to chemical environments of acidic and basic nature. By driving a wedge between the ends of two bonded beam adherends, an initial crack is introduced. When such a specimen is placed in an environment, the crack tip is exposed directly to the test environment while under opening stress. By following the propagation of the debond with time, the debond kinetics can be established. The main disadvantage of wedge test is that it requires sophisticated experimental set-up to measure the crack length (video camera, acoustic methods, or electrical). Also, the time for fluid saturation of the adhesive may be long because the adhesive is sandwiched between two impermeable substrates and only edge diffusion into the adhesive may occur. A test matrix consisting of test temperatures, preconditioning temperatures, preconditioning times, surface chemistry, and nature of adherends and adhesives, was developed to characterize subcritical debonding, study the debond mechanisms using empirical relationships for subcritical delamination observed in monolithic materials, evaluate the performance, and make durability and reliability predictions for the system.

4.3 Experimental Procedure

4.3.1 Sample Preparation

Borosilicate glass (100 mm×10 mm×2 mm) and silicon (77 mm×6 mm×0.98 mm) substrates were bonded using either a commercial (supplied by Hewlett Packard) or a model epoxy to make wedge test specimens. The borosilicate glass strips of required dimensions were supplied by the vendor and the silicon wafers were cut to dimensions and provided by Hewlett Packard. The model epoxy adhesive consists of bis-phenol-F diglycidyl ether (Epon 862), 10 phr (10 parts per hundred resin) 1, 4-butanediol, and 3 phr 4-methyl-2-phenylimidazole as curing agent. The Epon 862 resin has an epoxide equivalent weight of 171 g/mole. Figure 4.2 shows the chemical structure of the

components of model epoxy [49]. To prepare the epoxy, a relatively low viscosity clear liquid was obtained by stirring Epon 862 and 1, 4-butanediol together at about 80°C for several minutes. Subsequently, 4-methyl-2-phenylimidazole catalyst was dissolved in this mixture with stirring for about 15 minutes to obtain a homogenous mixture. This homogeneous epoxy mixture was used for casting the epoxy films. The bulk epoxy mixture or the epoxy mixture cast on silicon or glass substrates was cured at 150°C for 30 minutes. A Differential Scanning Calorimetry (DSC) study showed that a fully cured model epoxy polymer had a glass transition temperature of 110°C [49].

The substrates were first cleaned with an argon plasma treatment and then treated in a 0.1M of 3-aminopropyltriethoxysilane (3-APS) solution (with 5% v/v 0.1M HCl aqueous solution) for 30 minutes. Nonsilicone PTFE (polytetrafluoroethylene) release agent (McMaster-Carr Supply Company, Los Angeles, CA) was then carefully sprayed on the silicon and glass substrates 25 mm (the rest of the silicon or glass beam was covered by a plastic sheet during spraying) from the end of edge on one side of the silicon or glass beam where wedge is to be inserted and initial debond would be made. Where the mold release is sprayed on a specific surface, the epoxy adhered loosely to the substrate and provides a site for initial debonds to initiate at the surface as desired. Any migration or diffusion of the Teflon® release spray from the pre-crack to the bonded interface is unwanted, though possible. In order to confirm any significant migration of release agent from sprayed region to unsprayed region, both the sprayed and unsprayed surfaces were examined by SEM and XPS for borosilicate glass. Scanning electron microscopy (SEM) images of sprayed and unsprayed regions, for borosilicate glass, are shown in Figure 4.3. X-ray photoelectron spectroscopy (XPS) was performed, using a Perkin-Elmer PHI Model 5400 XPS spectrometer equipped with a Mg K_α X-ray source (1253.6 eV), operated at 300 W, on glass and silicon substrates at different locations, as shown in Figure 4.4 and Figure 4.5 respectively. The spot size of the XPS was 1 mm×3 mm. XPS results on borosilicate glass and silicon haven been summarized in Table 1 and Table 2 respectively. SEM and XPS results done on various samples confirmed the presence of fluorine, albeit trace, on surface far from the sprayed region.

Two surface treated silicon or glass strips were then bonded together with the epoxy polymer. The bonded specimens had a bond area of approximately 53 mm x 3 mm and 76 mm x 5 mm for silicon and glass specimens, respectively and a bond line thickness of

0.25 mm. The bond area was outlined on the substrates by using a 0.25 mm thick window-shaped Teflon® gasket with a pre-cut area (53 x 3 mm or 76 mm x 5 mm) placed between the two shim holders on the bottom part of the aluminum fixture (fixture was supplied by Hewlett Packard company). The surface prepared glass or silicon beam was then placed in a aluminum mold fixture, and epoxy was then dispensed on the bottom strip using a Automove 402 ASYM402-90036 Asymtek dispensing system, (ASYMTEK Incorporated, Carlsbad, CA) provided by Hewlett Packard. The microprocessor controlled adhesive dispensing system can be programmed to dispense a controlled amount of epoxy on the substrate. The fixture, when closed, ensured the proper alignment of strips on top of each other with the Teflon® shim and adhesive mixture in the middle. Small binder clips were used to hold the beams sandwiched geometry together, as shown for silicon substrate in Figure 4.6. The Teflon® shim along with restraining force provided by the binder clips (which held the entire bond assembly together) restricts the movement and dimension of the adhesive mixture within the bonded area during curing. The substrate/epoxy sandwiches were cured in a convection oven at 150°C for 30 minutes. The PTFE gasket in each specimen was removed after specimens cooled to room temperature. The sample preparation method is shown in Figure 4.6. The final bond dimensions are shown in Figure 4.7 for silicon and glass.

4.3.2 Environment

To study subcritical debonding behavior under varying environmental conditions, tests were performed inside an environmental chamber capable of controlling temperature. Subcritical debond growth rates were measured in DI water and three proprietary mixtures (supplied by Hewlett Packard) and referred to herein as liquid A, liquid B and liquid C at 60°C, 70°C, and 80°C. The pH levels of the liquids, measured at room temperature, are given as: liquid A = 6.65, Liquid B = 4.0 and liquid C = 9.0. Some samples were preconditioned in DI water and proprietary liquids before test, while others received no preconditioning exposure.

4.3.3 Specimen Preconditioning and Subcritical Adhesion Measurement

Preconditioning refers to soaking the wedge specimens at a desired temperature for a fixed amount of time before a wedge is inserted. The goal of preconditioning was to study the effect of exposure time in deionized water and other liquids on the durability of

the epoxy/silicon adhesive joint and to develop reliability and durability models based on the system behavior. Several proprietary liquids were also used along with DI water to precondition the wedge specimens. The specimens were placed in the liquids at different preconditioning temperatures for different preconditioning period. After the desired aging time was reached, the specimens were taken out of the liquids and dried with a paper towel. The crack was initiated in air at room temperature by first inserting a plastic shim of 0.5mm thickness between the two beams at Teflon® release spray end of the specimen before inserting a stainless steel wedge of 0.78 mm thickness. The plastic shim creates opening between two beams at one end sufficient enough to place the wedge between the beams. Placing a plastic shim prior to inserting metallic wedge ensures no damage to thin beams during wedge insertion which might happen if a metallic wedge were used in the first place. The shim was then slowly removed as soon as the stainless steel wedge was inserted and placed in position between the beams. Wedge specimens were then placed in a custom fixture (as shown in Figure 4.8) capable of holding 5 specimens. For silicon specimens, a ultrasonic scanning system HS1000 HiSPEED scanning acoustic microscope (Sonix Incorporated, Springfield, VA) was used to measure the debond lengths in water at room temperature. A 75 MHz transducer was used to image the debond tip through the opaque silicon. For transparent glass specimens, an optical stereomicroscope with a magnification range from 9X to 40X was used to measure the debond length. The step-by-step procedure is shown in Figure 4.8. Wedge specimens were then kept in desired liquid environment at 60°C, 70°C, and 80°C test temperatures in temperature controlled chambers. Initial crack lengths for the wedge specimen were recorded and subsequent crack length measurements were taken as a function of immersion time in different fluids. Some non-preconditioned samples were also tested in the same liquids. The crack length data were then used to determine the rate of crack propagation ($\frac{da}{dt}$) and the average value of strain energy release rate (G_{av}). A comparison between preconditioned and non-preconditioned samples provided us with valuable insights into the subcritical debonding behavior of the system. Calculations of G, used in this study, were obtained from the work of Cognard [50], and is given as:

$$G = \frac{3}{16}\frac{\Delta^2 E h^3}{a^4} \tag{1}$$

where the different terms are defined in Figure 2.4. The strain energy release rate decreases as a function of $\frac{1}{a^4}$ yielding a wide range of values of G which can rapidly approach a threshold value. The wedge was inserted in the specimens and crack length was then measured under the acoustic microscope (SAM) or optical microscope. Debond growth rates, $\frac{da}{dt}$, and strain energy release rate, G_{av} (both averaged over the increment in time between readings), were determined numerically using:

$$\frac{da}{dt} = \frac{a_{t+\Delta t} - a_t}{\Delta t} \tag{2}$$

$$G_{av} = \frac{G_{a_t} + G_{a_{t+\Delta t}}}{2} \tag{3}$$

where a_t is the crack length at time t and Δt is the time duration between crack length measurement. The wedge test results are presented in terms of growth rate (*da/dt*) as a function of strain energy release rate, G_{av}, in the following sections. See Appendix A for calculation of strain energy release rate values using different schemes to estimate the error introduced in the results.

In the following figures showing wedge test results, thick arrows pointing left or downwards indicate the samples that were debonded completely during testing and thin arrows pointing downwards indicate that either the crack ceased to propagate or growing very slow such that the crack growth is beyond the measurement capability of instruments used for measuring crack growth (SAM or optical microscope).

4.4 Results and Discussion

4.4.1 Effect of Test Temperature

Plots of $\frac{da}{dt}$ versus G_{av} are shown in Figure 4.9 to Figure 4.12 for wedge samples tested at room temperature (RT), 40°C, 60°C, 70°C, 80°C, and 90°C in DI water and proprietary liquid A. Wedge test data obtained from systems where model epoxy was used as the adhesive showed crack growth at 60°C and higher temperature but no apparent transport controlled or stress dependent chemically assisted debonding was observed at RT and 40°C. The crack growth rate is significantly higher at 70°C than at 60°C and samples tested at 70°C debonded completely (indicated by the thick arrow

pointing towards left or downwards) whereas the crack stopped or possibly growing at very low values of crack velocity at 60°C (indicated by the thin arrows pointing downwards). There is no apparent value of $G_{threshold}$ observed at 70°C for silicon/model epoxy and glass/model epoxy systems but data at 60°C for silicon/model epoxy system might suggest an apparent $G_{threshold}$ in the range of 5 J/m^2 to 10 J/m^2, as shown in Figure 4.9.

Similar effects of test temperature were also observed for commercial epoxy systems. For the glass/commercial epoxy system, significant crack propagation was seen at 70°C as compared against 60°C, as shown in Figure 4.11. For the silicon/commercial epoxy system, significant crack growth was observed at 80°C and 90°C and samples tested debonded completely with an apparent strain energy release rate value around 1 J/m^2, but at temperatures below 70°C, sufficient data could not be collected either because the crack stopped or growing very slowly (indicated by arrows pointing downwards) as shown in Figure 4.12. Moreover, the crack propagation rate and $G_{threshold}$ do not differ much between 80°C and 90°C.

As can be interpreted from the effect of temperature on subcritical debonding behavior, the crack velocity and $G_{threshold}$ values are affected significantly by the test temperature, i.e. the higher the test temperature, the higher the crack propagation rate and lower the apparent value of $G_{threshold}$. However, the apparent subcritical behavior holds true for a certain temperature range depending on the system Also, comparing the subcritical delamination behavior of the commercial epoxy systems with the model epoxy bonded systems suggests that the silicon/commercial epoxy and glass/commercial epoxy interface is more durable. This observation helped in interpreting that the subcritical crack propagation is not only governed by the test temperature but also depends on the substrate/epoxy interaction at the interface.

4.4.2 Effect of Preconditioning

Wedge specimens made of surface treated silicon substrate and a commercial epoxy were preconditioned in DI water and proprietary liquids A, B and C at RT, 40°C, 60°C, 70°C, and 80°C preconditioning temperatures for 20, 45, 50, and 70 days. Specimens were taken out of the conditioning liquids after desired preconditioning times and wedges were inserted to introduce sharp initial cracks. The wedged samples were then placed

again in the same liquid environment at a test temperature of either 70°C or 80°C, and crack length was measured periodically using SAM. The data obtained were compared against the standard wedge test results. Several interesting results were obtained, as shown in Figure 4.13 to Figure 4.16.

Figure 4.13 and Figure 4.14 show the data collected in DI water at 80°C and 70°C test temperatures, respectively, where the first term in the legend is the preconditioning time in number of days and the last term indicates the preconditioning temperature. As can be interpreted from the wedge test results, preconditioning in DI water doesn't affect the system behavior significantly. Wedge samples preconditioned in proprietary liquids B and C at 60°C for 30 days were also tested at 70°C and the data obtained were compared against the standard wedge test results. In this case, where more aggressive solutions were used for preconditioning, the system's behavior changed significantly after preconditioning, as suggested by higher debond propagation rate (and possibly lower values of $G_{threshold}$), as shown in Figure 4.15 and Figure 4.16.

The observations discussed above may be explained by the diffusion phenomenon where any liquid tends to penetrate the adhesive and swell the polymer network, resulting in adhesive and interface degradation and a change in the material properties. Adhesive degradation is a result of a slowly progressing chemical reaction in the bulk adhesive and/or interface [51]. It is argued that in a bonded system bond durability depends on how soon a liquid can diffuse through the adhesive layer and cause degradation in the interfacial area. The preconditioning wedge test results discussed above suggests that faster interfacial diffusion and resulting interfacial degradation may be the controlling mechanisms for the higher debond propagation in aggressive solutions.

4.4.3 XPS Characterization and Failure Mechanism

X-ray Photoelectron Spectroscopy (XPS) surface analyses of wedge test specimens immersed in the proprietary solutions were carried out in an effort to determine the failure mode/mechanism and the results presented here are taken from the work of Dingying Xu [52] on wedge samples fractured in different environments. All samples were characterized using a Perkin-Elmer PHI Model 5400 XPS spectrometer equipped with a Mg K_α X-ray source (1253.6 eV), operated at 300 W. The spot size analyzed was a 1 mm x 3 mm area. Photoelectrons were analyzed in a hemispherical analyzer and were

detected using a position-sensitive detector. Wedge samples were retrieved from solutions after crack propagation arrested and DCB strips were separated by mechanical force. To analyze the failure mode, surfaces near the arrested crack front on the failed epoxy side and failed substrate side of the specimens were examined, and compared to the spectral features for the as-prepared epoxy and silicon surfaces prior to bonding, as shown in Figure 4.17. XPS spectral features indicate the presence or absence of particular elements and chemical functionalities on the failed surfaces.

The atomic % results in Table 3 show that the compositions for the as-prepared model epoxy surface and the as-prepared 3-APS treated silicon surfaces. Nitrogen was absent on the as-prepared model epoxy surface even though nitrogen (at low concentration) in the 4-methyl-2-phenylimidazole curing agent was in the epoxy formulation. Nitrogen is likely buried in the bulk epoxy matrix at chain ends. The 3-APS modified silicon surfaces showed a significant amount of nitrogen. For the as-prepared model epoxy surface, silicon was not detected. For the as-prepared 3-APS surface, the Si 2p spectrum (see Figure 4.18) showed the SiO_x (SiO_2 + silane) at ~103.1 eV and Si^o (elemental silicon) at ~98.8 eV. The C 1s spectra for the as-prepared model epoxy surface showed a significant C-O photopeak at ~285.6 eV, which can be attributed to the epoxy functionality.

For specimens that failed at 70^{o}C in proprietary liquid B, the respective failed epoxy and silicon surfaces showed surface compositions that were similar to the respective as-prepared surfaces. The C content on the failed silicon surface was slightly higher than that for the as-prepared silane/silicon surface, which suggests that minor failure occurred in the surface of the epoxy film. A small amount of SiO_2 was detected by XPS on the failed model epoxy surface. This is likely due to a few silane chains that are detached from the silicon surface via hydrolysis of the Si-O-Si bond in the aqueous environment. This observation is consistent with the assumption of a diffusion driven debond, in which interfacial degradation (i.e. disruption of chemical bonds) occurs in the presence of water. These findings support the conclusion that failure occurred primarily at the silane/epoxy interface (Figure 4.19).

The second section of the XPS results considers the question regarding whether there is a change of failure mode/mechanism between 60°C and 70°C for the silicon/3-APS/model epoxy system. The results provided helpful insights in explaining the vast differences in crack velocity and $G_{threshold}$ behavior for experiments conducted at 60°C

and 70°C in the wedge testing. The elemental surface compositions for as-prepared and failed bonded surfaces after wedge test are shown in Table 3 for silicon/3-APS/model epoxy system at 60°C and 70°C in proprietary liquid C. As shown in Figure 4.20, at 60°C, primary interfacial failure was observed at the model epoxy/3-APS interface and minor debonding at the 3-APS/SiO_2-Si interface. This mechanism is very similar to that for the glass/3-APS/model epoxy system under the diffusion drive regime at 60°C as discussed earlier. At 70°C, the major difference is that substantial epoxy functionality was detected on the failed silicon surface; a source can only come from the model epoxy film. This suggests that minor cohesive failure has happened at 70°C in the model epoxy film. The overall failure mechanism at 70°C may be a mix of interfacial failure at the model epoxy/3-APS interface and some cohesive failure in the model epoxy adhesive. This finding could explain in part the differences in debond behavior and durability of wedge testing specimens at different temperatures.

4.5 Summary and Conclusions

Wedge specimens consisting of silicon or glass substrates and commercial or model epoxy were subjected to different environments. Subcritical debonding behavior of these systems has been studied using a wedge test geometry. The crack growth rate, $\frac{da}{dt}$, has been measured as a function of the average value of strain energy release rate, G_{av}. The adhesion degradation of the interface was found to be transport controlled at higher temperatures and for aggressive solution environments. Higher temperatures may result in more severe interaction between strained atomic bonds and liquid molecules causing faster crack propagation.

The wedge test data showed that there may exist threshold values, $G_{\text{threshold}}$, below which no significant crack growth will occur. No apparent value of $G_{\text{threshold}}$ was observed for model epoxy systems at 70°C and 80°C but a threshold value in the range of 8 J/m^2 to 12 J/m^2 did exist at 60°C, depending on the substrate. The values of $G_{\text{threshold}}$ for commercial epoxy system in DI water were found to be about 8 J/m^2 and 1 J/m^2 at 70°C and 80°C, respectively. Also, a decrease in $G_{\text{threshold}}$ value with increasing temperature indicates that a weaker interface may be resulting in higher crack propagation rate.

The detrimental effect of preconditioning was evident in aggressive solution environments. The diffusing species diffuse through the polymer or wick along the

interface and degrade the adhesion at the interface. The rate of diffusion has been known to be dependent on the nature of diffusant, the preconditioning temperature, the nature of the polymer, and the area of the polymer exposed to the diffusant. The extent of damage to the interface and observed adhesion degradation may depend on the interaction of liquid with the polymer.

The XPS data revealed the failure pattern for model epoxy/3-APS interface. The failure was observed to be interfacial at 60°C, whereas a mix of interfacial failure and some cohesive failure in the model epoxy adhesive occurs at 70°C. This observation might suggest a possible weakening of the adhesive at higher temperatures, giving rise to cohesive failure in the adhesive. The XPS results suggested that the interaction at the commercial epoxy/3-APS interface may be stronger than that between the model epoxy/3-APS surface. XPS results revealed weaker model epoxy/3-APS interface and corroborates the wedge test result where diffusion controlled debonding was observed with higher crack propagation rate for model epoxy system as compared to the stronger commercial epoxy interface.

The viscoelastic changes in the polymer in the presence of aggressive environment may be a possible explanation for system behavior at lower and higher temperatures. An understanding of the interface adhesion can provide guidance for developing new processes and materials to enhance surface integrity. Several conclusions drawn from the wedge test data are listed here:

1. The debond growth rate, da/dt, and threshold value of strain energy release rate, Gthreshold, depends on the adhesive system under testing and environmental conditions.
2. The adhesion degradation of the interface is diffusion controlled at higher temperatures and for aggressive solution environments.
3. Weak interfaces, aggressive environments, and high testing temperatures result in higher crack propagation rate without an apparent value of Gthreshold.
4. Preconditioning in DI water does not have a significant effect on subcritical behavior of the systems whereas aggressive environments affect subcritical behavior significantly.
5. The failure pattern of the system tends to be a mix of interfacial and cohesive at higher temperatures.

6. The reliability of an adhesive joint may depend on surface chemistry, temperature, preconditioning and other factors and their mutual interactions.

4.6 References

1 L. Jacobs, "Technology Gaps and Research Needs in Electronic Packaging-An Industry", *Presentation at Cornell Industry Alliance for Electronic Packaging*, Cornell University, New York, 1997.

2 W. B. Hillig and R. J. Charles, "Surfaces, Stress-dependent Surface Reactions, and Strength", *High-Strength Materials* (Edited by V. F. Zackey), John Wiley and Sons Incorporated, New York, **17**, 682–705, 1962.

3 R. J. Charles and W. B. Hillig, "The Kinetics of Glass Failure by Stress Corrosion", Published as part of the *Symposium on the Mechanical Strength of Glass and Ways of Improving it*, Union Scientifique Continentale du Verre, Florence, 511–527, 1961.

4 S. M. Wiederhorn, "Influence of Water Vapor on Crack Propagation in Soda-lime Glass", *Journal of the American Ceramic Society***, 50**, 407–414, 1967.

5 S. M. Wiederhorn and L. H. Bolz, "Stress Corrosion and Static Fatigue of Glass. *Journal of the American Ceramic Society***, 53**, 543–548, 1970.

6 S. M. Wiederhorn, S. W. Freiman, E. R. Fuller, and C. J. Simmons, "Effect of Water and Other Dielectrics on Crack Growth", *Journal of Materials Science,* **17**, 3460–3478, 1982

7 J. D. Helfinstine, S. T. Gulati, D. G. Pickles, "Slow Crack Growth in High-Silica Glasses", *Physics of Non-Crystalline Solids*, (Edited by L. D. Pye, W. C. La Course, & H. J. Stevens), Taylor & Francis, U.K., **3**, 654–658, 1992.

8 D. Maugis, "Subcritical Crack Growth, Surface Energy, Fracture Toughness, Stick-slip and Embrittlement", *Journal of Materials Science,* **20**, 3041–3073, 1985.

9 C. J. Simmons and S. W Freiman, "Effect of Corrosion Processes on Subcritical Crack Growth in Glass", *Journal of the American Ceramic Society,* **64**, 683–686, 1981.

10 J. J. Mecholsky, A. C. Gonzalez, and S. W. Freiman, "Fractographic Analysis of Delayed Failure in Soda-lime Glass", *Journal of the American Ceramic Society*, **62**, 577–580, 1979.

11 G. W. Weidmann, and D. G. Holloway, "Slow Crack Propagation in Glass", *Physics and Chemistry of Glasses*, **15**, 116–122, 1974.

12 S. W. Freiman, D. R. Mulville, and P. W. Mast, "Crack Propagation Studies in Brittle Materials", *Journal of Materials Science*, **8**, 1527–1533, 1973.

13 S. W. Freiman, "Effect of Alcohols on Crack Propagation in Glass", *Journal of the American Ceramic Society*, **57**, 350–353, 1974.

14 S. W. Freiman, "Temperature Dependence of Crack Propagation in Glass in Alcohols", *Journal of the American Ceramic Society*, **58**, 340–341, 1975.

15 N. E. W. Hartley, and T. R. Wilshaw, "Deformation and Fracture of Synthetic Quartz", *Journal of Materials Science*, **8**, 265–278, 1973.

16 J. S. Nadeau, "Subcritical Crack Growth in Vitreous Carbon at Room Temperature", *Journal of the American Ceramic Society*, **57**, 303–306, 1974.

17 A. Tonneau, G. Henaff, C. Mabru, and J. Petit, "Environmentally-Assisted Fatigue Crack Propagation in Aluminides at Room Temperature", *Scripta Materialia*, **39**, 1503–1508, 1998.

18 A. G. Evans, M. Linzer, “Failure Prediction in Structural Ceramics Using Acoustic Emission”, *Journal of the American Ceramic Society*, **56**, 575–581, 1973.
19 S. M. Wiederhorn, E. R. Fuller, R. Thomson, “Micromechanisms of Crack-Growth in Ceramics and Glasses in Corrosive Environments”, *Metal Science*, **14**, 450-462, 1980.
20 S. N. Crichton, M. Tomozawa, J. S. Hayden, T. I. Suratwala, J. H. Campbell, “Subcritical Crack Growth in a Phosphate Laser Glass”, *Journal of the American Ceramic Society*, **82**, 3097-3104, 1999.
21 M. K. V. Chan and J. G. Williams, “Slow Stable Crack Growth in High Density Polyethylenes”, *Polymer*, **24**, 234-244, 1983.
22 K. Tonyali and H. R. Brown, "On the Applicability of Linear Elastic Fracture Mechanics to Environmental Stress Cracking of Low Density Polyethylene", *Journal of Materials Science*, **21**, 3116-3124, 1986.
23 A. J. Kinloch, L. S. Welch, and H. E. Bishop, “The Locus of Environmental Crack Growth in Bonded Aluminium Alloy Joints”, *Journal of Adhesion*, **16**, 165–178, 1984.
24 S. Mostovoy and E. J Ripling, “Flaw Tolerance of a Number of Commercial and Experimental Adhesives”, *Polymer Science and Technology* (edited by L Lieng-Huang), Plenum Press, New York, **9**, 513–562, 1975.
25 E. J. Ripling, C. Bersch, and S. Mostov, “Stress Corrosion Cracking of Adhesive Joints”, *Journal of Adhesion*, **3**, 145–163, 1971.
26 J. E Ritter, J. R. Fox, D. I. Hutko, and T. J. Lardner, “Moisture -Assisted Crack Growth at Epoxy-Glass Interfaces”, *Journal of Materials Science*, **33**, 4581–4588. 1998.
27 K. M. Conley, J. E. Ritter, and T. J. Lardner, “Subcritical Crack Growth along Epoxy/Glass Interfaces”, *Journal of Materials Research*, **7**, 2621–2629, 1992.
28 M. W. Lane, J. M. Snodgrass, R. H. Dauskardt, “Environmental Effects on Interfacial Adhesion”, *Microelectronics Reliability*, **41**, 1615-1624, 2001.
29 M. W. Lane, R. H. Dauskardt, Q. Ma, H. Fujimoto, N. Krishna, “Subcritical Debonding of Multilayer Interconnect Structures: Temperature and Humidity Effects,” *Material Reliability in Microelectronics*, Materials Research Society, San Francisco, CA, **9**, 251-256, 1999.
30 R. J. Hohlfelder, D. A. Maidenberg, R. H. Dauskardt, W. Wei, J.W. Hutchinson, “Adhesion of Benzocyclobutene-Passivated Silicon in Epoxy Layered Structures,” *Journal of Materials Research*, **16**, 243-255, 2000.
31 S. Y. Kook and R. H. Dauskardt, “Moisture-Assisted Subcritical Debonding of Polymer/Metal Interface,” *Journal of Applied Physics*, **9**, 1293-1303, 2002.
32 A. Bhatnagar, M. J. Hoffman, R. H. Dauskardt, “Fracture and Subcritical Crack Growth Behavior of Y-Si-Al-O-N Glasses and Si_3N_4 Ceramics,” *Journal of the American Ceramic Society*, **83**, 585-596, 2000.
33 R. H. Dauskardt, M. W. Lane, Q. Ma, and N. Krishna, “Adhesion and Debonding of Multi-layer Thin Film Structures”, *Engineering Fracture Mechanics*, **61**, 141–162, 1998.
34 E. J Ripling, S. Mostovoy, and C. Bersch, “Stress Corrosion Cracking of Adhesive Joints,” *Journal of Adhesion*, **3**, 145-163, 1971.

35 J. E. Ritter, T. J. Lardner, W. Grayeskl, G. C. Parkash, and J. Lawrence, "Fatigue Crack Propagation at Polymer Adhesive Interface," *Journal of Adhesion*, **63**, 265-284, 1997.
36 A. J. Kinloch, "The Durability of Adhesive Joints", Adhesion Science and Engineering, Volume - I: The Mechanics of Adhesion, (Edited by D. A. Dillard and A. V. Pocius), Elsevier, New York, **17**, 661-698, 2002.
37 J. W. Holubka, and W. Chun, "Evaluation of Adhesively Bonded Composite/Metal Bonds in Simulated Automotive Service Environments", *Adhesives, Sealants, and Coatings for Space and Harsh Environments*, (Edited by L. H. Lee,) *Polymer Science and Technology*, Plenum Press, New York, **37**, 213–225, 1988.
38 A. J. Kinloch, "Mechanisms of Adhesion," *Adhesion and Adhesives: Science and Technology*, Chapman and Hall, New York, **3**, 57-66, 1987.
39 W. J. Van Ooij, "Metal-Polymer Interfaces," *Industrial Adhesion Problems* (Edited by D. M. Brewis and D. Briggs), John Wiley and Sons, New York, **4**, 87–127, 1985.
40 A. H. Landrock, "Effect of Environment on Durability of Adhesive Joints," *Adhesive Technology Handbook*, Noyes Publication, New Jersey, **9**, 251–253, 1985.
41 E. P. Plueddemann, "Silane Coupling Agents", Plenum Press, New York, **9,** 114-235, 1982.
42 R. A Gledhill, A. J. Kinloch, and S. J. Shaw, "A Model for Predicting Joint Durability", *Journal of Adhesion*, **11**, 3–15, 1980.
43 W. D. Bascom, "The Surface Chemistry of Moisture-Induced Composite Failure", *Interfaces in Polymer Matrix Composites*, (edited by E. P. Plueddemann), Academic Press, New York, **6,** 79–109, 1974.
44 I. Goodman, and J. A. Rhys, "Polyesters", *Saturated Polymers*, American Elsevier Publishing Company, New York, **1,** 99-102**,** 1965.
45 J. W. Hutchinson and Z. Suo, "Mixed Mode Cracking in Layered Structures", *Advances in Applied mechanics*, **29**, 65-187, 1992.
46 C. K. Gurumurthy, E. J. Kramer, C. Y Hui, "Water-Assisted Sub-Critical Crack Growth along an Interface between Polyimide Passivation and Epoxy Underfill", *International Journal of Fracture*, **109**, 1-28, 2001.
47 B. R. Lawn, "Diffusion-Controlled Subcritical Crack Growth in the Presence of a Dilute Gas Environment," *Material Science Engineering*, **13,** 277–83, 1974.
48 A. J Curley, J. K. Jethwa, A. J. Kinloch, A. C. Taylor, "The Fatigue and Durability Behavior of Automotive Adhesives. Part III: Predicting the Service Life", *Journal of Adhesion*, **66**, 39-59, 1998.
49 S. L. Case, "Fundamental Importance of Fillers, Cure Condition, and Crosslink Density on Model Epoxy Properties," *Ph.D. Dissertation*, Virginia Tech, Chapter 4, 2003.
50 J. Cognard, "The Mechanics of the Wedge Test", *Journal of Adhesion*, **20**, 1-13, 1986.
51 Y. J. Weitsman, M. Elahi, "Effects of Fluids on the Deformation, Strength and Durability of Polymeric Composites - An Overview", *Mechanics of Time Dependent Materials*, **4**, 107-126, 2000.
52 D. Xu, "Durability and Adhesion of a Model Epoxy Adhesive Bonded to Modified Silicon Substrates", *Ph.D. Dissertation*, Virginia Tech, Chapter 7, 2004.

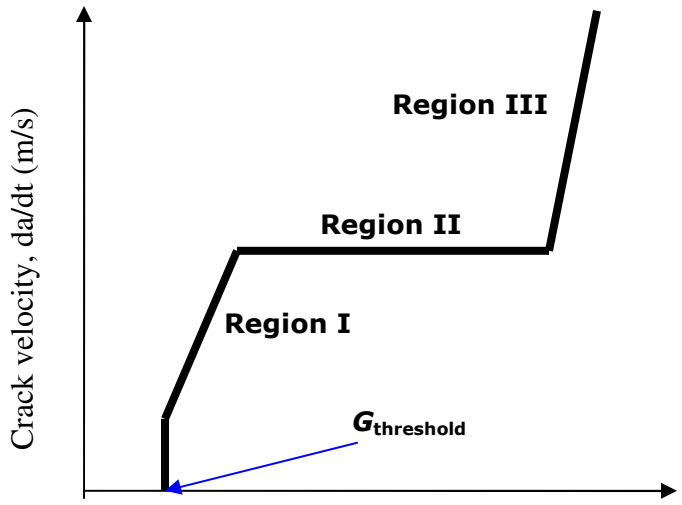

Figure 4.1 Schematic illustration of a typical $\frac{da}{dt}$ versus G curve illustrating three region of crack growth for subcritical crack growth.

.

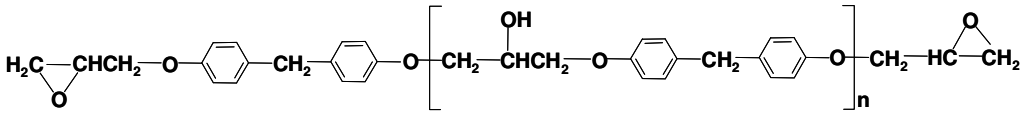

bis-phenol F diglycidyl ether (Epon 862)

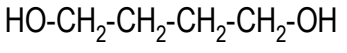

1, 4-butanediol

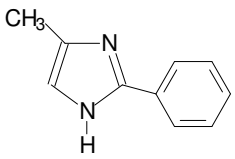

4-methyl-2-phenylimidazole

Figure 4.2 Chemical structures of the model epoxy components.

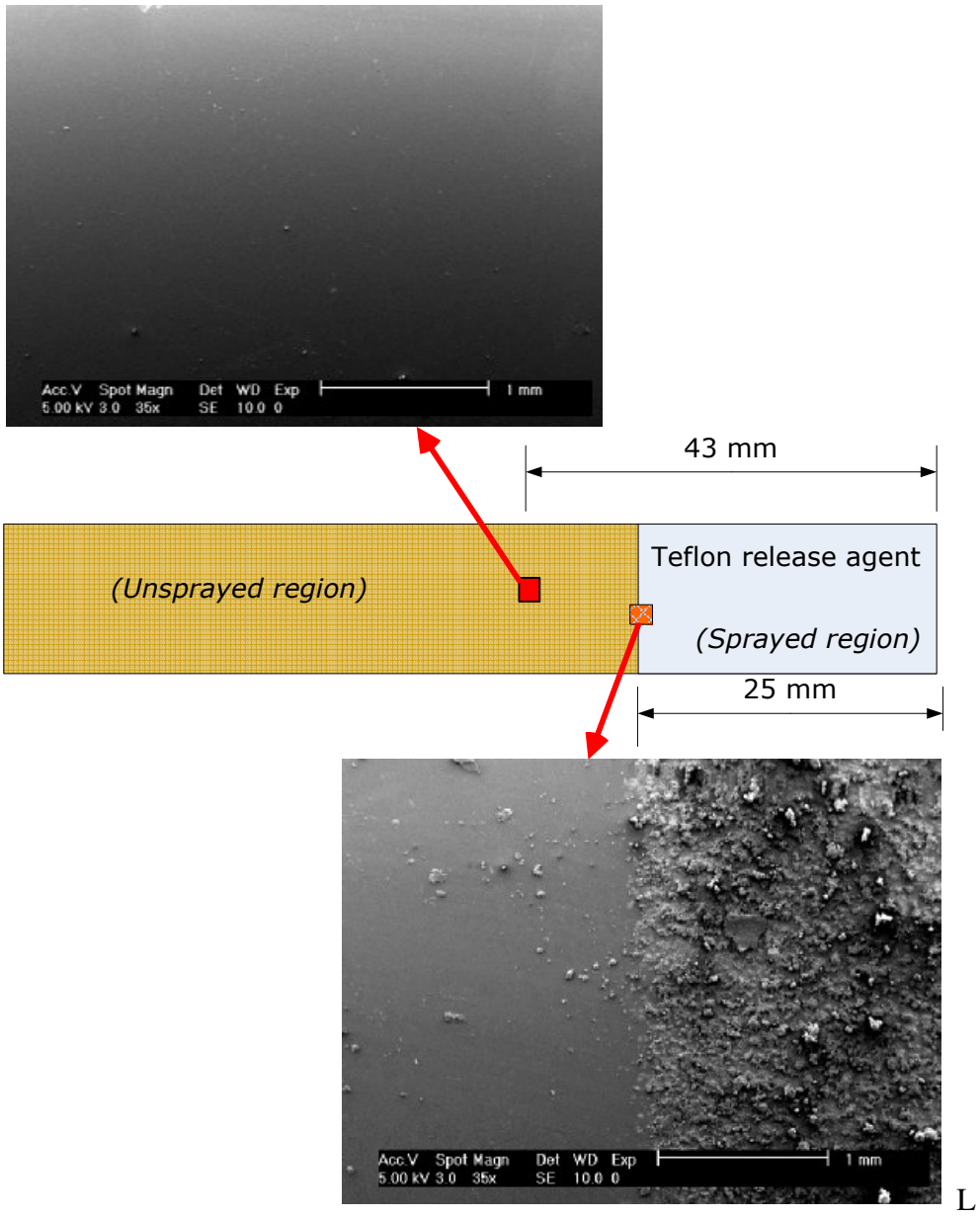

Figure 4.3 Illustration of the PTFE mold release sprayed and unsprayed region showing SEM image near the PTFE release agent sprayed region and the unsprayed region for borosilicate glass substrate.

Atomic concentration table (%)								
	B	**C**	**N**	**O**	**F**	**Al**	**Si**	**Sn**
Glass as received from vendor	3	20	1	56	**< 0.5**	1	21	0.5
Surface treated (3-APS) glass substrate	1	14	2	60	**< 0.5**	1	25	
PTFE release agent sprayed region	-	35	-	1	**63**	-	1	-
6 mm from the spray	2	18	2	55	**2**	1	23	< 0.1
23 mm from the spray	2	14	3	58	**2**	1	24	< 0.1
43 mm from the spray	2	14	3	60	**< 0.5**	1	24	< 0.1

Table 1 Atomic concentration table showing the percentage of elements present on the glass surface as determined by XPS.

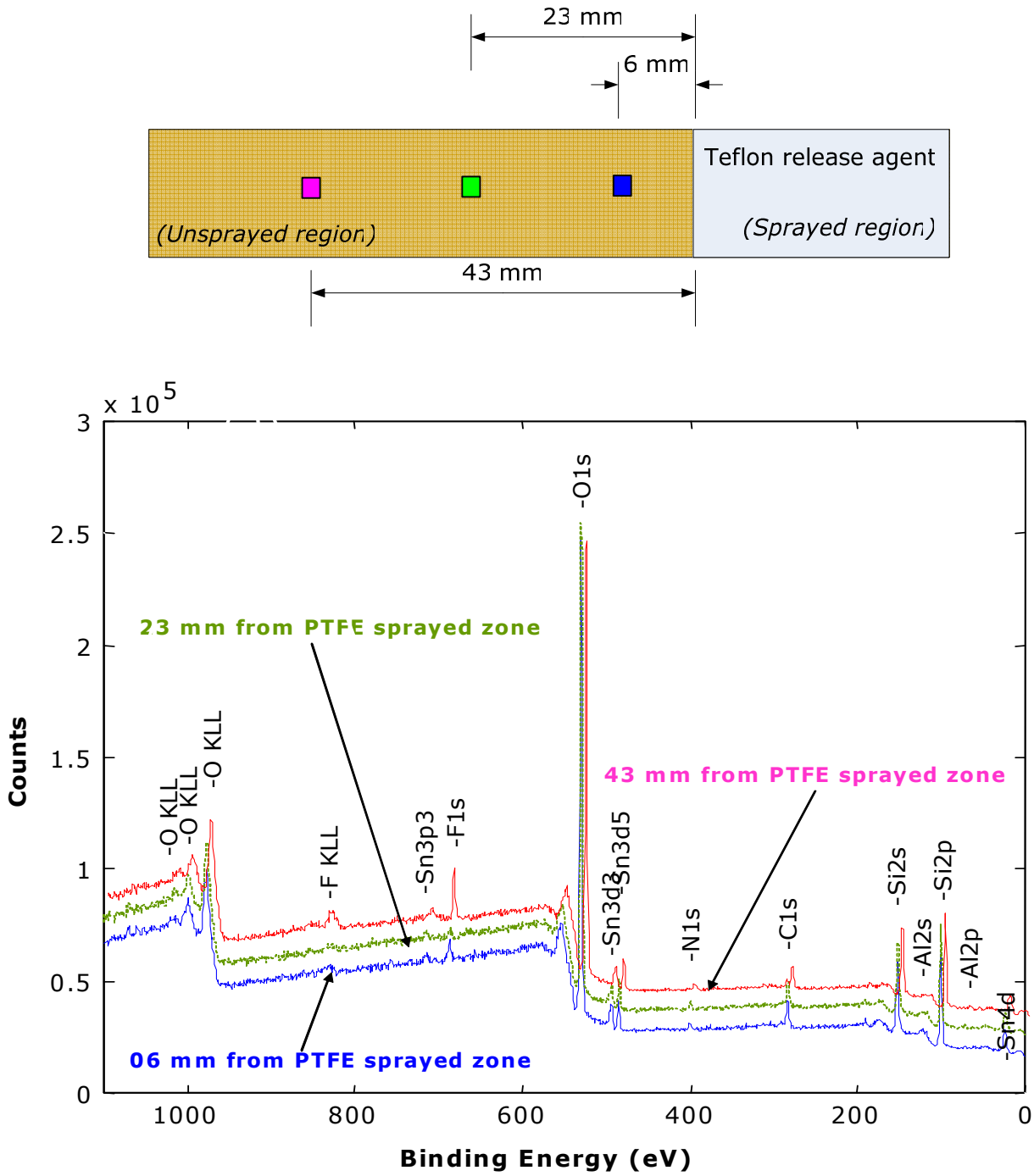

Figure 4.4 XPS spectral regions at various locations of the glass substrate sprayed with PTFE release agent.

	B	C	N	O	F	AL	SI
Silicon as received from vendor	-	20	1	40	**2**	-	21
Surface treated (3-APS) silicon substrate	1	19	2	60	**2**	1	25
PTFE release agent sprayed region	-	35	-	1	**63**	-	1
6 mm from the spray	-	23	3	48	**2**	-	24
23 mm from the spray	-	22	3	49	**1**	-	24
43 mm from the spray	-	19	3	53	**1**	-	24

Table 2 Atomic concentration table showing the percentage of elements present on the silicon surface as determined by XPS.

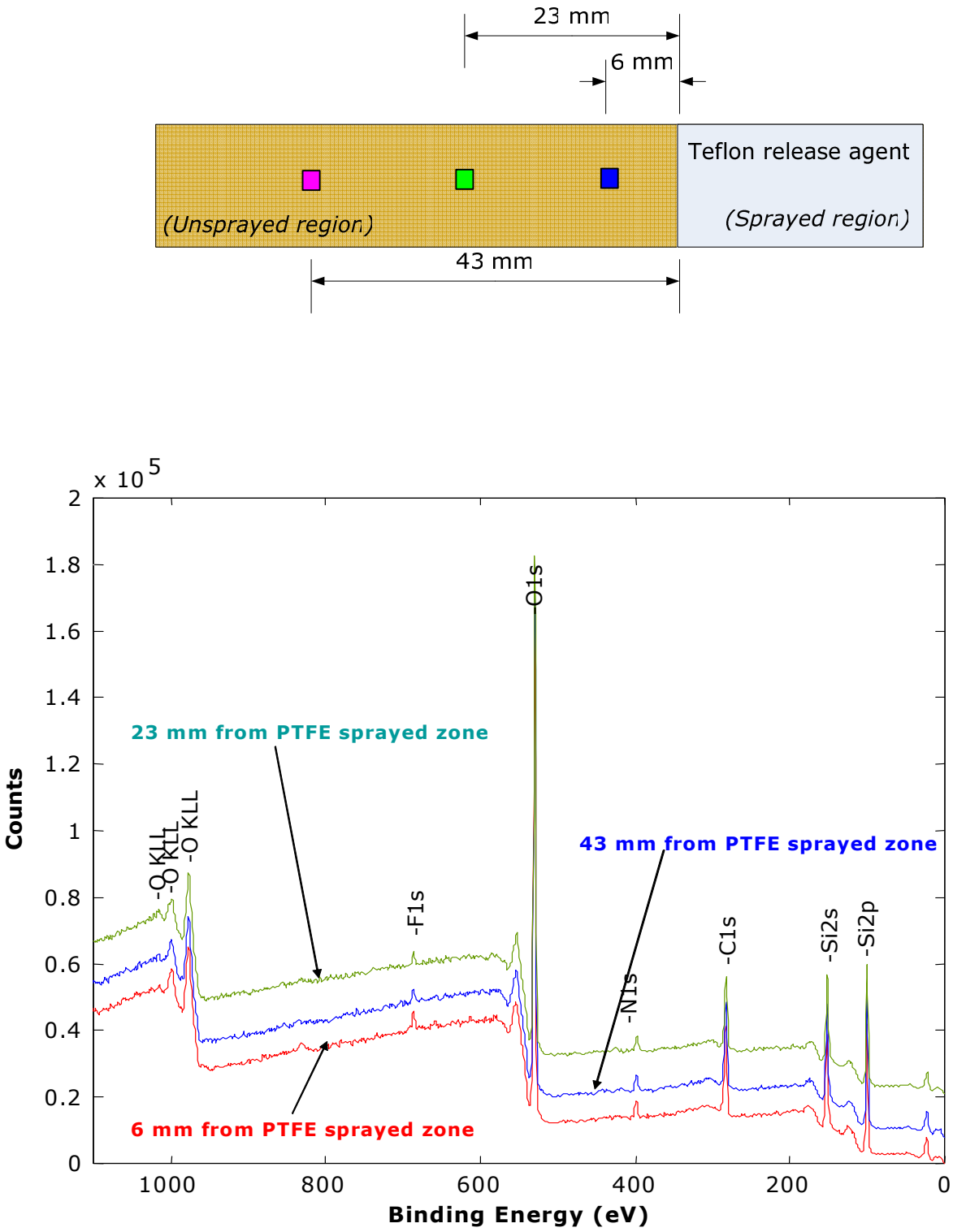

Figure 4.5 XPS spectral regions at various locations of the silicon substrate sprayed with PTFE release agent.

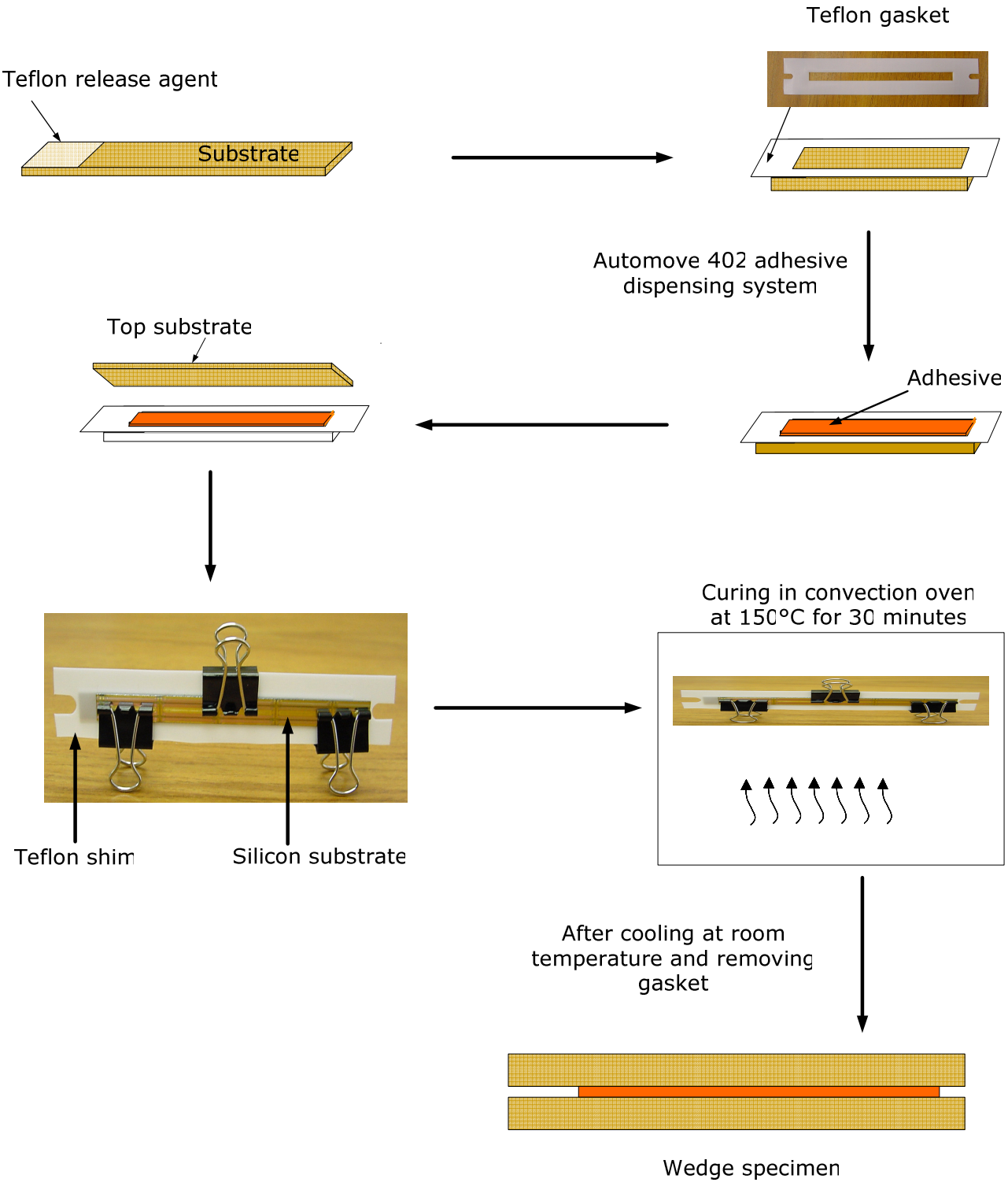

Figure 4.6 Schematic illustration of the sample preparation procedure.

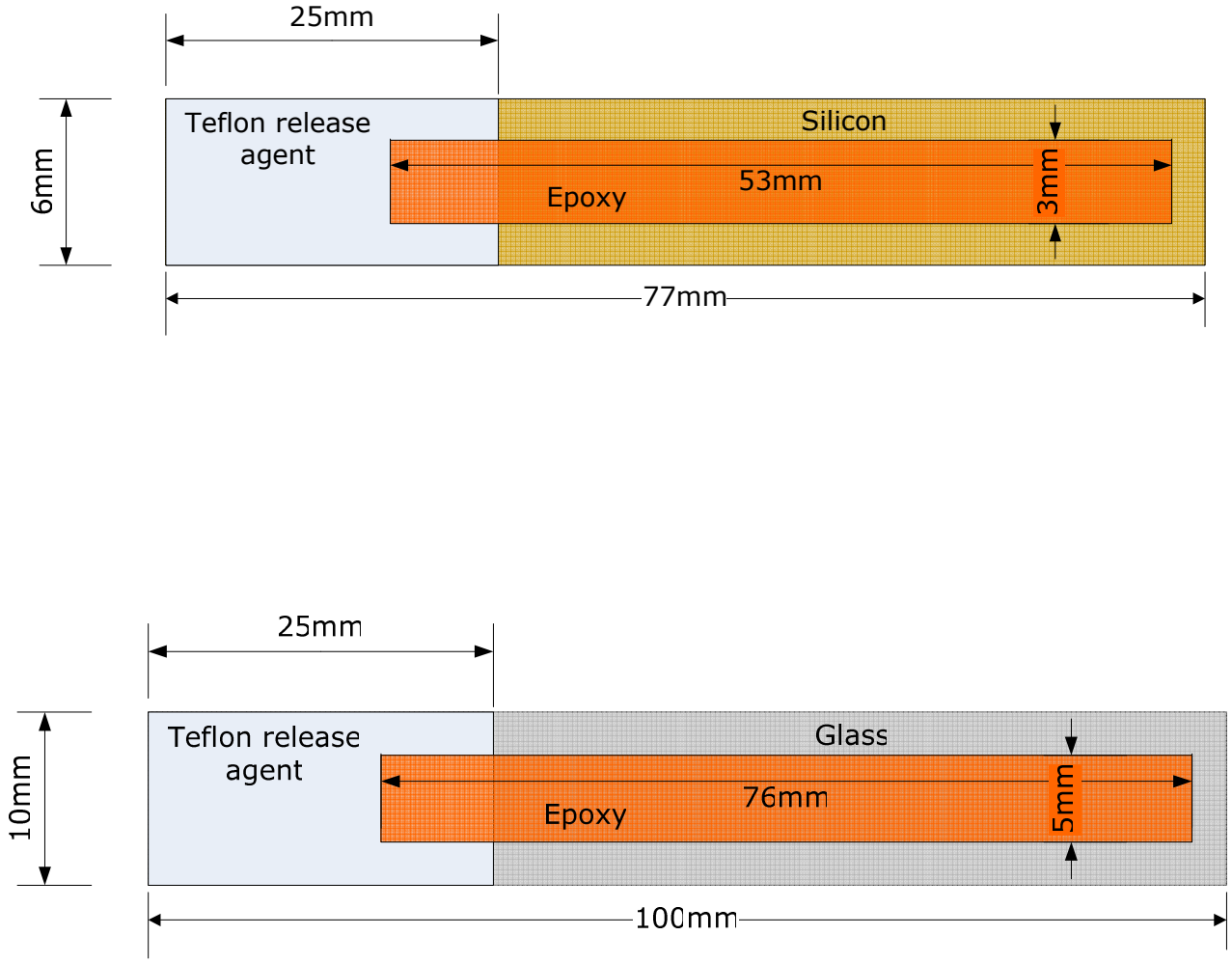

Figure 4.7 Illustration of the final bond dimensions for silicon and glass specimens.

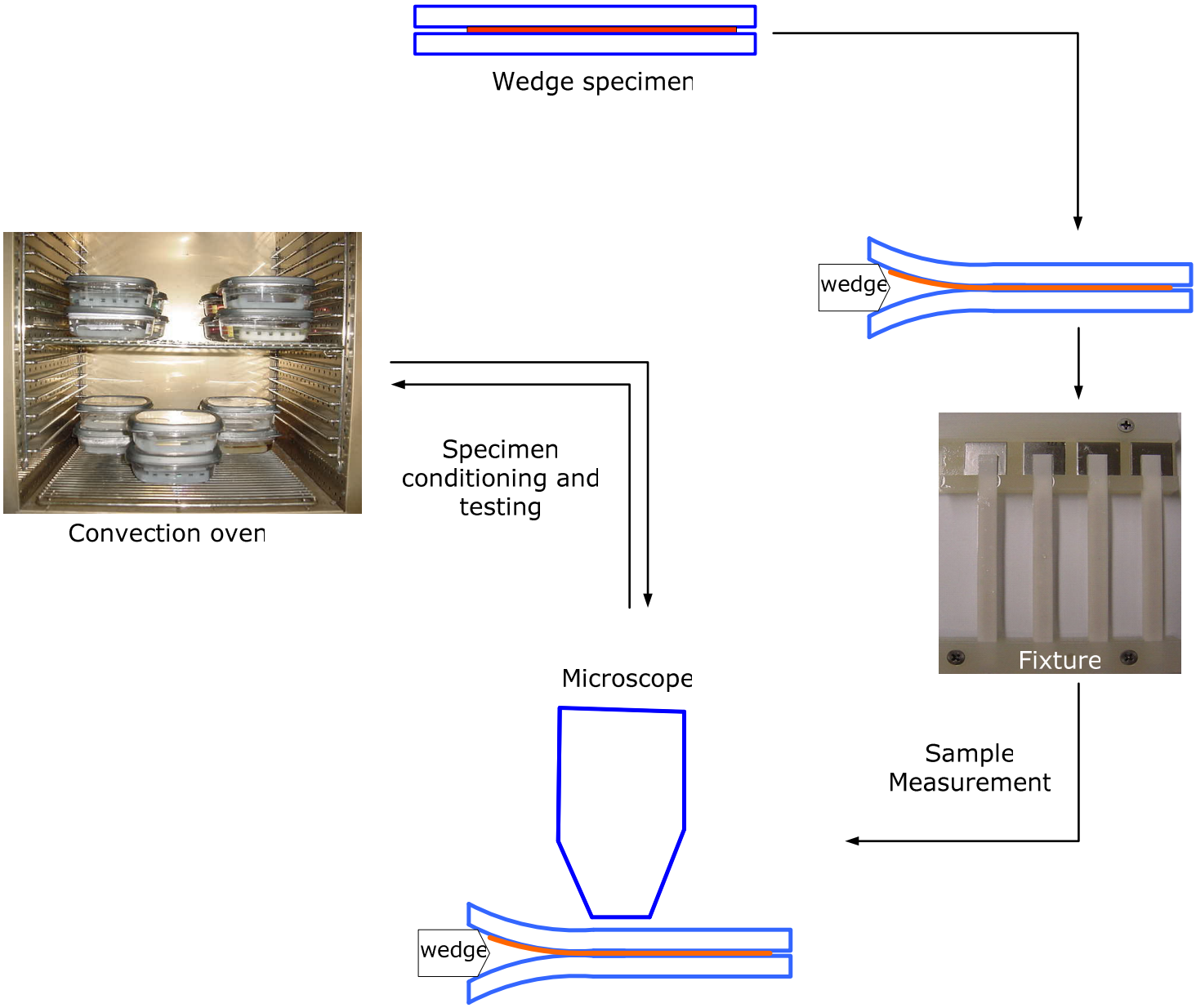

Figure 4.8 Schematic illustration of wedge insertion, crack length measurement and conditioning.

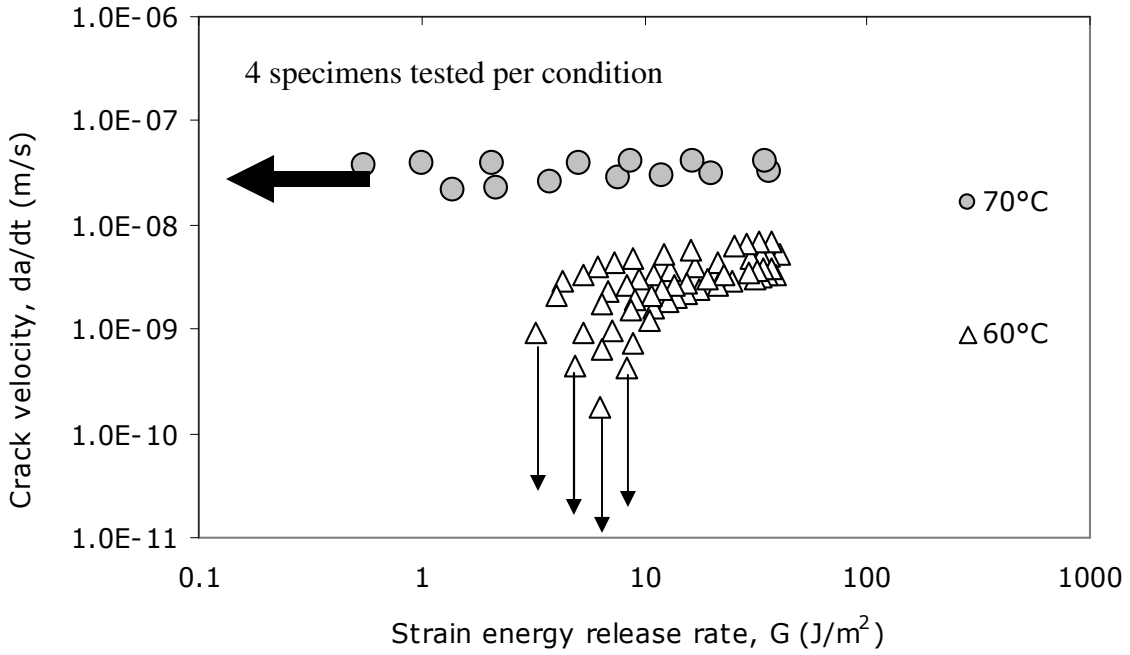

Figure 4.9 Effect of test temperature on debond kinetics for silicon/model epoxy system in proprietary solution A.

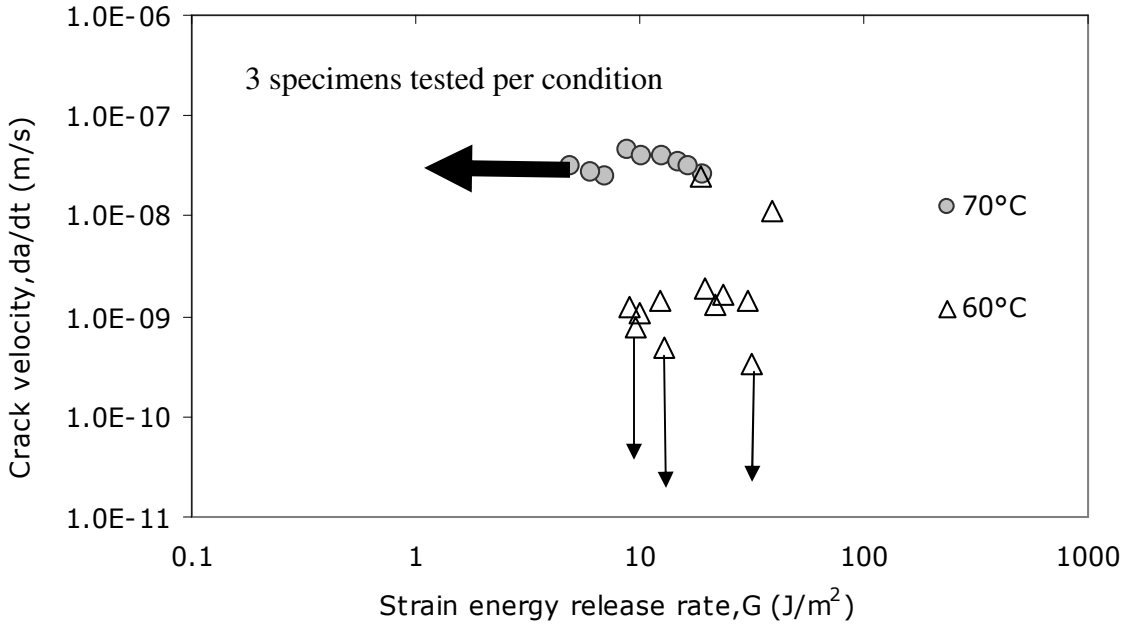

Figure 4.10 Effect of test temperature on debond kinetics for glass/model epoxy system in proprietary solution A.

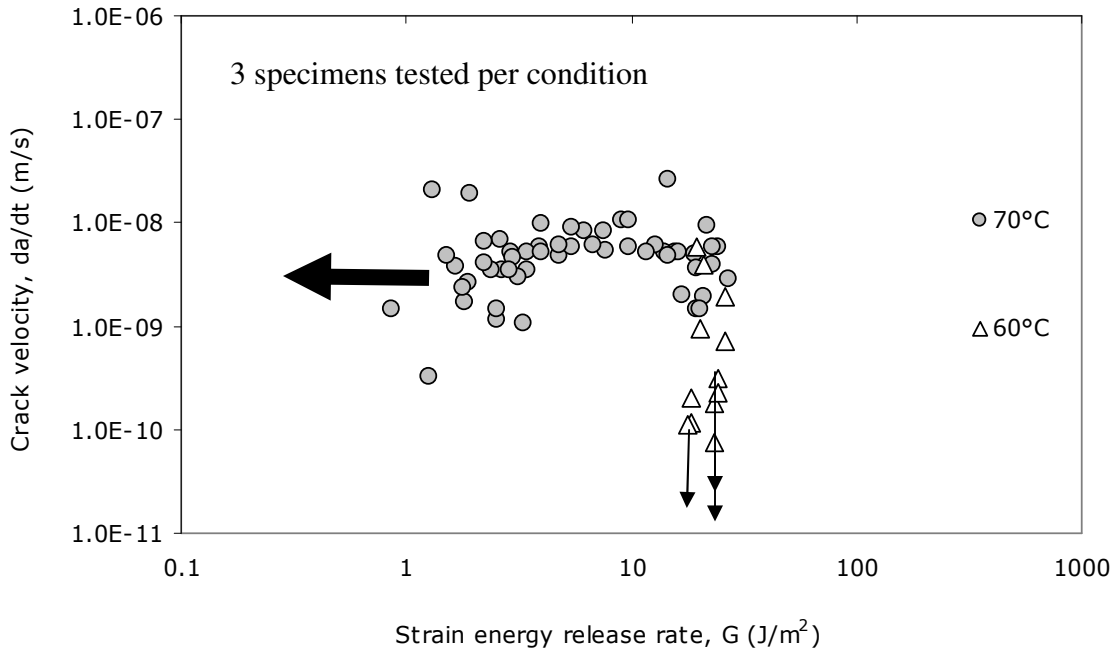

Figure 4.11 Effect of test temperature on debond kinetics for glass/commercial epoxy system in proprietary solution A.

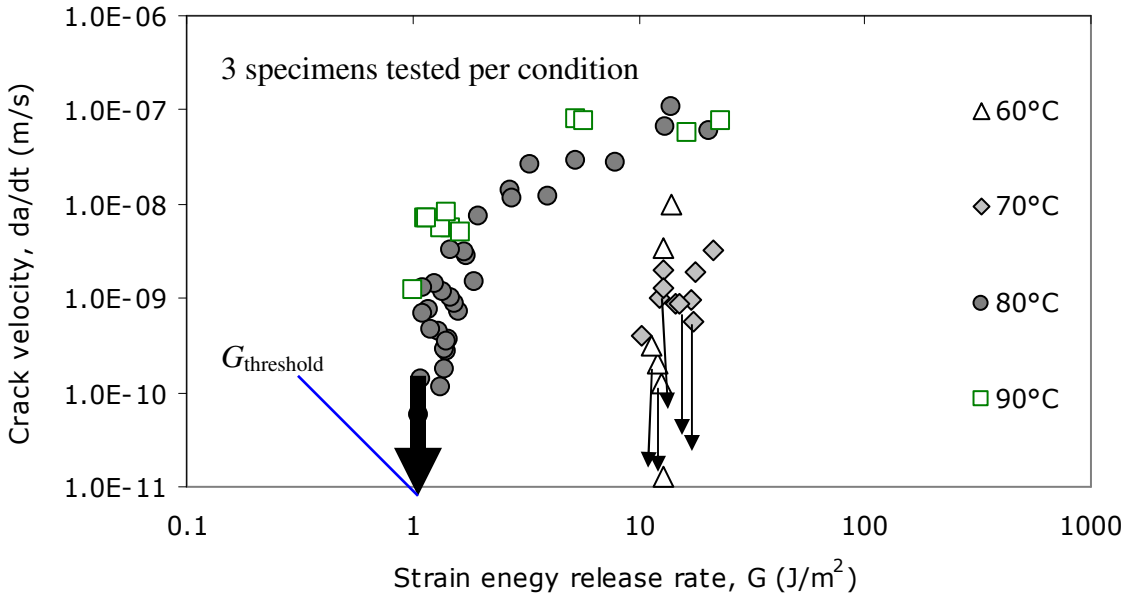

Figure 4.12 Effect of test temperature on debond kinetics for silicon/commercial epoxy system in DI water.

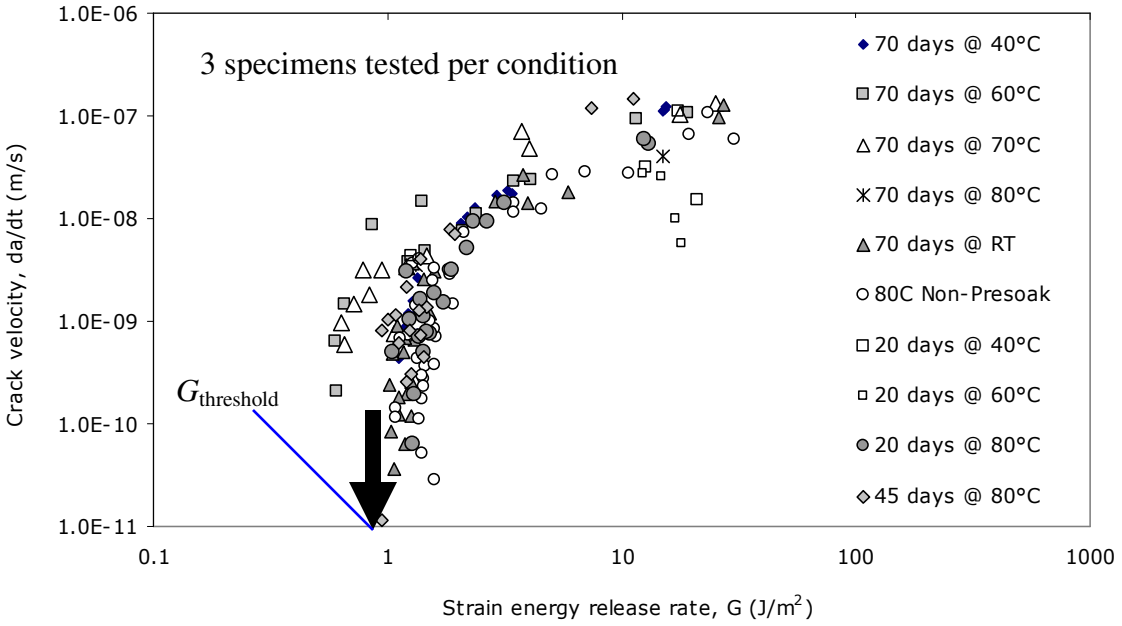

Figure 4.13 Effect of preconditioning on debond kinetics for silicon/commercial epoxy system at 80°C test temperature in DI water.

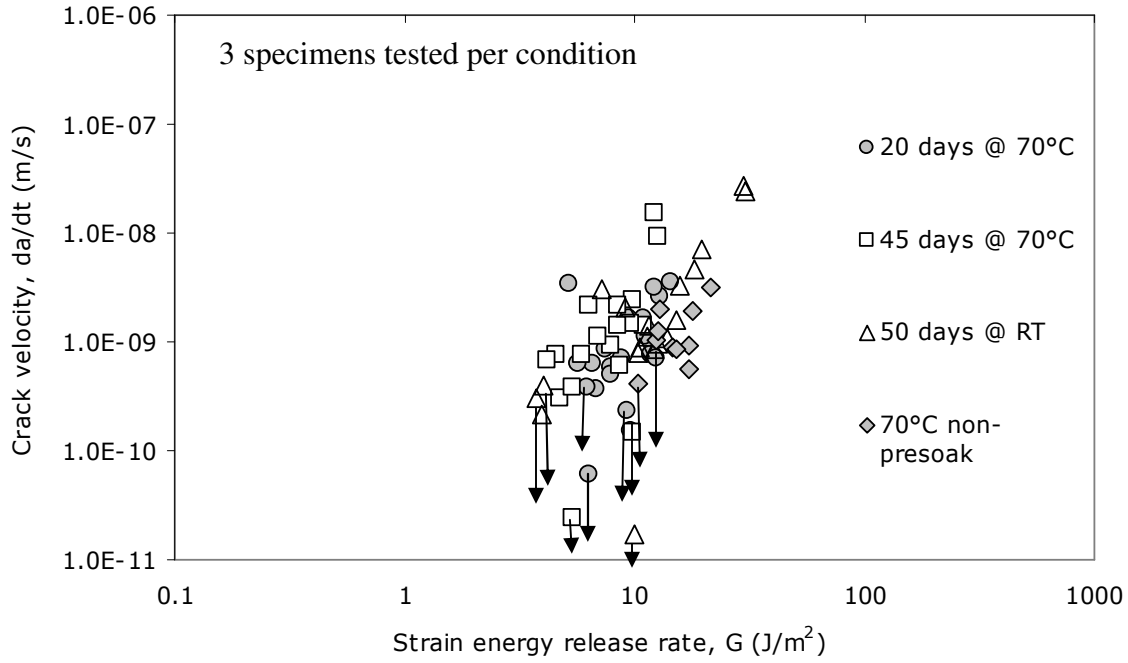

Figure 4.14 Effect of preconditioning on debond kinetics for silicon/commercial epoxy system at 70°C test temperature in DI water.

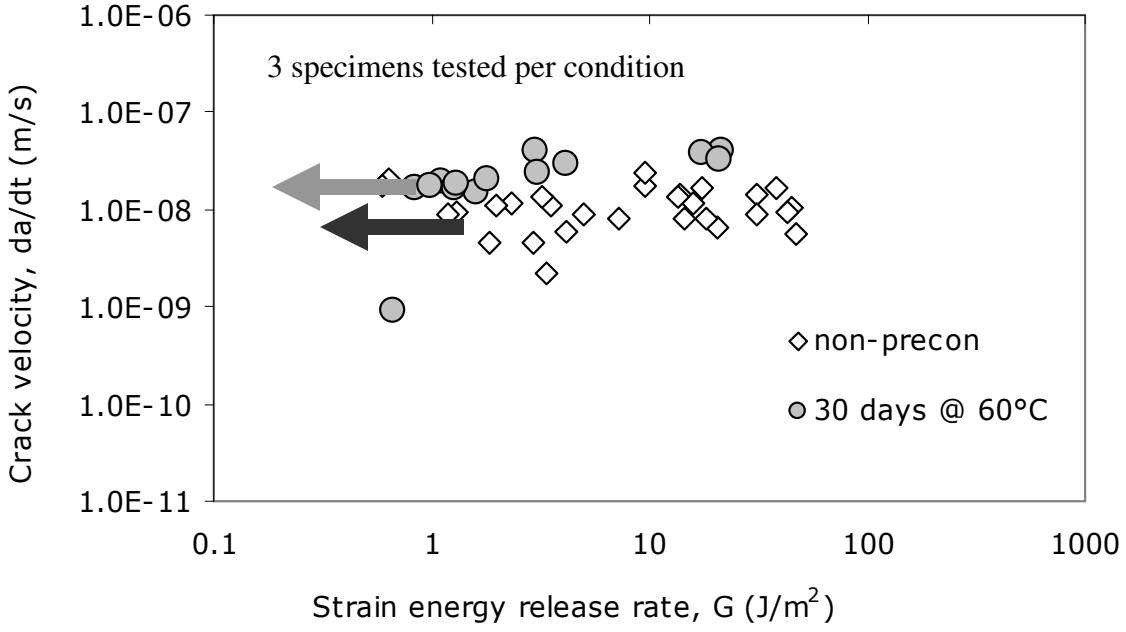

Figure 4.15 Effect of preconditioning on debond kinetics for silicon/commercial epoxy system at 70°C test temperature in proprietary solution B.

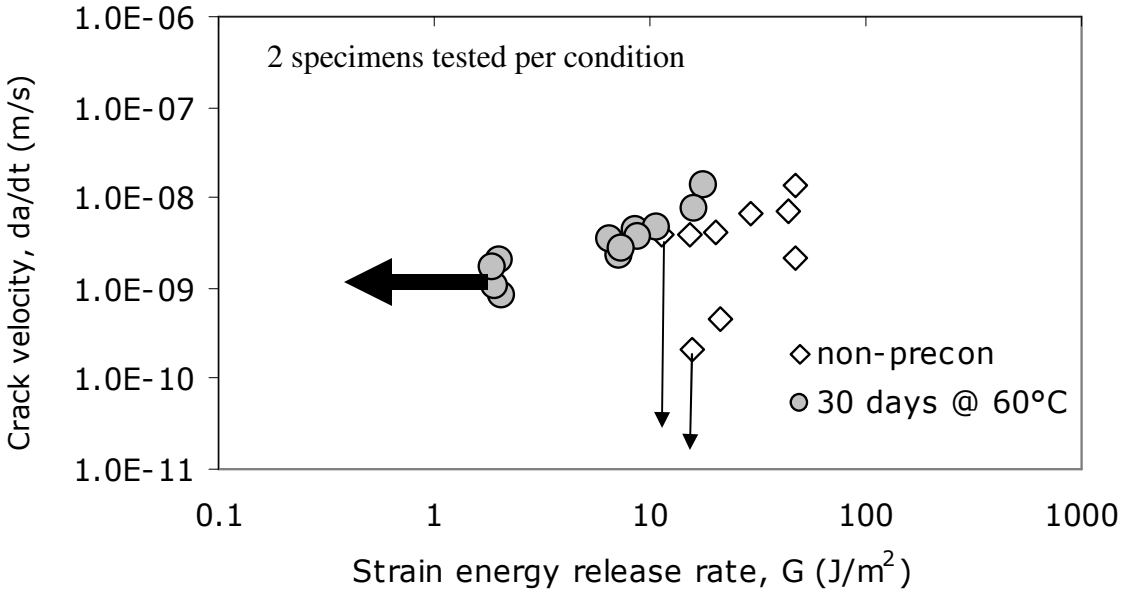

Figure 4.16 Effect of preconditioning on debond kinetics for silicon/commercial epoxy system at 70°C test temperature in proprietary solution C.

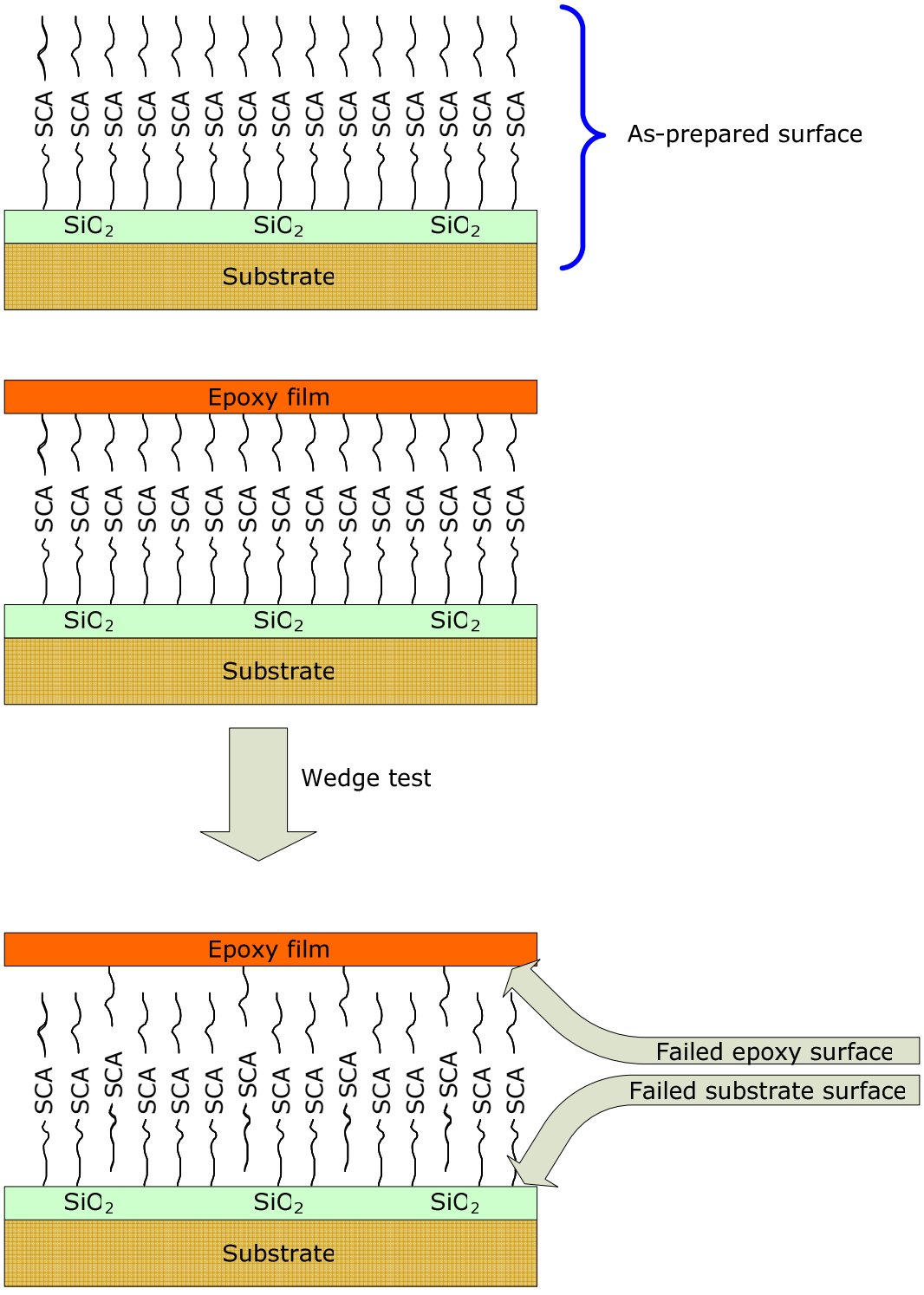

Figure 4.17 Illustration of the wedge test specimen investigated for bond failure using XPS.

Type of Surfaces	Sample	C	O	Si	N
As-prepared surfaces **(prior to bonding)**	Model epoxy, as prepared	81.6	18.4	<0.1	<0.1
	Silicon + argon plasma + 3-APS	38.5	31.2	27.1	3.2
Failed surfaces **(after debonding)**	Failed epoxy side	77.9	21.2	0.5	0.4
	Failed silicon side	45.3	34.6	18.3	1.9

Table 3 Elemental surface compositions (atomic %) for as-prepared and failed wedge specimen surfaces in proprietary liquid A at 70°C [reference 52].

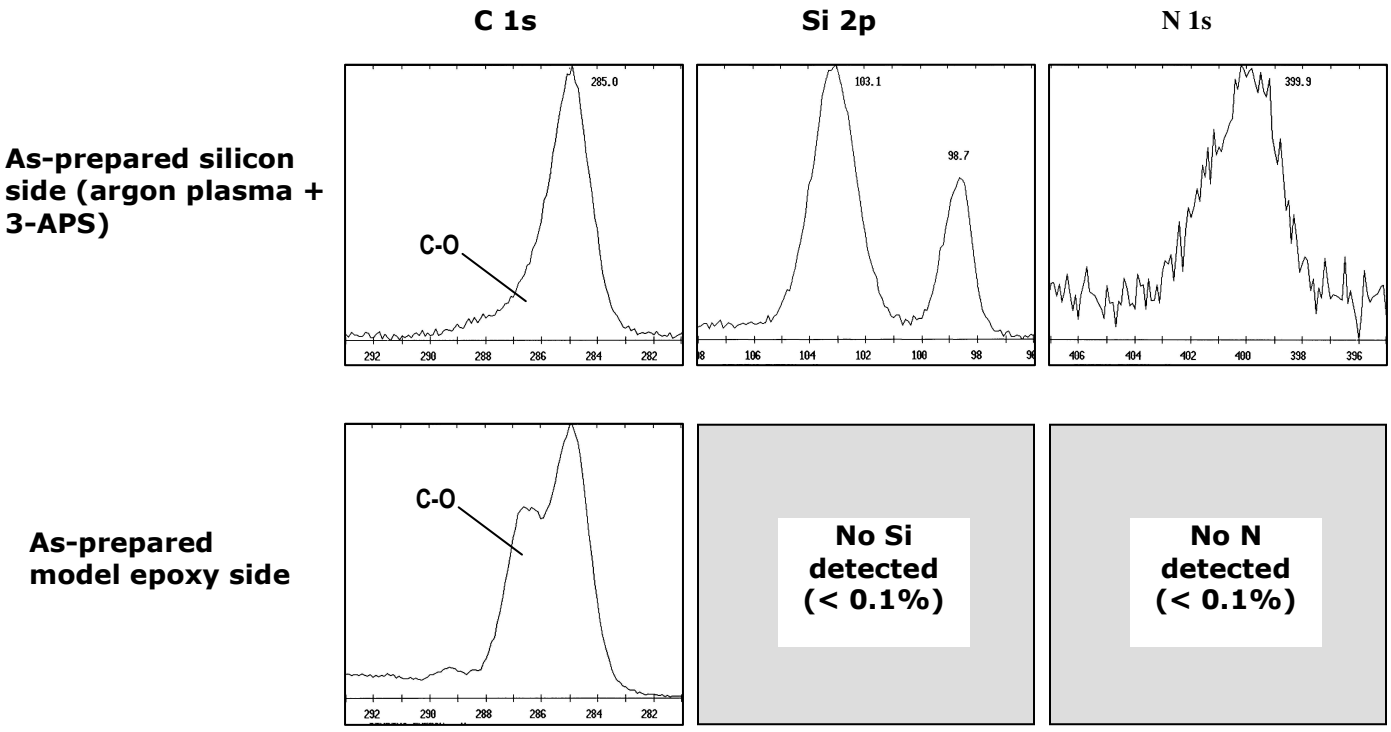

Figure 4.18 C 1s, Si 2p, and N 1s XPS spectral regions for as prepared model epoxy and silicon/3-APS surfaces [reference 52].

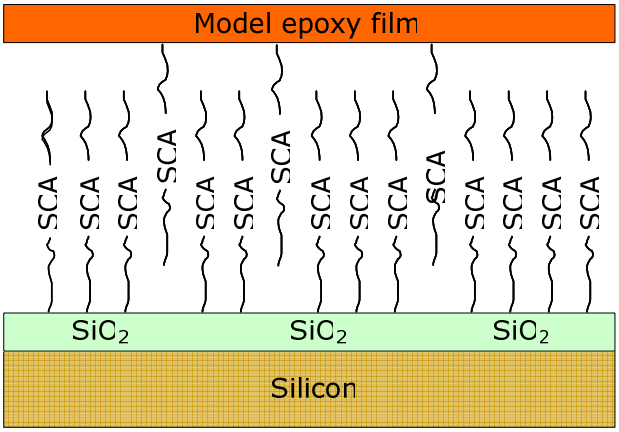

Figure 4.19 Proposed failure mode for silicon/3-APS/model epoxy bonded sample failed in the wedge test in proprietary liquid B (pH = 4) at 70°C (refer Table 3).

Type of Surfaces	**Sample**	**C**	**O**	**Si**	**N**
As-prepared surfaces **(prior to bonding)**	Model epoxy, as prepared	81.6	18.4	<0.1	<0.1
	Silicon + argon plasma + 3-APS	33.2	31.2	32.1	3.5
Failed surfaces **(after debonding)**	**60°C immersion**				
	Failed epoxy side	76.4	22.3	1.0	0.4
	Failed silicon side	25.5	47.4	25.6	1.5
	70°C immersion				
	Failed epoxy side	73.0	24.0	1.9	1.2
	Failed silicon side	21.9	52.2	24.3	1.5

Table 4 Elemental surface compositions (atomic %) for as-prepared and failed bonded surfaces after wedge test for silicon/3-APS/model epoxy system in proprietary liquid C at 60°C and 70°C [reference 52].

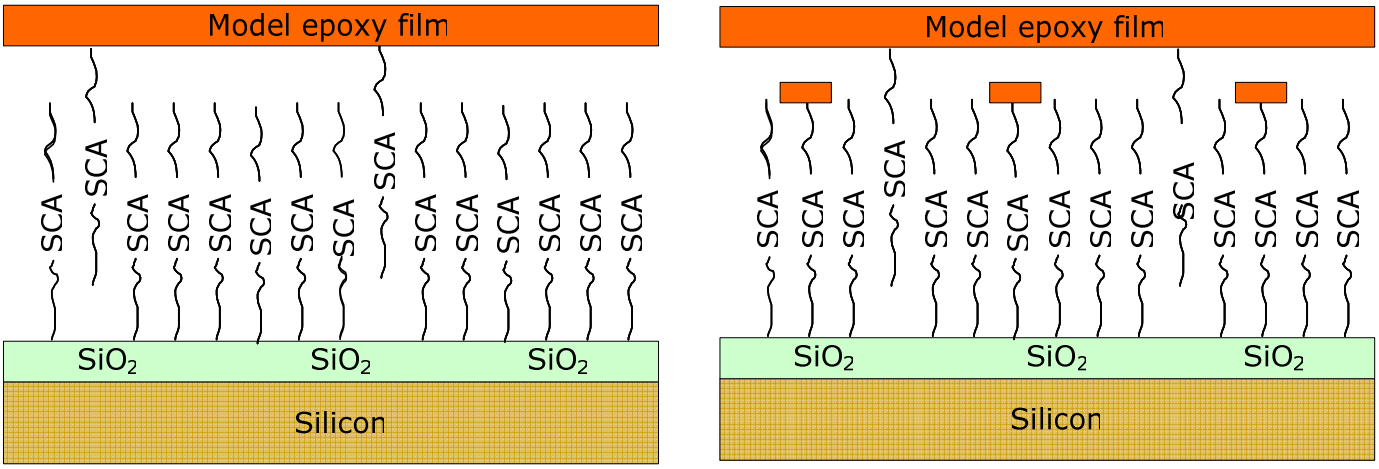

Figure 4.20 Comparison of the effect of temperature on debond mechanisms at 60°C and 70°C of failed wedge specimen for silicon/3-APS/model epoxy bond failed in proprietary liquid C (pH = 9).

Appendix A

This study was prompted by concerns over the calculation of the value of strain energy release rate. Figure 4A shows two methods that can be used to calculate the average value of strain energy release rate between two consecutive crack length values over the increment in time Δt. Vertical axis represents the value of strain energy release rate and horizontal axis represents the crack length where a_t is the crack length at time t *a*nd $a_{t+\Delta t}$ is the crack length after time increment Δt. Calculation of strain energy values using integral formula (G^*) and average value formula (G_{av}), as shown in Figure 4A, and the percentage difference between the respective values is presented here. The purpose is to show that either of the two methods can be used to calculate the value of strain energy release rate without introducing significant amount of error. A brief calculation of % error is presented here for the case of silicon/commercial epoxy system (as an example). The formula for calculating *G* (derived from Equation 1) can also be written as:

$$G = \frac{2.935 \times 10^6}{a^4} \tag{4A}$$

where *a* is the value of crack length in millimeters. The values of other constants used, to drive Equation 4A from Equation 1, are given below:

Modulus of Elasticity for Silicon (E) = 186 MPa

Width of the beam (B) = 6mm

Thickness of the silicon substrate (h) = 0.675mm

Width of the adhesive on the substrate (b) = 3mm

Opening displacement (Δ) = 0.52mm

Thickness of the wedge = 0.78mm

Thickness of the adhesive layer between beams = 0.26mm

For a maximum crack length increment Δa =1mm (as observed during subcritical debonding of the silicon system), the percentage error between *G* values for two methods, as given in Equation 4B, is calculated to be less than 0.3%.

$$\%error = \frac{G_{av} - G^*}{G_{av}} \times 100 \tag{4B}$$

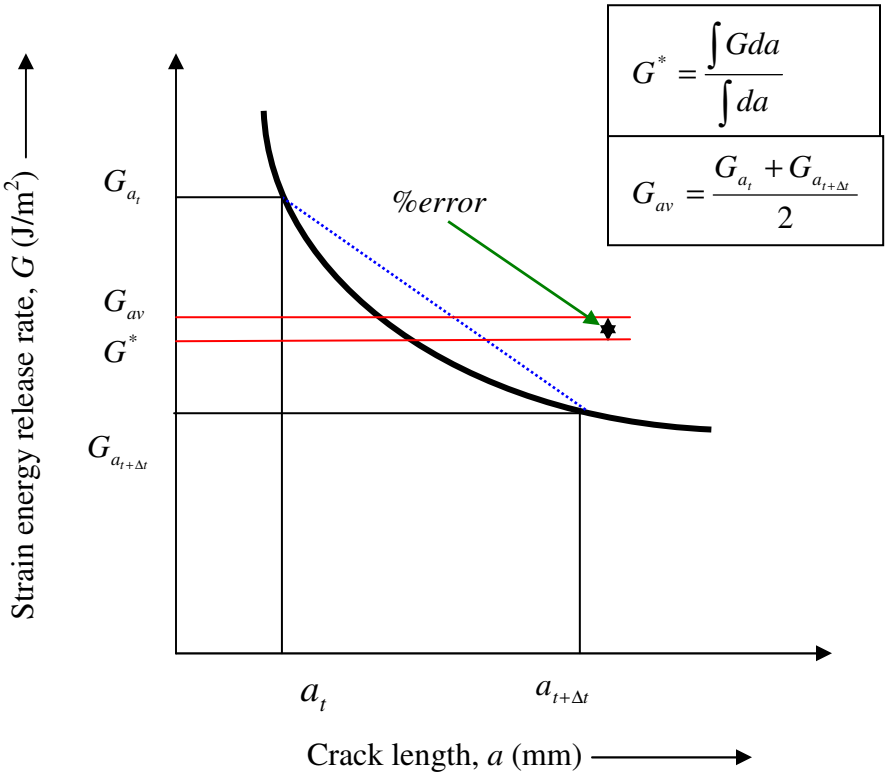

Figure 4A Estimation of % error in strain energy release rate calculation using two methods.

5 DATA ANALYSIS

Since understanding the subcritical delamination mechanisms of adhesive joints under environmental attack is very important for reliability and durability predictions, the kinetic behavior of the system needs to be addressed. The ability to quantitatively describe the change in performance, based on molecular interactions between epoxy and coupling agent at the interface and linear elastic fracture mechanics, and to predict the lifetime of bonded joints would be a powerful tool to help predict long-term deterioration of interfacial adhesion. Several models have been proposed by different researchers [1, 2, and 3] to describe the stress corrosion cracking observed in bulk glasses and have been found to accurately predict the relationship between moisture content and crack velocity for different regions shown in Figure 4.1. Region III is independent of environmental factors and is dominated by critical fracture events [4-6]. Data in this region were not collected in this study.

In region II, crack growth rate is transport controlled in what is known as the plateau region and the crack velocity depends strongly on the environment. Diffusion effects are dominant in this region and debonding is caused by the interaction of environmental or absorbed moisture with strained atomic bonds near the debond tip, and the crack growth rate is found to be linearly dependent on the activity of water molecules at the crack tip. Such debond growth rate has been studied by several researchers [7-10], and a wide amount of experimental evidence has been accumulated to demonstrate that the central, moisture-assisted mode I sub-critical crack growth rate, $\frac{da}{dt}$, of region II (as shown in Figure 4.1) may be modeled by means of the expression based upon the Paris Law [11] (as given in Equation 1) which has been found to adequately represent the observed moisture-assisted debond growth rate behavior [12]:

$$\frac{da}{dt} = \Omega G^n \tag{1}$$

where Ω and n are fitting parameters which depend on the material and test conditions and can be considered to be constant in a given physico-chemical environment. The exponent n is significant because it is a measure of the crack growth to the applied G; a

higher n signifies a greater resistance to "stress-corrosion" crack growth as described elsewhere [13]. Also, the dependence of crack growth on applied G in region II, given by the value of n, depends on the testing conditions, i.e. test temperature, solution chemistry, surface chemistry etc.

The crack velocity in region I is controlled by bond rupture and healing events, the ratio of which is governed by the applied driving energy [4]. Wiederhorn et al. [1] treated the rupture process (for humid air environment) at the crack tip in region I as a chemical reaction between strained atomic bonds and water molecules at the crack tip, and assumed the crack growth rate, $\frac{da}{dt}$, was proportional to the rate of chemical reaction:

$$\frac{da}{dt} = A^* \left(\frac{P_{H_2O}}{P^0}\right)^n \exp\left(\frac{bG}{RT}\right) \tag{2}$$

where $A^* = A\left[-E^*/RT\right]$ is a constant at fixed temperature, E^* is the stress free activation energy, b is an activation area related to the activation volume, P_{H_2O} is the partial pressure of water vapor, P^0 the standard state pressure (1 atmosphere), and G is the crack tip strain energy release rate. The above equation predicts an exponential increase in crack velocity with G and an Arrhenius-like increase with temperature, and has been used successfully to fit region I data for tests conducted on a wide range of bulk glasses [1, 14, 15, and 16]. However, at very low values of debond driving energies, the opening behind debond may become too narrow for H_2O molecules to reach the crack tip, leading to a steric hindrance threshold as suggested by Michalske and Bunker [14]. According to Wiederhorn [17-19], the three possible limiting steps for the chemically enhanced fracture process are diffusion, chemisorption, and chemical reaction. The latter two processes involve a chemical reaction and are expected to depend on the stress at the crack tip, perhaps obeying a reaction law similar to that suggested by Charles and Hillig [20, 21]. Therefore, if fracture were controlled by chemisorption or another chemical reaction at the crack tip, one might expect the crack velocity to be exponentially dependent on the applied value of strain energy release rate, as given in Equation 2. According to Charles and Hillig, the crack propagation in region I is due to the corrosive attack of environment at the crack tip and rate of stress-dependent chemical reaction at the crack tip depends on the state of

stress, the rate increasing with increasing stress [20-22]. The stress is greatest at the roots of cracks, and consequently the reaction proceeds at its greatest rate from these roots.

Although the exact debond mechanisms of crack propagation under subcritical loading conditions are not completely understood, it is generally accepted that the crack front movement in region I and region II involves the transport of H_2O through the crack and the subsequent reaction between water and crack tip. Various models have been developed to describe crack growth in region I and II with the most widely accepted being that of Wiederhorn [10-12]. Wedge test results on silicon and glass systems revealed subcritical debond growth mainly in region II i.e. region I behavior was not observed for all systems whereas data in region II behavior, where a plateau is observed, was evident for most systems. Because of the lack of sufficient data and the sensitivity of the system with respect to the testing conditions involved, a comparison between experimental results observed in region II is discussed in order to understand the delamination mechanisms responsible for debond propagation.

An investigation of the applicability of Equation 1 to describe region II behavior in terms parameters Ω and n have been presented here. From Equation 1, a value of n approximately close to zero indicates the plateau region (defined for diffusion controlled debonding) where the crack propagation does not depend on strain energy release rate and the value of constant Ω is given by the crack velocity. Such a behavior has been observed for silicon/model epoxy (Figure 4.9), glass/model epoxy (Figure 4.10), and glass/commercial epoxy (Figure 4.11) in solution A and silicon/commercial epoxy (Figure 4.15) in solution B at 70°C. The value of n greater than zero indicates the dependence of crack growth on strain energy release rate which has been observed for silicon system in DI water at 80°C and in solution C at 70°C. Analysis of silicon/commercial epoxy system at 70°C indicate that acidic solution B (Figure 4.15) causes the diffusion controlled debonding with no dependence of crack growth on debond driving energy whereas basic solution C (Figure 4.16) exhibit dependence of crack growth on crack driving energy. Figure 5.1 shows the power law fit for the silicon/commercial epoxy system tested at 70°C in DI water, liquid B and liquid C and the corresponding values of Ω and n are shown in Table 3. A comparison of the value of n indicates that crack growth is less dependent on G in acidic environment (liquid B) as

compared to basic environment (liquid C) and DI water. Also, as the value of n increases, the value of Ω decreases or the debond propagation rate in diffusion controlled region II goes down. Although, the accuracy of the results presented here is questionable owing to the limited amount of data, a preliminary conclusion drawn from this observation might suggest that the solution chemistry is one of the important factors among testing temperature, surface chemistry, epoxy, substrate etc., that affect the dependence of crack growth on crack driving energy.

Wedge tests performed in this study helped to gain valuable insights by learning how the reliability and durability of an adhesive joint may depend on solution chemistry, testing temperature, and preconditioning time and temperature. The system behavior was observed to be different for different environment, for example, the higher the temperature, the higher the debond propagation. Also, the adhesion degradation of the interface was found to be diffusion controlled at higher temperatures and for aggressive liquid environments where no apparent value of G_{th} was observed which can be attributed to a number of reasons one of which could be the viscoelastic changes or diffusion induced plasticization and swelling of the polymer in the presence of liquid. Subcritical debonding data was analyzed using empirical relationships proposed by various researchers, and empirical constants Ω and n (the resistance to "stress-corrosion" crack growth) were obtained in an attempt to understand the system behavior. However, limited amount of data and unpredictability of the system response limited the modeling efforts and analysis to region II behavior only (See Appendix B for a brief discussion on region I and region III behavior) and a fundamental understanding of the delamination mechanisms is still not apparent. The behavior of the system appears to be environment specific and since several different factors like liquid environment, epoxy, surface treatment, temperature, residual stresses etc. play a significant role during subcritical debonding, a well thought out Design of Experiment (DOE) is critical to understand their interaction with one another and possible effect on the performance of adhesive joint.

5.1 References

1 S. M. Wiederhorn, E. R. Fuller, R. Thomson, "Micromechanisms of Crack-Growth in Ceramics and Glasses in Corrosive Environments", *Metal Science,* **14**, 450-458, 1980.

2 B. R. Lawn, "An Atomistic Model of Kinetic Crack Growth in Brittle Solids," *Journal of Materials Science,* **18**, 469-480, 1975.

3 R.F. Cook and E.G. Liniger, "Kinetics of Indentation Cracking in Glass," *Journal of American Ceramic Society*, **76**, 1096-1106, 1993.

4 M. W. Lane, J. M. Snodgrass, R. H. Dauskardt, "Environmental Effects on Interfacial Adhesion", *Microelectronics Reliability*, **41**, 1615-1624, 2001.

5 S. W. Freiman, "Effect of Alcohols on Crack Propagation in Glass", *Journal of American Ceramic Society*, **57**, 350-353, 1974.

6 S. M. Wiederhorn, S. W. Freiman, E. R. Fuller, and C. J. Simmons, "Effects of Water and Other Dielectrics on Crack Growth", *Journal of Materials Science*, **17**, 3460-3478, 1982.

7 R. J. Hohlfelder, D. A. Maidenberg, R. H. Dauskardt, W. Wei, J.W. Hutchinson, "Adhesion of Benzocyclobutene-Passivated Silicon in Epoxy Layered Structures," *Journal of Materials Research*, **16**, 243-255, 2000.

8 M. W. Lane, R. H. Dauskardt, Q. Ma, H. Fujimoto, N. Krishna, "Subcritical Debonding of Multilayer Interconnect Structures: Temperature and Humidity Effects," *Symposium on Material Reliability in Microelectronics*, Materials Research Society, San Francisco, CA, **9**, 251-256, 1999.

9 S. Y. Kook and R. H. Dauskardt, "Moisture-Assisted Subcritical Debonding of Polymer/Metal Interface," *Journal of Applied Physics*, **9**, 1293-1303, 2002.

10 W.B. Hillig and R.J. Charles, "Surfaces, Stress-dependent Surface Reactions, and Strength", *High Strength Materials* (Edited by V. F. Zackay), John Wiley and Sons Incorporated, New York, **14**, 682-705, 1962.

11 P.C. Paris and F. Erdogan, "A Critical Analysis of Crack Propagation Laws," *Journal of Basic Engineering*, **85**, 528–534, 1963.

12 J. M. Snodgrass, D. Pantelidis, M. L. Jenkins, J. C. Bravman, R. H. Dauskardt, "Subcritical Debonding of Polymer/Silica Interfaces Under Monotonic and Cyclic Loading," *Acta Materialia*, **50**, 2395-2411, 2002.

13 J. E. Ritter, J. R. Fox, D. I. Hutko, and T. J. Lardner, "Moisture Assisted Crack Growth at Epoxy-Glass Interfaces," *Journal of Materials Science*, **33**, 4581-4588, 1998.

14 T. Michalske and B. Bunker, "Steric Effects in Stress Corrosion Fracture of Glass," *Journal of the American Ceramic Society*, **70**, 780-784, 1987.

15 T. A. Michalske and B. C. Bunker, "A Molecular Mechanism for Stress Corrosion in Vitreous Silica," *Journal of the American Ceramic Society*, **66**, 284-288, 1993.

16 A. Bhatnagar, M. J. Hoffman, R. H. Dauskardt, "Fracture and Subcritical Crack Growth Behavior of Y-Si-Al-O-N Glasses and Si_3N_4 Ceramics," *Journal of the American Ceramic Society*, **83**, 585-596, 2000.

17 S. M. Wiederhorn, "Influence of Water Vapor on Crack Propagation in Soda-Lime Glass," *Journal of American Ceramic Society*, **50**, 407-414, 1967.

18 S. M. Wiederhorn, "Chemical Interaction of Static Fatigue," *Journal of American Ceramic Society*, **55**, 81–85, 1971.

19 S. M. Wiederhorn and C. H. Bolz, “Stress Corrosion and Static Fatigue of Glass,” *Journal of American Ceramic Society*, **53**, 543–548, 1970.
20 R. J. Charles, “A Review of Glass Strength”, *Progress in ceramic Science* (edited by J. E. Burke), Pergamon Press, New York, **1**, 1-38, 1961.
21 W. B. Hillig, “Source of Weakness and Ultimate Strength of Brittle Amorphous Solids”, *Modern aspects of the Vitreous State* (Edited by J. D. Mackenzie), Butterworth, Washington DC, **2**, 152-194, 1962.
22 C. J. Phillips, “Strength and Weakness of Brittle Materials,” *American Scientist*, **53**, 20-51, 1965.

Power Law Fit: $\frac{da}{dt} = \Omega G^n$		
	Ω	n
DI Water	2×10^{-11}	1.5
Liquid C	2×10^{-10}	0.9
Liquid B	5×10^{-9}	0.1

Table 5 Values of Ω and n for silicon/commercial epoxy system in DI water, liquid C, and liquid B at 70°C using Paris Law.

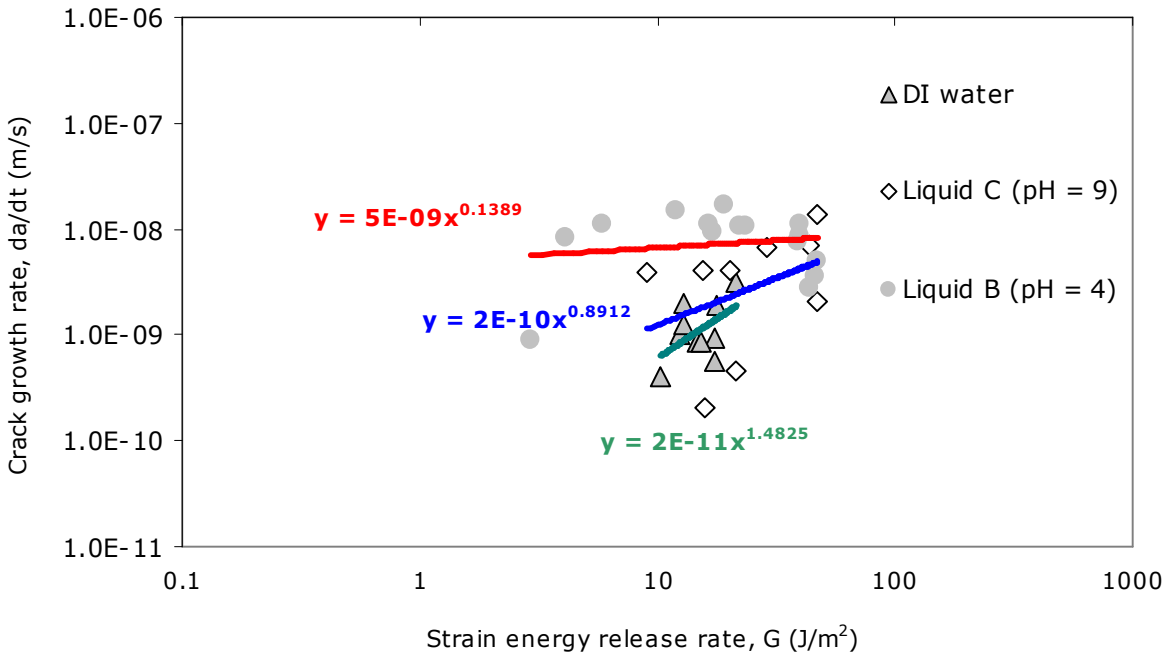

Figure 5.1 Paris Law fit to region II data for silicon/commercial epoxy system in DI water, liquid C, and liquid B at 70°C.

Appendix B

Several models have been proposed by different researchers to predict the behavior of subcritical debonding mechanisms. The rupture process at the crack tip in region I (adopted from the work of Wiederhorn), for humid air environments, is treated as a chemical reaction between strained atomic bonds and water molecules , and the crack growth rate, $\frac{da}{dt}$ is assumed to be proportional to the rate of chemical reaction, as shown in Equation 5A:

$$\frac{da}{dt} = A^* \exp(\frac{bG}{RT}) \tag{5A}$$

where $A^* = A\left[-E^*/RT\right]$ is a constant at fixed temperature, E^* is the stress free activation energy, b is an activation area related to the activation volume, and G is the crack tip strain energy release rate. The above equation predicts an exponential increase in crack velocity with G and an Arrhenius-like increase with temperature, and has been used successfully to fit region I data.

Figure 5A shows the temperature response of silicon/commercial epoxy system in DI water, where region I and II are presumed as shaded areas. Since no sharp distinction is evident for the transition from region I to region II, an overlap of two regions is also shown. Fitting Equation 5A to the wedge test data at different testing temperature yields different values of A^* and b. Since the data collected in region I was not observed at 60°C, 70°C and 90°C, Figure 5B shows the exponential fit for region I at 80°C. If region I data were also available at other temperatures, then an Arrhenius kind of relationship between crack velocity, $\frac{da}{dt}$, and temperature, T, would yield the value of activation energy (E^*) and activation volume (b) for the system at a given value of strain energy release rate G.

Region III is found to be independent of environmental factors and is dominated by critical fracture events where the crack velocity is no longer limited by mass transport. The onset of region III is indicated by a rapid increase in crack velocity at the end of region II. This typically occurs as G approaches the critical value G_C. No satisfactory theory has been proposed to explain the fracture data in region III. However, a fracture mechanics approach (proposed by Curley et al) may be introduced to capture the

sigmoidal form of the kinetics. Specifically, the relationship between the debond growth rate and the energy release rate may be expressed by a modified form of the Paris law,

$$\frac{da}{dt} = CG^n \left[\frac{1-(G_{th}/G)^{n_1}}{1-(G/G_c)^{n_2}} \right] \tag{5B}$$

where G_{th} and G_C are the subcritical threshold energy release rate and critical fracture energy, respectively. Since $G_C >> G$, we can assume $1-\left(G/G_C\right)^{n_2} \approx 1$. Therefore, Equation 5B can be rewritten as:

$$\frac{da}{dt} = CG^n \left[1-(G_{th}/G)^{n_1}\right] \tag{5C}$$

A curve fitting was used (shown in Figure 5C using Equation 5C) for silicon/commercial epoxy system in DI water to calculate the values of constant C and exponent n and n_1 at 70^0C and 80^0C, as shown in Table 5A. The values of constant C and exponent n do not exhibit a significant change with change in temperature whereas the exponent n_1 was found to have higher value for higher temperature. The model discussed above may be useful to quantify the system response provided the sufficient amount of data in all three regions of crack propagation is available. Limited amount of data discouraged the modeling efforts for reliability and durability predictions for the system under study. For a full fundamental understanding of the debond mechanisms at the interface and utilizing molecular modeling and/or kinetic modeling approach to understand subcritical crack growth mechanisms, a model epoxy system may be employed where each parameter controlling subcritical debonding could be adjusted to understand it's role in delamination.

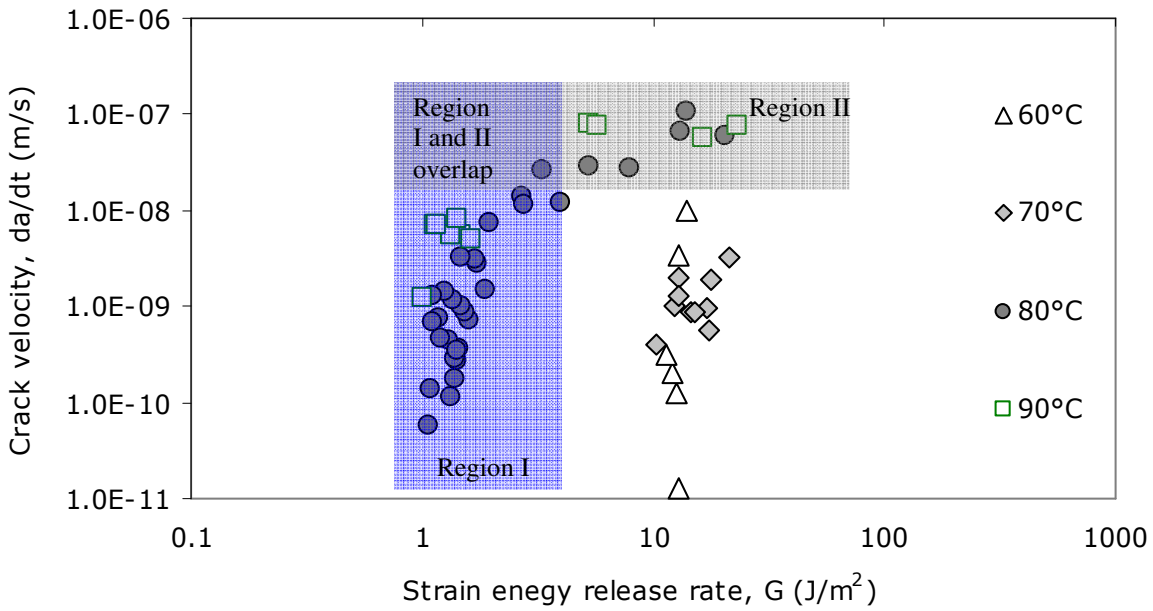

Figure 5A Silicon/commercial epoxy system in DI water at different testing temperatures.

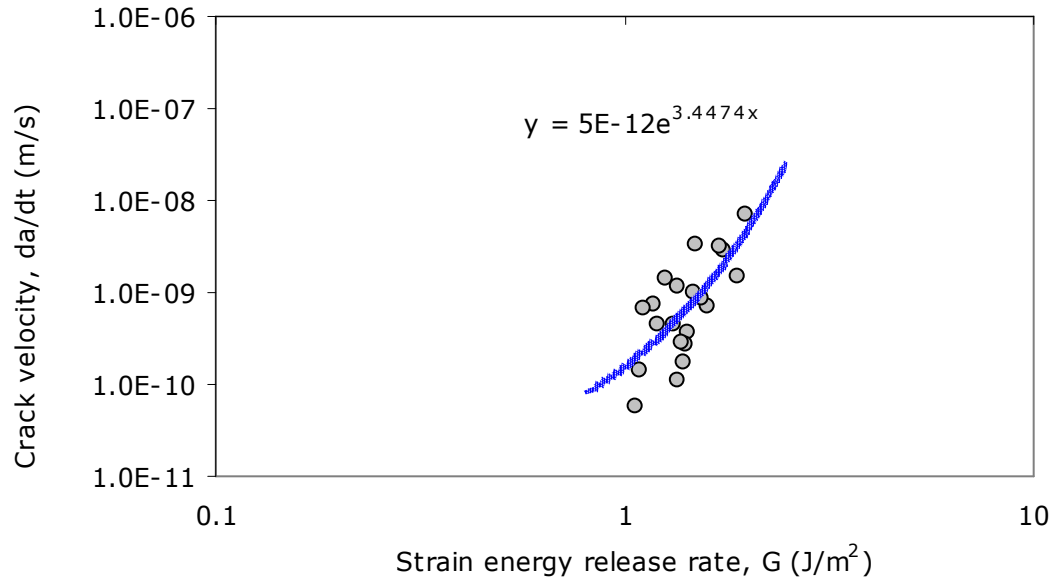

Figure 5B Exponential fit to region I data at different temperatures for silicon/commercial epoxy system in DI water at 80^0C.

Modified Paris Law: $\frac{da}{dt} = CG^n\left[1-(G_{th}/G)^{n_1}\right]$			
	C	n	n_1
70°C	-9	0.89	1.29
80°C	-8.6	1.17	3.6

Table 5A Values of constants at 70°C and 80°C for silicon/commercial epoxy system using modified Paris Law.

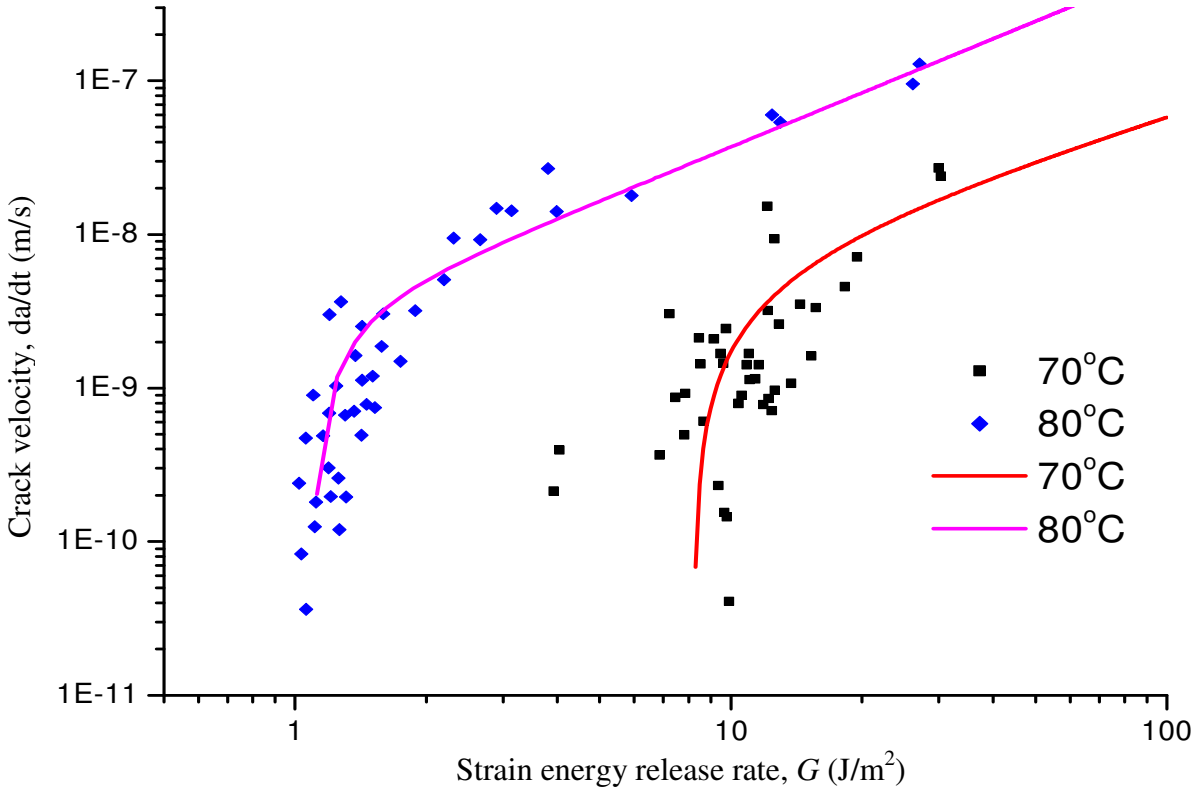

Figure 5C Modified Paris Law fit at 70°C and 80°C for silicon/commercial epoxy system in DI water.

6 CONCLUSIONS

6.1 Summary and Conclusions

Polymers have been used in electronics applications for a long time, and are still gaining much attention because of their unique properties. Epoxy resin systems are used extensively in such diverse as matrix resin for printed circuit board, die-attach adhesives, and encapsulants for different levels of packaging. Adhesion between polymeric materials and various kinds of inorganic, even polymer materials, and the corresponding durability property against environmental attack of the bonded structures are among the key requirements for such materials for their successful service application. Subcritical failure of the adhesively bonded devices is very common in the products composed of different materials, and the initiated debond may propagate when subjected to both mechanical stress and environmental attack simultaneously. Many methods have been proposed to measure subcritical delamination, and the wedge test is commonly utilized to test the durability of fractured and stressed adhesive joints when exposed to different environments.

In this thesis, I have tried to generate an understanding of subcritical delamination mechanisms of the adhesively bonded systems in different environments, which may provide insights to the application of polymers in the microelectronics industry. Subcritical adhesion testing closely resembles the failures observed in the actual application or service of the adhesive. In these more realistic situations, degradation and failure takes place over long periods of time and the environment is the main driving force. Subcritical debond propagation along glass/epoxy and silicon/epoxy interfaces was explored. The following sections summarize this research, and detail some of the findings related to this study.

Subcritical debonding behavior of wedge specimens consisting of silicon or glass substrates and commercial or model epoxy, subjected to different environments, has been studied. The crack growth rate, $\frac{da}{dt}$, was measured as a function of the strain energy release rate, G. The adhesion degradation of the interface was diffusion controlled at higher temperatures and for aggressive liquid environments. The results showed that

there exist threshold values, G_{th}, below which no significant crack growth will occur. No apparent value of G_{th} was observed for model epoxy systems at 70°C and 80°C, whereas the values of G_{th} for commercial epoxy system in DI water were found to be about 8 J/m^2 and 1 J/m^2 at 70°C and 80°C respectively which suggest that the existence of G_{th} depends on the epoxy-substrate interaction at the interface. Also, the higher the test temperature, the higher the debond propagation rate and lower the value of G_{th}.

Wedge tests on preconditioned specimens were also conducted to investigate the effect of preconditioning on the system behavior. Wedge specimens were preconditioned in different liquids at 60°C for 30 days and tested at 70°C. The data obtained helped us in learning that the introduction of aggressive environments significantly degrades the adhesion resulting in poor performance of adhesive joint whereas the same adhesive joint perform better in non-aggressive environments.

XPS study of fractured surfaces revealed some important aspects of delamination. The XPS data revealed the failure pattern for model epoxy/3-APS interface. The failure was observed to be interfacial at 60°C, whereas a mix of interfacial failure and some cohesive failure in the model epoxy adhesive occurs at 70°C. This observation might suggest a possible weakening of the adhesive at higher temperatures, giving rise to cohesive failure in the adhesive. The XPS results suggested that the interaction at the commercial epoxy/3-APS interface may be stronger than that between the model epoxy/3-APS surface. XPS results revealed weaker model epoxy/3-APS interface and corroborates the wedge test result where diffusion controlled debonding was observed with higher crack propagation rate for model epoxy system as compared to the stronger commercial epoxy interface. The failure of the adhesively bonded system, interfacial or cohesive, may depend on the environmental conditions, e.g. test temperature, surface chemistry, epoxy etc.

The data obtained from subcritical wedge testing in different environments was analyzed using empirical relationships proposed by various researchers and empirical constants were calculated. The value of Ω and n obtained by fitting the power law relationship to region II exhibited a particular trend as regards to crack growth rate. The decrease in the value of n (the resistance to "stress-corrosion" crack growth) and the increase in the value of Ω were observed with decrease in the pH of the test environment.

The observed trend for the value of Ω and n may be specific to a particular system and testing conditions.

6.2 Future Directions

Wedge tests performed in this study helped to gain valuable insights by learning the behavior of the selected systems with respect to temperature, preconditioning, and surface chemistry, but a fundamental understanding of the delamination mechanisms is still not apparent. The behavior of the system appears to be environment specific and since several different factors like liquid environment, epoxy, surface treatment, temperature, residual stresses etc. play a significant role during subcritical debonding, a well thought out Design of Experiment (DOE) is critical to understand their interaction with one another and possible effect on the performance of adhesive joint. For a full fundamental understanding of the debond mechanisms at the interface and utilizing molecular modeling and/or kinetic modeling approach to understand subcritical crack growth mechanisms, a model epoxy system may be employed where each parameter controlling subcritical debonding could be adjusted to understand it's role in delamination. The approach can be summarized as follows:

1. A detailed experimental investigation and design of experiment (DOE) evaluation of various parameters and evaluate crack velocity as a function of strain energy release rate.
2. Durability assessment of bond system, utilizing wedge test data and bimaterial curvature techniques to evaluate the role and interactions of residual stresses and various other factors involved in degradation and debonding.
3. A model epoxy system may be employed where each parameter controlling subcritical debonding could be adjusted to understand the delamination mechanisms.
4. A full fundamental understanding of the debond mechanisms at the interface utilizing molecular modeling and/or kinetic modeling approach to understand subcritical crack growth mechanisms to make reliability and durability predictions.